Universitatea
Transilvania
din Brașov

INTERDISCIPLINARY DOCTORAL SCHOOL
Faculty: Product and Environmental Design

Eng. Cezar-Ioan FRINCU

# DOCTORAL THESIS

Scientific Advisor
Prof. Dr. Eng. Ioan Stroe

BRAȘOV, 2024

Eng. Frîncu Cezar-Ioan

*DOCTORAL THESIS*

TITLE (romanian): Sistem de prehensiune autoadaptiv pentru piese solide cu forme neregulate
TITLE (english): Self-adaptive prehension system for solid pieces with irregular shapes.

Doctoral field: MECHANICAL Engineering

Thesis analysis committee:
Univ. Prof.PhD. Eng. Prof. – Eneșca Alexandru, Vice Dean of the Faculty of Product and Environmental Design, Transilvania University of Braşov
Univ. Prof. PhD. Eng. – Stroe Ioan, Transylvania University in Braşov
Univ. Prof. PhD. Eng. – Doroftei Ioan, "Gheorghe Asachi" Technical University from Iasi
Univ. Prof. PhD. Eng. – Pîslă Doina, Technical University of Cluj-Napoca
Univ. Prof. PhD. Eng. – Zamfira Sorin, Transylvania University of Brașov

# CUPRINS

# LIST OF NOTATIONS

| Symbol | Description |
|---|---|
| $M_{t_{c1}}$ | The moment of calculation on the auger |
| $M_t$ | Engine torque |
| $M_{pp}$ | Stepper motor |
| $P_e$ | The pitch of the screw propeller corresponding to the rolling diameter |
| $\beta$ | The angle of inclination of the spiral of the auger |
| $d_{r1}, r_{r1}$ | The diameter, respectively the rolling radius of the auger |
| $F$ | Force |
| $p$ | Axial pitch (apparent) of the screw |
| $s$ | The number of starts of the snail |
| $D_{\min}$ | Minimum clamping diameter |
| $D_{\max}$ | Maximum clamping diameter |
| $C_m$ | Maximum travel of the module |
| $F_{\min}$ | The minimum pulling force of the object |
| $F_{contact}$ | The frictional force between the module's tip and the surface of the grasped object. |
| $s_1, s_2, s_3,$ $s_4, s_5, s_6$ | Sides of the parallelogram |
| $a_1, a_2, a_3, a_4,$ $a_5, a_6, a_7, a_8$ | Angles from the kinematic structure |
| $l_1, l_2, l_3$ | Variable distances |
| $A, B, C, D,$ $F, O, O'$ | Torques of rotation |
| $F, H$ | Translational torques |
| $F_c$ | Composite force |
| $F_r$ | Reaction force |
| $F_x, F_y, F_z$ | Resultant forces in the x, y, z directions |
| $M_x, M_y, M_z$ | Resultant moments in the x, y, z directions |
| $R$ | Transmission report |
| $F_a$ | Axial force |
| $H_I, H_{II}, H_{III}$ $V_{I_1}, V_{II_1}, V_{III_1}$ | Reactions due to force |
| $V_{I_2}, V_{II_2}, V_{III_2}$ $F_{r_I}, F_{r_{II}}, F_{r_{III}}$ | Reactions due to force |

## THANKS

On the occasion of the completion of this doctoral internship, I feel marked by happiness, emotions and fulfillment, feelings that come from both the professional and personal satisfaction of doctoral studies.

I am deeply grateful to Professor Ioan STROE, the coordinator of this doctoral thesis, for his scientific guidance and support throughout the writing of this paper, his complete trust, availability and professional collaboration throughout the internship period.

Sincere thanks, professors Luciana CRISTEA, Ionel STAREȚU, Cătălin ALEXANDRU, for agreeing to be members of the analysis committee, for the kindness and patience with which they analyzed this paper, for the comments and suggestions sent when supporting the reports.

At the same time, I want to thank my colleagues, Constantin TORCĂTORU, Lucian ULMANU, Alexandu DIACONU, Marius BĂSESCU, as well as the other colleagues from the ARKA team, for their encouragement in difficult moments, advice and activities during the internship period.

Last but not least, I would like to take this opportunity to thank my wife, parents, sister and close friends, for supporting me and being with me throughout the writing of this doctoral thesis.

Thank you!
Sincerely,
Ph.D. Eng. Cezar FRiNCU

## INTRODUCTION

The use of industrial robots in the modern industry puts a lot of emphasis on robotic gripping to replace humans and many of the errors they used to make through inattention or accumulated fatigue. At the same time, through the implementation of industrial robots, all kinds of gripping systems such as grippers are used. Robotic technology is especially relevant in high- and middle-income countries, where manual labor is expensive. In such cases, economic benefits can be made by replacing human labor with autonomous robotic manipulation.

Robots were introduced into the industry in 1912 by the UnimationTM company and implemented within the General Motors Company.

Industrial handling robots are essential in the automation of industrial processes. These robots are designed to manipulate, move and place objects precisely and efficiently, thereby reducing the need for human intervention in repetitive or dangerous tasks. They play a crucial role in increasing productivity and improving quality in various industries.

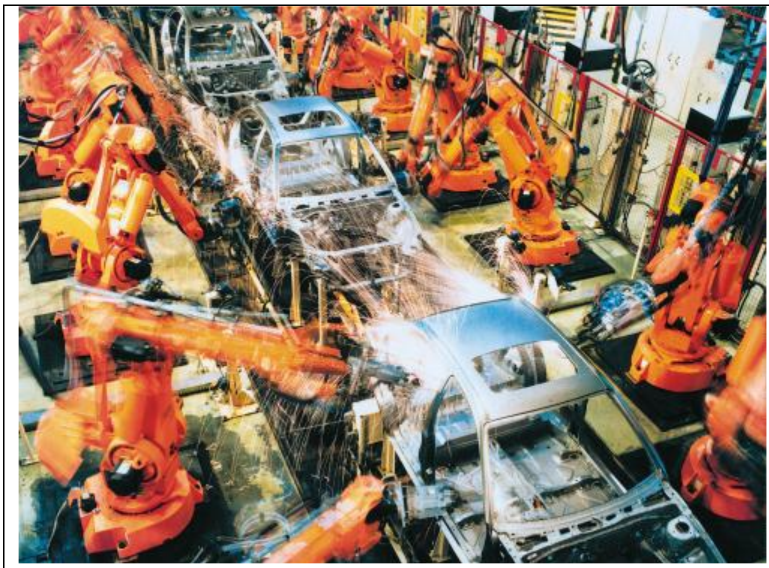

*Figure. 1.01. Modern car manufacturing factories with robots*

All handling robots are designed with a gripper system to handle objects. These gripping systems are implemented according to the field of activity, the type of object they are gripping and the environment in which they work.

Grippers are advanced mechatronic structures predominantly used by industrial robots to perform the operations of gripping and manipulating objects, transferring them from a starting position to a final position required for various automated technological processes. These systems are classified, depending on the type of prehension force applied, into three main categories: mechanical, vacuum and magnetic.

# 1. GRIP SYSTEMS. CURRENT STATE

The prehension systems were taken from real life, where we have animals and insects that describe a grasper through their movements, these being called natural prehension systems (Figure 1.1).

Prehensoarele sunt sisteme mecatronice complexe cu ajutorul cărora se pot prinde obiecte de diferite forme și dimensiuni. Ele pot fi cu două degete, de tipul gripper, dar și cu 3, 4 sau 5 degete constituind tipuri de prehensoare, similar antropomorfelor care imită mâna umană.


*Figure. 1.1. Examples of natural grippers [1]*

Grippers are complex mechatronic systems that can be used to grip objects of various shapes and sizes. They can be with two fingers, of the gripper type, but also with 3, 4 or 5 fingers constituting types of grippers, similar to anthropomorphs that imitate the human hand.[2].

In terms of operation, grippers are of several types. Depending on the applicability and the object to be grasped, the grippers can be operated in several ways:

• With contact gripping method – these grippers are resistant and can grip rigid objects with arms or fingers;

• With intrusive grasping method – with this method you can grasp objects made of glass, fiberglass, carbon;

• With an astringent gripping method - it can be vacuum, magnetoadhesive, electroadhesive and is used to grip non-porous objects, thin materials, sheet metal;

• With the contiguous grasping method – it can be thermal, chemical, with surface tension and is used to grasp objects such as textiles, carbon, small and light objects.

In general, each gripping method has a specific applicability, but there are also cases where a gripping method can be used in many types of processes to grip various objects of different materials [3].

## 1.1. The Study of Complex Contact Prehension Systems

### 1.1.1. Adaptive grippers

Sistemele de prehensiune adaptive sunt sisteme mecatronice complexe în care sunt incluse sisteme senzoriale, mecanice şi sunt programabile.

These adaptive grippers have the ability to make certain decisions individually, therefore they are not pre-programmable. They orient themselves in space according to several parameters generated by the system in which they are implemented. These mechatronic systems are designed to handle objects safely by controlling torque and clamping force.

Humans can grasp an object and take into account external parameters. They can grip controlled depending on the weight and the adhesion to the touch between the object and the skin. This has been very well studied, and many systems have been made trying to mimic all of these things.

Finger grippers differ in the number of actuated and un-actuated joints, the coupling of the various joints, and the way in which the drive torque is transmitted to these joints.

All these grippers have in common under-actuation and self-adaptation resulting in a reduction in weight and a simple controllable gripper with the ability to understand the shape of different objects. They also have the ability to adapt to different surfaces and shapes for holding objects.

At first, these systems were created for controlled gripping of fragile objects, where the force must be very well determined.

The Roboticq 2-Finger Adaptive Gripper has two versions, 85 and 140. The 2-Finger version shows resizing for objects of different sizes **(Error! No reference source.)**[10].

An interesting example of the use of an adaptive clamping technology that Festo has developed can be seen in the Figure. 1.2, where the target objects are of variable shape. In addition, the fragile nature of bulbs requires a gripper to handle them with care. They must be held firmly enough not to slip from the claws of the gripper and at the same time, they must not be crushed by a strong grip.

This may also be true in the food industry, where economic losses could be avoided if product handling did not lead to destruction or damage [4].

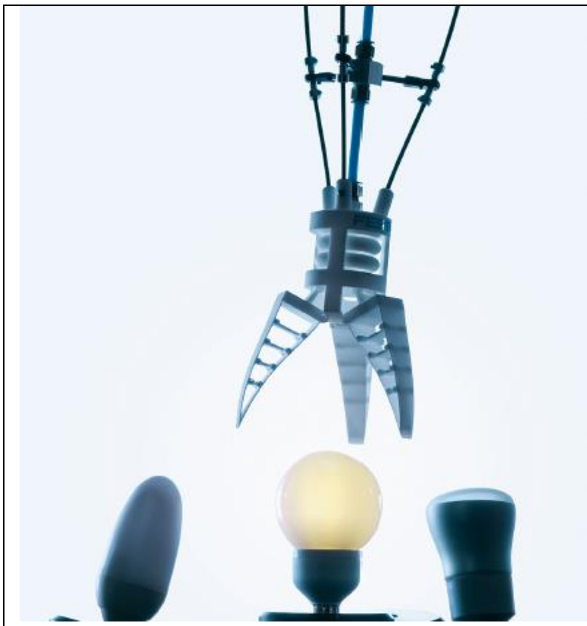

*Figure. 1.2. Adaptive gripper for sensitive objects Bionic Tripod 3.0*[11]

The gripper with a multi-functional 3-finger system SCHUNK SDH molds to the shape. This system is also suitable for sensitive objects with a hole, where it clamps with a controlled force into the holes even if they are extremely wide [11].

This adaptive gripper is capable of grasping different objects and can bring the fingers up to an anthrax of 57.2 mm. From that moment, the system can only juggle from the upper joints to be able to bring the bins closer together, as can be seen in the Figure. 1.3.

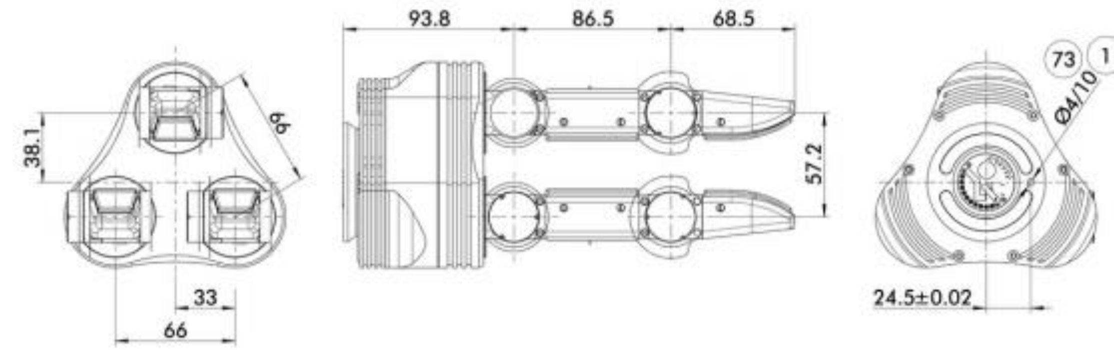


*Figure. 1.3. 2D assembly drawing of SCHUNK SDH adaptive gripper*

### 1.1.2. Self-adaptive grippers

As a result of research, the most advanced application in the field of grippers was discovered by Marc Manz and Sebastian Bartsch. The gripper is designed as a module to be mounted on different manipulators. This requirement led to the choice of electric motor actuation instead of hydraulic or pneumatic systems. Moreover, sensors for object detection, grip force control and force measurement between gripper and manipulator are integrated into the system [2].

## 1.2. Conclusion

- An adaptive prehension system must be created that does not change its size during operation;
- It is necessary to move the bins parallel to the horizontal of the work table;
- Without a complex sensory system, an adaptive system cannot be realized;
- It is very important to control the forces on the object;

# 2. DESIGN OF THE GRIPPER MODULE WITH PARALLEL PLANE MOVEMENT

The self-adaptive gripper allows the gripping of objects of small sizes, different geometries and reduced thickness by the parallel movement of the gripper with the surface on which the object is placed compared to other gripping systems that describe arcs of a circle in movement for gripping objects, which is why it does not serve to catch small objects [12], [12], [13].

The gripper has self-adaptive force control, it can grip objects of different shapes, not just regular-shaped objects because each arm of it is independently controlled and actuated according to the prehension force applied to the object, so that the object does not slip during movement [14]–[16].

Mechanical 5-finger grippers are complex systems that mimic a human hand, and the hand is an ideal gripper. Grippers have the role of transporting objects in a controlled and well-determined way in a defined space. The imposed conditions of this type of gripper are flatness with respect to the gripped object and the work table, and the movement must be very precise, with 1 kg gripped [17]–[20].

The proposed objective of this chapter is: **Analysis and design of a self-adaptive gripper with five independent fingers, using a parallelogram-type kinematic configuration to ensure adaptability, precision, and flexibility in handling objects of different shapes and sizes. 3D modeling, kinematic simulation, and detailed structural analysis were considered to optimize the design of a gripper for application in robotics and automation.**

## 2.1. Designing the kinematic scheme of the prehension module

In order to establish a concept, the details necessary for its realization are needed. In the case of making a gripper module, it is necessary to establish the principle and mode of operation. According to the imposed conditions, the gripper system created fulfills the function of parallelism with respect to the grasped object and the function of parallelism with respect to the work table on which the object stands.

**Input data:**

Dmin = 9mm, for the minimum clamping diameter,

Dmax = 90mm, for the minimum clamping diameter.

**Ipoteze:**

- Dispozitivul trebuie să fie proiectat în așa fel încât să poată efectua prehensiunea de corpuri caracterizate de forme neregulate.
- Obiectele supuse prehensiunii trebuie să aibă o masă maximă de 1 kilogram.
- Dispozitivul trebuie să fie conceput pentru a putea prehensa obiecte cu o înălțime minimă de 2 mm.

**În urma studiilor s-au concluzionat următoarele:**

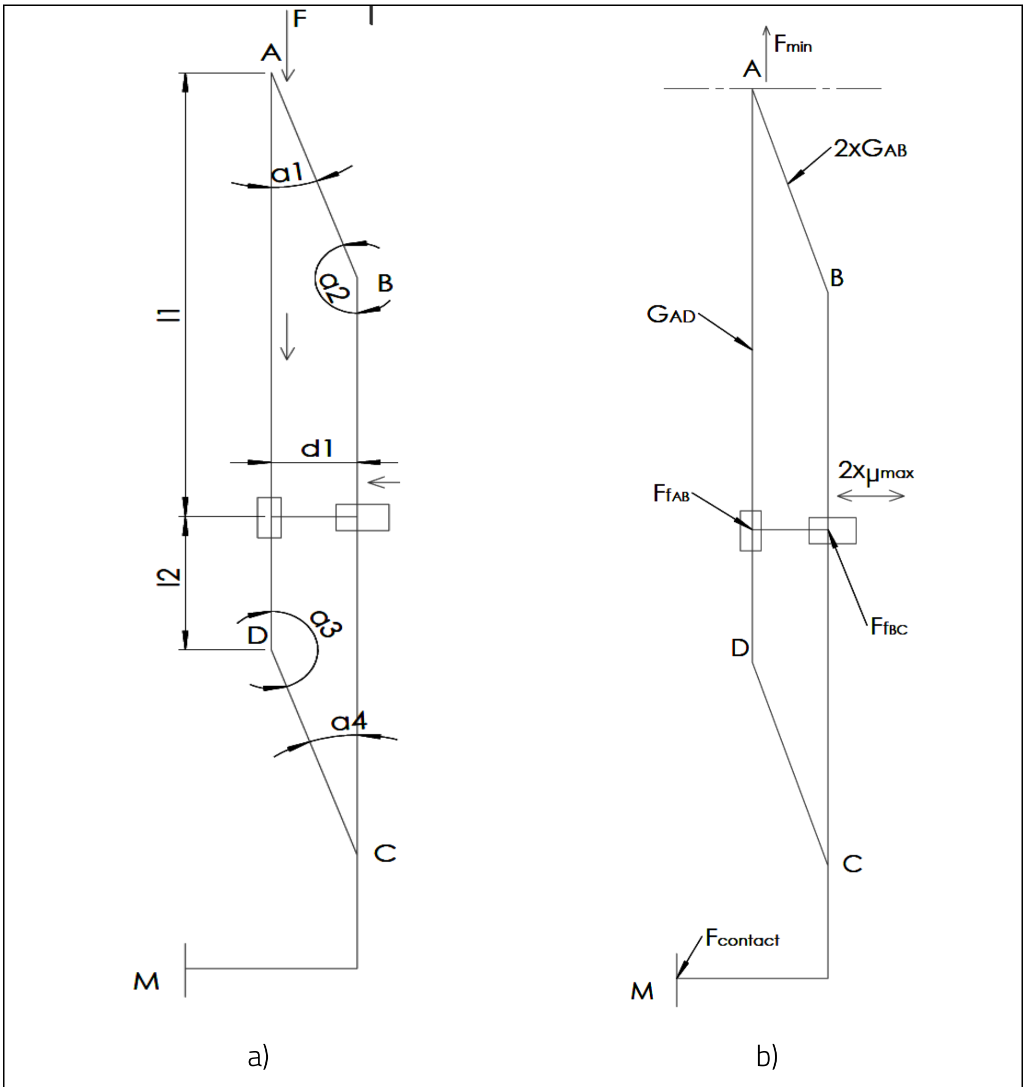


*Figura. 2.1. Schema cinematica a modulului de prehensare*

- The gripping device will be designed with 5 arms;
- The 5 gripper arms are mechanically, electrically and software independent;
- The description of the movement of the 5 arms of the gripper is a plane-parallel movement.

Maximum stroke of the module:

$$C_m = \frac{D_m}{2} = \frac{90}{2} = 45 \text{ mm}, \tag{2.1}$$

- In order to achieve parallel plane movement, a parallelogram-type kinematic configuration will be implemented, characterized by the presence of two fixed translation points located centrally.

$$\begin{cases} \overline{AB} = \overline{DC}, \\ \overline{AD} = \overline{CB}. \end{cases} \tag{2.2}$$

where:

$$\begin{cases} \overline{AB}, \overline{BC}, \overline{AD}, \overline{DC} = \text{fixe}, \\ d_{1\min} = \text{variabil}, \\ L_1 = \overline{AO} = \text{variabil}, \\ L_2 = \overline{OD} = \text{variabil}. \end{cases} \quad (2.3)$$

The minimum distance between the two sides of the parallelogram $\overline{AD}$ and $\overline{BC}$ is reached when the mechanical system is in a closed position:

$$d_{1\min} = 27 \text{ mm}, \quad (2.4)$$

The maximum distance between the two sides of the parallelogram $\overline{AD}$ and $\overline{BC}$ is reached when the mechanical system is in an open position:

$$d_{1\max} = 73 \text{ mm}, \quad (2.5)$$

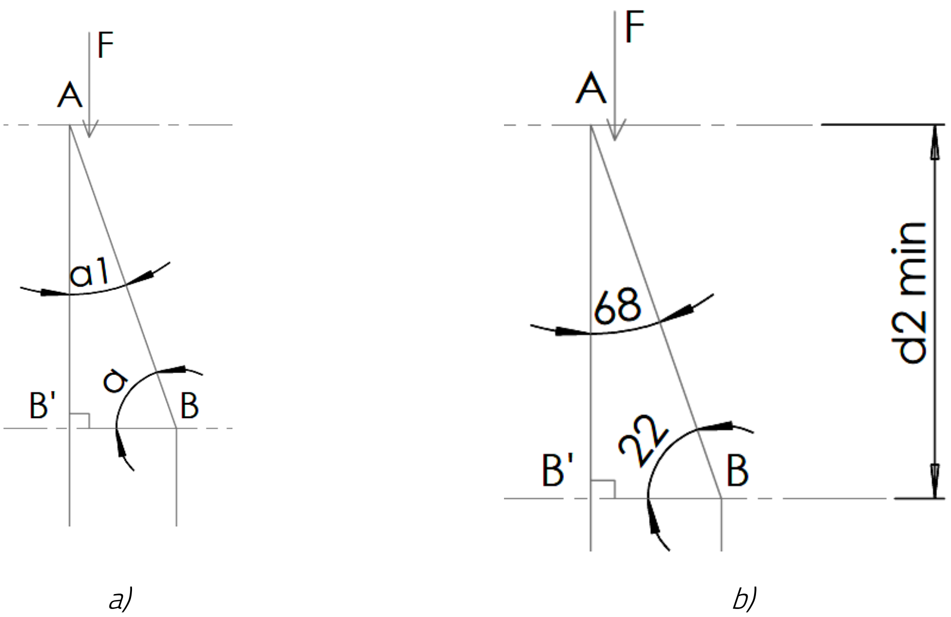


*Figure. 2.2. Determination of segment BB'*

- $d_{1\min}$ - is determined by the mechanical components that are in motion, this value being variable.

$$d_{1\min} = 27 \text{ mm} \Rightarrow \overline{AB} = \overline{DC} > d_{1\max}. \quad (2.6)$$

$$\text{Din } ABCD \Rightarrow \sphericalangle a_1 \text{ din } A, \sphericalangle a_4 \text{ din } C \quad (2.7)$$

$$\begin{cases} \sphericalangle a_1 = \sphericalangle a_3 \\ \sphericalangle a_2 = \sphericalangle a_4 \end{cases} \quad (2.8)$$

For an italic motion of segment AB, it cannot be ⊥ on BC and must be > 20˚, $\alpha$>20 ˚:

$$\overline{BB'} = d_{1\max} = 75 \text{ mm, pentru } \alpha = 20^\circ, \quad (2.9)$$

$$a_1 = 70^\circ, \text{ for } \sphericalangle B' = 90^\circ, \quad (2.10)$$

$$\cos 20^{\circ} = \frac{75}{\overline{AB}} \Rightarrow \overline{AB} = \frac{75}{\cos 20^{\circ}} = 80.5 \text{ mm}, \tag{2.11}$$

For a margin of error it will be approximated:

$$\overline{AB} = 82 \text{ mm} \Rightarrow \cos\alpha = \frac{73}{82} = 0.89 \tag{2.12}$$

$$\text{for } arccos\, 0.89 \Rightarrow \alpha \simeq 22^{\circ}. \tag{2.13}$$

$$82^2 = 75^2 + \overline{AB'^2} \tag{2.14}$$

For the retreat position, where $d_1 = \overline{BB'} = 30 \text{ mm}$:

$$\Rightarrow \begin{cases} \overline{AB} = 82 \text{ mm}, \\ \overline{AB'} = 33 + 45 = d_2, \\ \overline{AB} = 78 \text{ mm}. \end{cases} \tag{2.15}$$

From a structural point of view, $\overline{AD}$ □ $\overline{BC}, \overline{AD} = \overline{BC},$ throughout the travel and matters kinematically.

Calculation of the force required for prehension

The maximum weight is 1kg for a prehension system with 5 modules, the minimum lifting weight is 1000g.

$$\frac{1000}{2} = \frac{200 \text{ g}}{\text{module}}. \tag{2.16}$$

The minimum pulling force of the object considering inertia $i = 0$ and friction $\mu = 0$.

$$F_{\min} = 0.2 \text{ N}. \tag{2.17}$$

In the kinematic system:

$$F_{\min} = F_{contact} + G_{structura} + F_{frecare} \tag{2.18}$$

In the calculation, the friction force in the bearings with bearings in the rotation points A, B, C, D is neglected, they have a coefficient of friction of $\mu = 0.0010 \ \mu\text{m}$.

$$F_{\min} = G_{AD} + F_{f_{AD}} + F_{f_{BC}} + F_{contact} \tag{2.19}$$

$$\begin{aligned} F_{\min} &= 9.8 \cdot m_{AD} + 0.04 \cdot m_{AD} + 2 \cdot 9.8 \cdot m_{AB} + 0.08 \cdot m_{BC} \\ &= (9.8 + 0.04) \cdot m_{AD} + 18 \cdot m_{AB} + 0.08 \cdot m_{BC} \\ &= 9.84 \cdot m_{AD} + 18 \cdot m_{AB} + 0.08 \cdot m_{BC} \end{aligned} \tag{2.20}$$

$$\begin{aligned} F_{f_{BC}} &= 2\mu m g \\ &= 2 \cdot 0.004 \cdot m \cdot 9.89 = 0.08 \cdot m_{BC} \text{ [N]}. \end{aligned} \tag{2.21}$$

The coefficient of friction between rubber and steel is: $\mu_c$=0.3

To be able to lift the object, the minimum traction force (Fmin) must be greater than the contact force ($F_{contact}$):

$$F_{\min} > F_{contact}, \quad F_{contact} > G_{obiect}. \tag{2.22}$$

$$F_{contact} = \mu_c \cdot m_{obiect} \cdot g = 0.588 \text{ [N]} \tag{2.23}$$

$$F_{\min} = G_{AD} + 2 \cdot G_{AB} + 0.04 \cdot m_{AB} + 0.08 \cdot m_{BC} + 0.588 \tag{2.24}$$

To choose the motor, the motor moment is calculated according to Fmin: $M_t = 9.55 \cdot 10^{-6} \dfrac{P}{n}$ (2.25)

Where, n = the number of revolutions, which will adjust according to the gripping speed.

3D modeling of the designed module

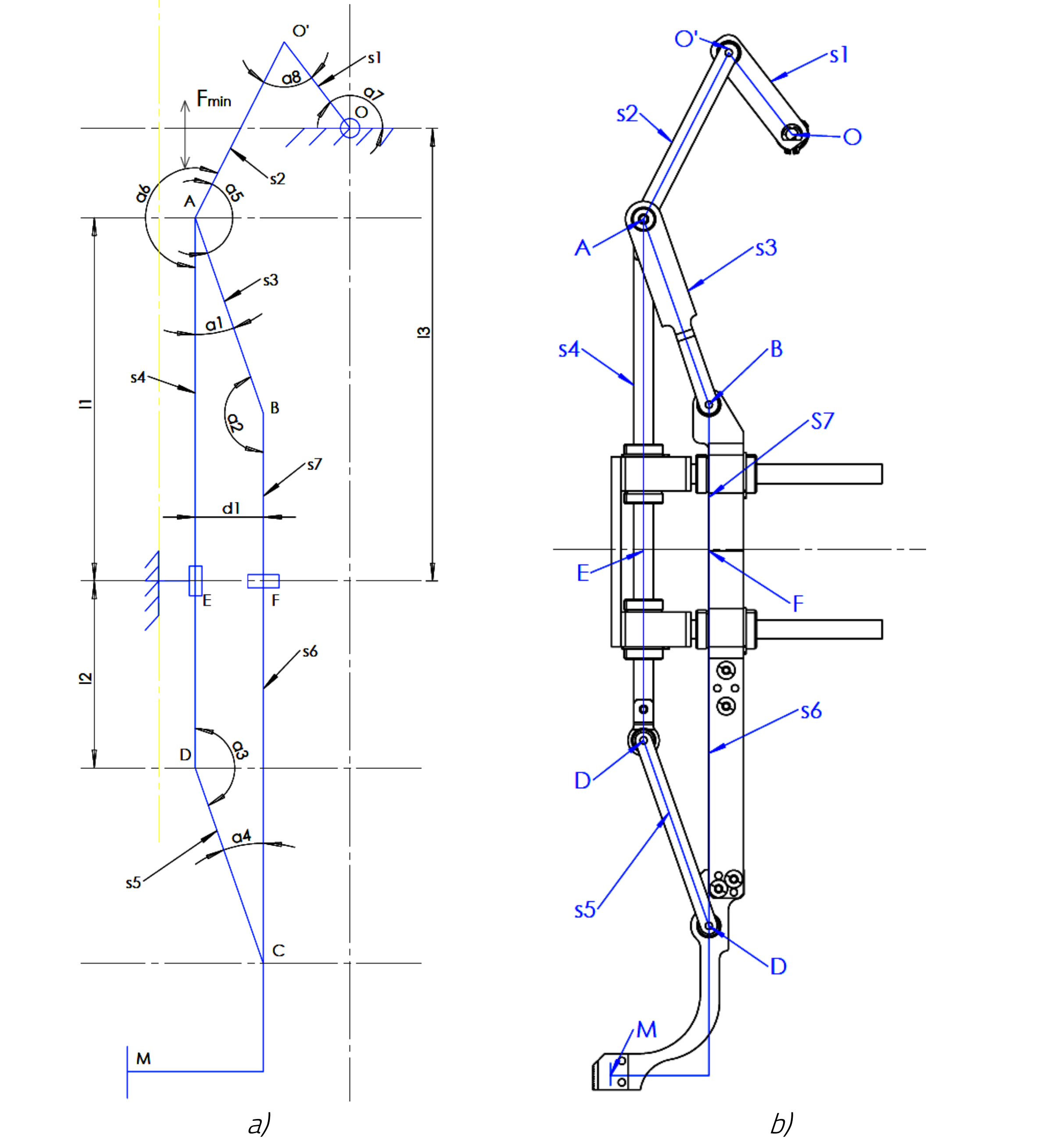


*Figure. 2.3. Schematic representation of compliance with the kinematic scheme*

After going through the stages of 3D modeling and observing the kinematic conditions, the gripper module was made. The respect of the kinematic scheme and the mechanical realization are represented, so that the kinematic couples have the necessary degrees of freedom. The rotation torques (A), (B), (C), (D), (F) and (G) are of the bearing type between the parts that form the arms of the levers and the radial-axial bearings, to reduce friction from the movement of the gripper module .

The translational movements are made with the help of linear guides with balls (E) and (H), which allow a very good continuity in the movement of the gripper module. With the help of bearings and guides, a very low coefficient of friction is obtained between the couplings, which helps in 3D simulation, because it is ideal and therefore friction is neglected [10].

## 2.2. Virtual prototyping of the module

### 2.2.1. Importing and simulating the gripper module in Adams software

**a. Importing the gripper module into Adams**

After completing the design in a design program such as Catia, the parts are imported into Adams or, depending on the Adams version, the entire gripper module can be imported directly. Once the gripper module is imported, the material type is specified for each part to apply constraints.

With the help of these tools, all components of the gripper module (Figure. 2.4) were constrained to allow its movement. Along with these constraints, you must declare which of the constrained couplings is primary, and then define the secondary ones [21], [22].

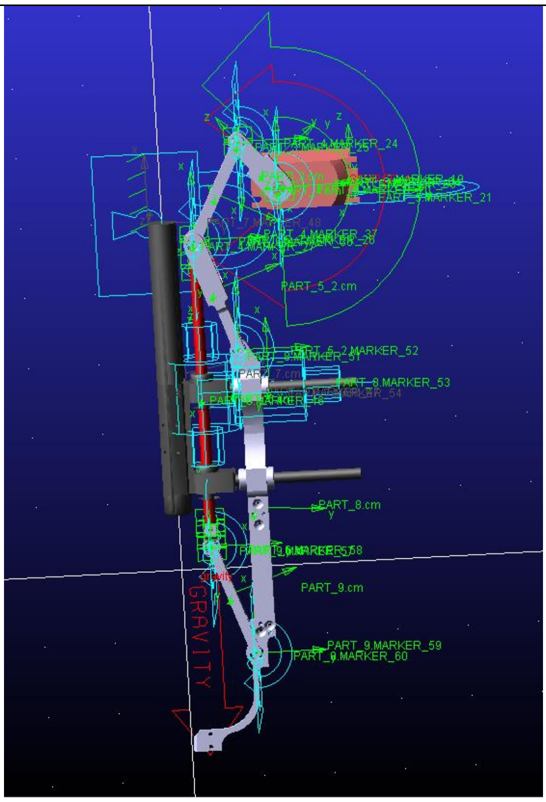


*Figure. 2.4. Representation of couples in Adams*

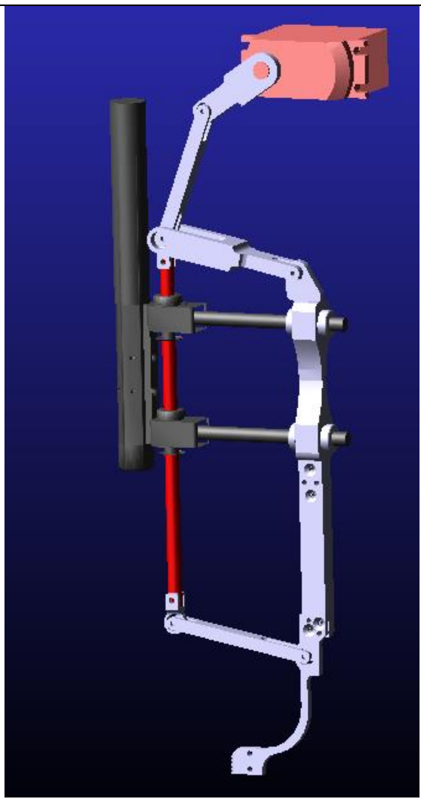

*Figure. 2.5. Realization of kinematics*

**b. Realization of virtual prototyping and simulation in Adams**

After all the couplings were placed, the forces necessary for movement were applied to the components of the gripper module, and one of these forces is constant namely the gravitational force. By fulfilling all the functionality conditions, the 3D simulation of the gripper module can be applied.

After determining the time and steps necessary to generate the complete movement of the gripper module, it is moved to the start stage and the gripper module will move to the advance position relative to the origin, as in the Figure. 2.5 [23].

### 2.2.2. Motion analysis and graphical simulation in the Adams program.

Following the simulation in the Adams program, an acceleration sensor was applied to the entire module. This simulation was performed applying the force of the gripper module drive motor of 2Nm, to which was added the gravitational acceleration of 9.8 m/s2.

In the graph in Fig. 2.6 the maximum demands are observed for a complete cycle performed by the module (advance-retraction). These stresses are amplified over time as mechanical wear occurs in the couplings and bearings or mechanical backlash may occur and these may create vibrations in the system. In the performed simulation, frictional forces are not taken into account, which means that the system is considered to perform ideal movements [23].

The frictional forces that can appear in the system and are not taken into account are multiple and can be:

• Frictional forces in bearings,
• Frictional forces between components,
• Frictional forces of the system due to non-observance of dimensions.

Due to the parallelogram-type mechanical structure driven by a rotational movement, it has a slight acceleration when retracting and a slight deceleration when advancing.

Due to the parallelogram-type mechanical structure driven by a rotational movement, it has a slight acceleration when retracting and a slight deceleration when advancing.

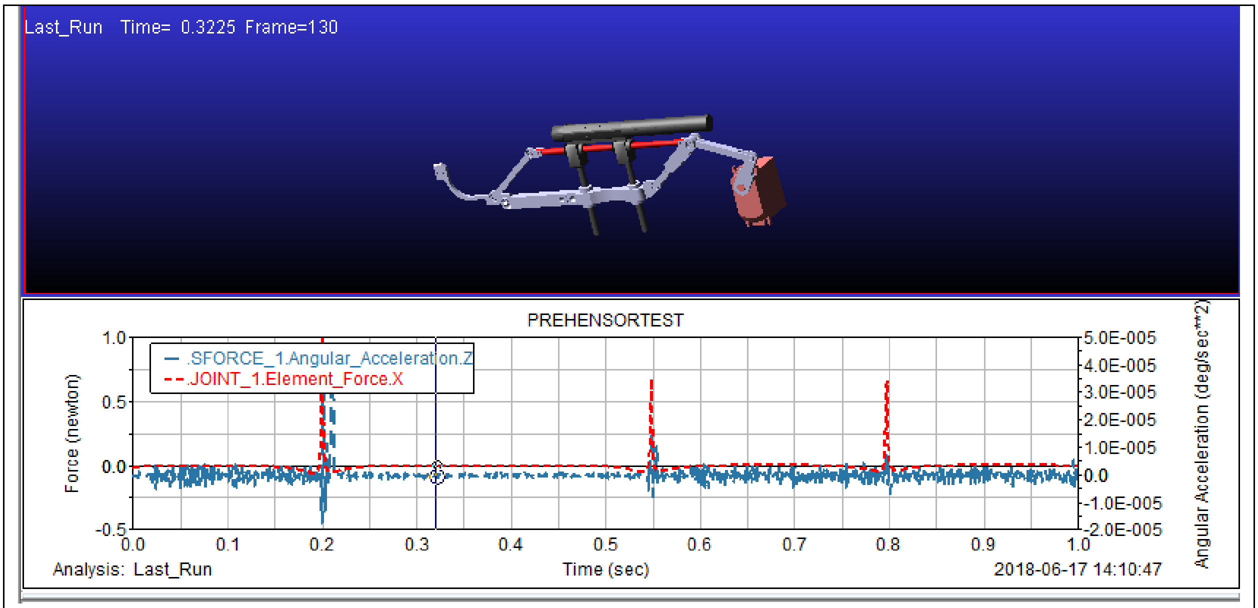


*Figure. 2.6. Graph in the Adams program*

## 2.3. Structural analysis of the module and determination of the stress state of the structure

### 2.3.1. Selection and analysis of mechanical components subject to wear

The gripper module is driven by an electric stepper motor that generates a torque of 8.2 Kg*cm, which means it exerts a force on the components of 0.911 Nm.

In Figure. 2.7 two images are represented; the first image represents the front view of an adaptive gripper module where the mechanical components that have greater wear over time due to their rotational movement are represented in red. The second image is a 2D representation of the gripper module in which the rotation couplers are represented (a red line at points A, B, C, D, E), where the components can be mechanically locked and their numbering. The mechanical component locks in coupling A, mechanical component 2 locks in coupling B, mechanical component 3 locks in coupling C, and mechanical component 4 locks in coupling D, respectively coupling E depending on the advance or retreat movement.

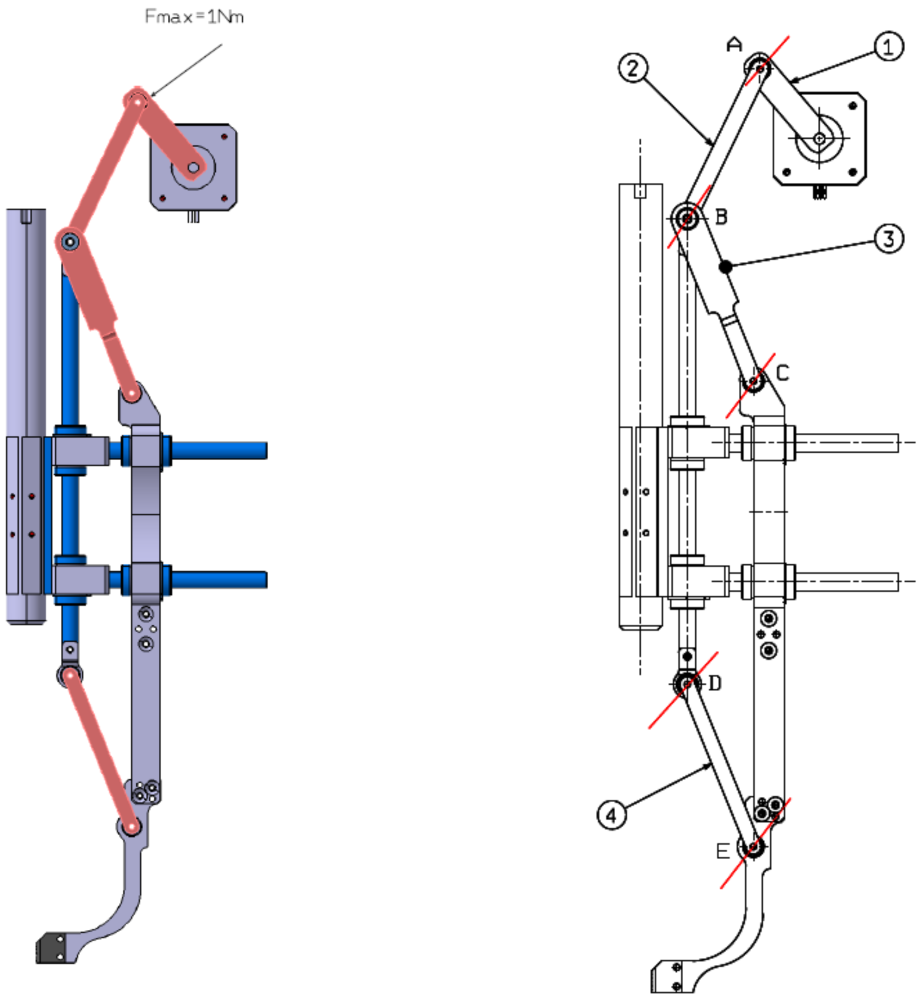


*a)* *b)*

*Figure. 2.7. Representation of rotation torques and choice of components with the greatest wear.*

#### 2.3.2. Application and decomposition of forces on mechanical components that perform rotational movements

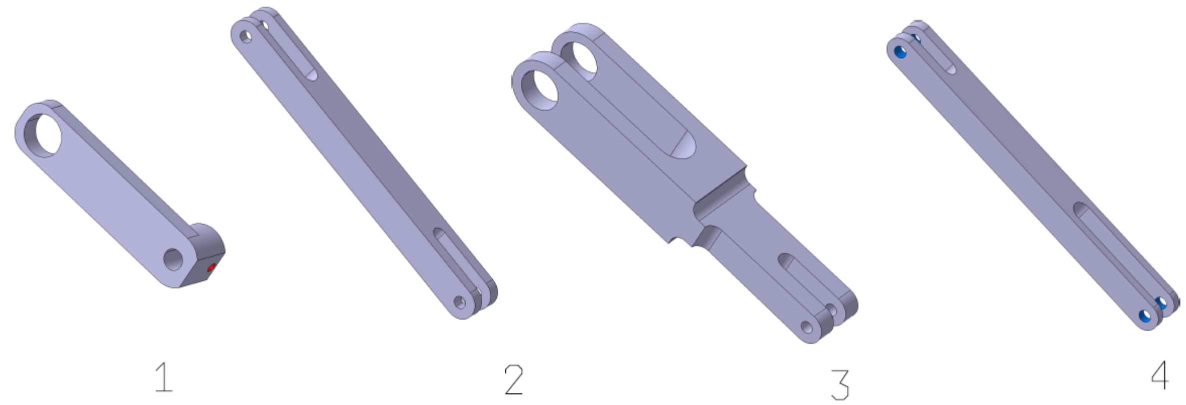


*Figure. 2.8. Representation of 3D components*

Remove components 1, 2, 3 and 4 (Fig. 2.8) separately and apply the necessary forces and constraints to simulate locking at points A, B, C, D and E.
Each component must be positioned and the applied force must apply in the sense generated by the entire module, where Fc is the composite force between the parallel force and the perpendicular force on the analyzed mechanical component. The application forces are equal and opposite, in our case, Figure. 2.9, denoted by Fr (reaction force).

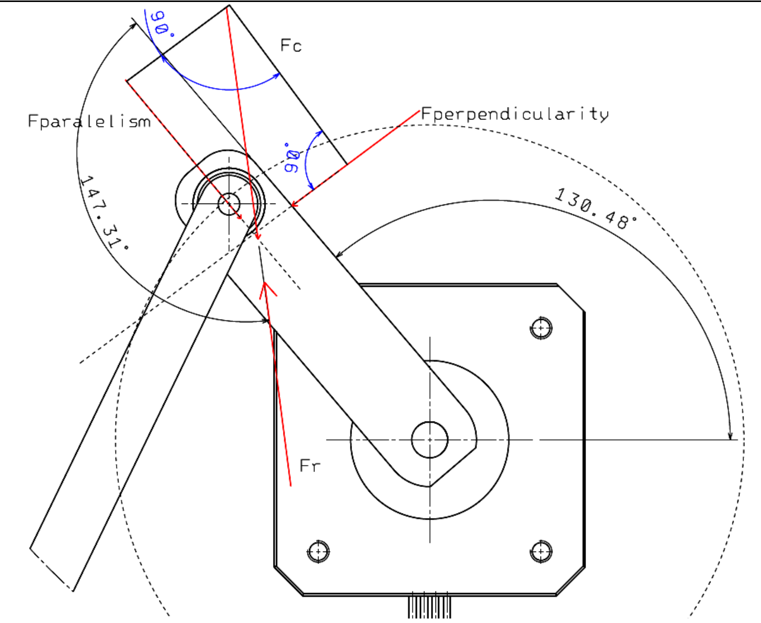


*Figure. 2.9. Example of composition of forces for mechanical component 1*

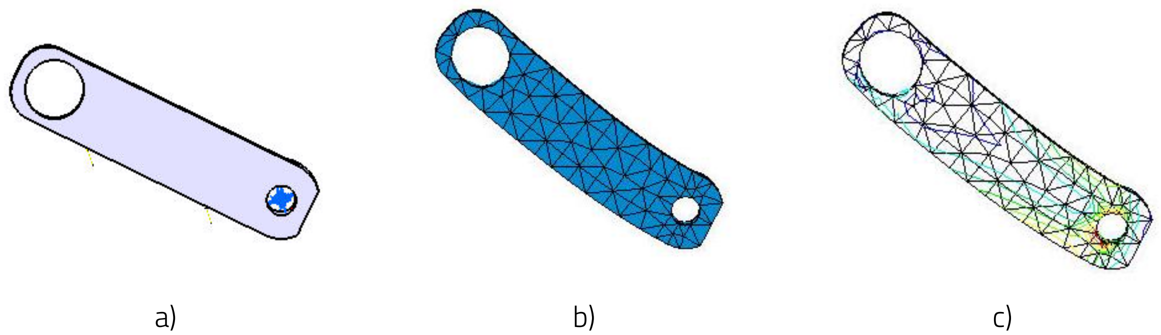


*Figure. 2.10. Stages of amplified deformations of the mechanical component 1*

Vectorial summing of the forces Fx, Fy, Fz, Mx, My and Mz generates the vector orientation of the reaction force Fr. Once the forces are applied, the finite element method can be applied to the mechanical component, where the plastic and elastic deformation can be observed (Figure. 2.10), with an amplification of 107.

a) **Generation of the stress-type parameters of the mechanical component 1**

b) Following the analysis of the stress-type finite element, an automatic report was generated from the Catia program, where you can observe the areas influenced and subject to small deformations, but also the areas where there are no deformations. The generated report is in the form of a graduated column from red to blue, where red signifies the greatest deformation, and blue the least (Figure. 2.11)[3].

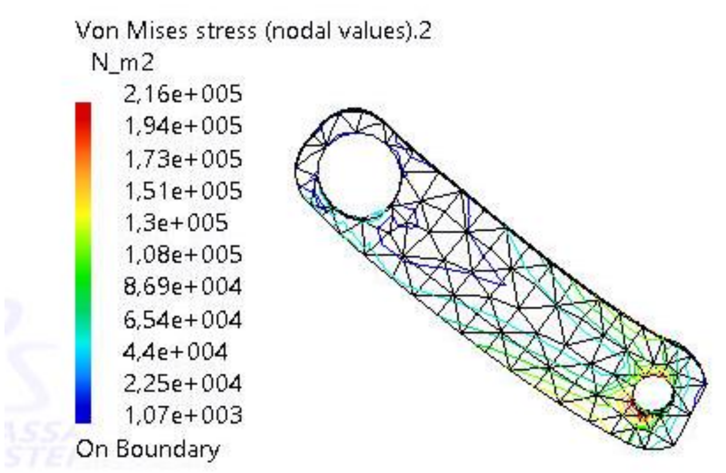


*Figure. 2.11. Finite element ratio*

To generate the position of the force Fr at an angle of approximately 147o, , it is necessary to generate the position Fr from the summation of the values of the forces Fx, Fy, Fz, Mx, My and Mz (Table 2.1).

*Table 2.1. Composition of the forces of the mechanical component 1*

| Force | Force value | Unit |
|---|---|---|
| Fx | 3*817e-012 | N |
| Fy | -1 | N |
| Fz | -1 | N |
| Mx | 2*900e-002 | N |
| My | -2*500e-003 | N |
| Mz | 2*500e-003 | N |

Respecting the conditions of mechanical component 1, the reaction force Fr is generated for the other mechanical components 2, 3 and 4.

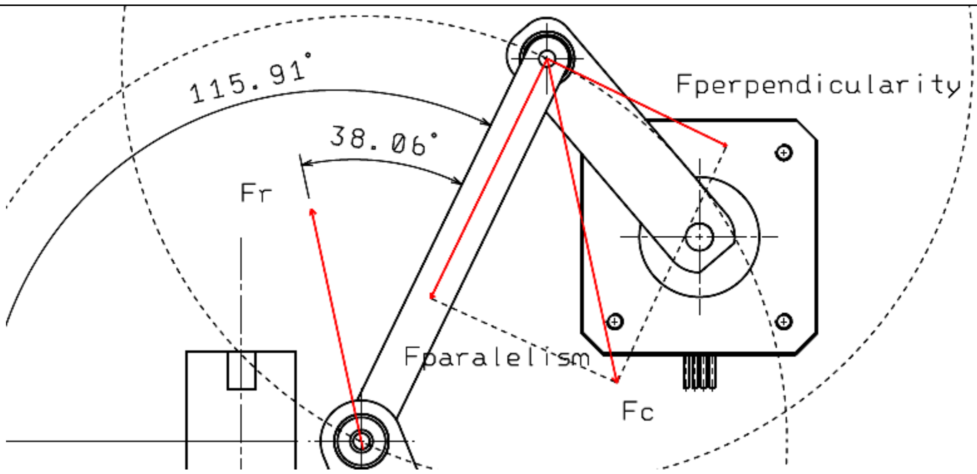


*Figure. 2.12. Composition of forces for the mechanical component 2*

### 2.3.3. Application and analysis of forces on mechanical components that perform a horizontal translation movement

The translational movement is achieved with the help of ball bushings (linear guides). With their help, the gripper module makes its translational movements easily, because they take over from the friction of the system. Over time, this system that makes the movement with the help of guides can get stuck or braking phenomena can occur due to lubrication or impurities accumulated between the balls.

When the linear guides are locked, the force exerted on the system is distributed to the mechanical components. In Figure. 2.13 a scheme with the composition of the forces was made where the force is applied at a chosen position of 30° from the horizontal to simulate the distribution of the force in the translation system.

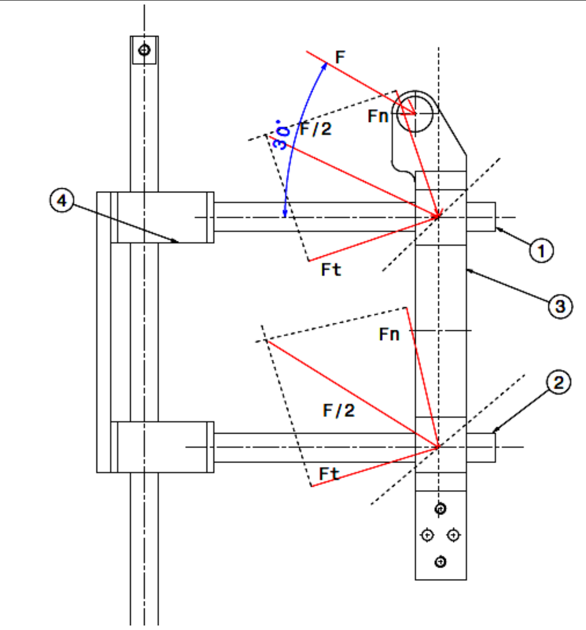


*Figure. 2.13. The composition of the forces of the translation system*

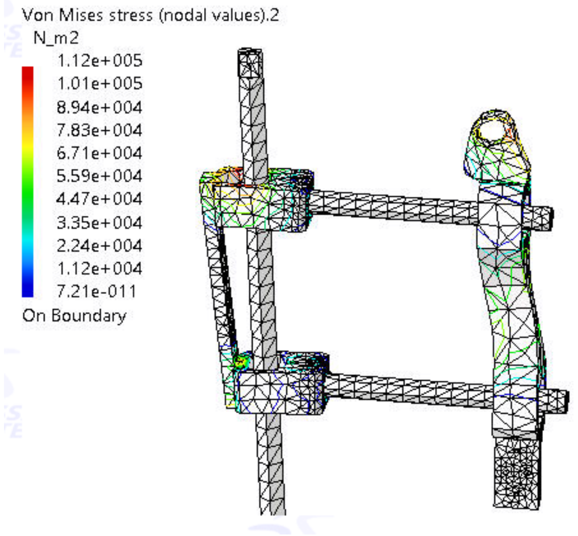


*Figure. 2.14. The ratio of resistance forces in the translation system*

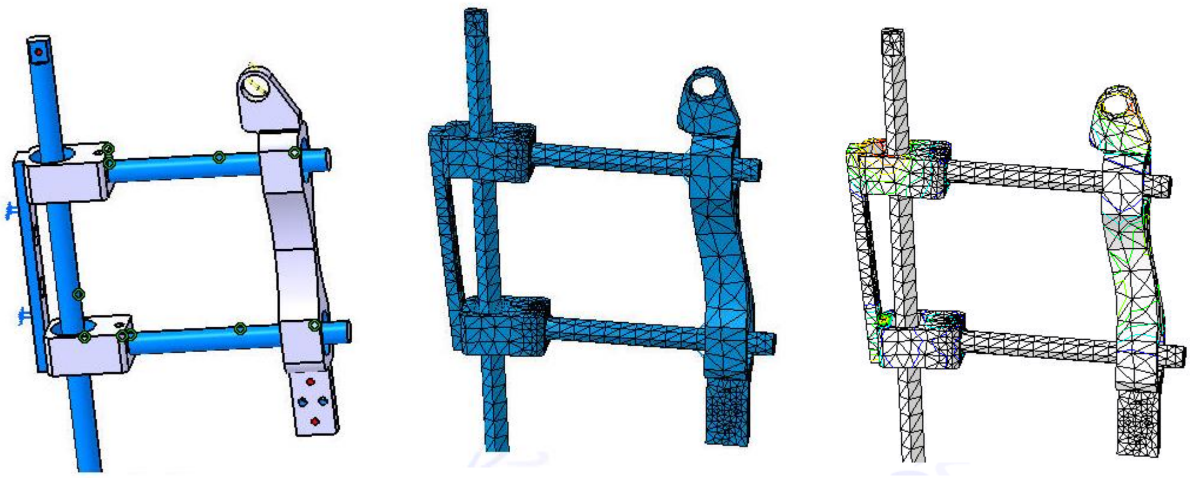

*a) b) c)*

*Figure. 2.15. The stages of deformation of the translational system*

The force (F) is applied to the mechanical component (3) which performs a translational movement with respect to the mechanical components (1), (2). At the moment of locking, the force is distributed equally in the two rods, and they in turn transmit the force to the component 4 where they are embedded.

After the locking moment, the force (F) tends to go in the direction of the normal force (Fn) because the component (3) is locked and no longer makes any movement. After the distributed force reaches the direction of the normal force, the system tends to deform downwards (Fig. 2.15).

In order to find out the resistance values of the forces Fx, Fy, Fz, Mx, My and Mz, the finite element method was applied to the system, after which a force ratio was generated (Figure 2.14) and which are completed in Table 2.2.

*Table 2.2. The value of the resistance of the forces generated on the system*

| Force | The value of force | Unit |
|---|---|---|
| Fx | -1* 037e-012 | N |
| Fy | -2 | N |
| Fz | -2 | N |
| Mx | -6* 946e-002 | N |
| My | 4* 747e-011 | N |
| Mz | -1* 533e-010 | N |

## 2.4. Conclusions

The self-adaptive gripper design with five independent fingers demonstrates high flexibility and adaptability in gripping objects of various shapes and sizes. Thanks to the plane-parallel movement and individual control of each arm, this system is able to handle irregularly shaped objects and apply the required prehension force without damaging or dropping them.

The implementation of a parallelogram-type kinematic configuration ensures the precision and flatness of the gripper movements in relation to the manipulated object and the work surface. This design is essential to achieve precise and controlled movement, especially in the context of gripping small objects, where movement errors could compromise the efficiency and accuracy of the operation.

The design of the gripper module included detailed stages of 3D modeling, kinematic simulation and structural analysis to evaluate the performance and strength of the components. The use of design and simulation software such as CATIA and Adams enabled an in-depth evaluation of the gripper's mechanical behavior, identifying areas of wear and optimizing the design to minimize friction and ensure long-term durability.

# 3. DESIGN OF THE SELF-ADAPTIVE GRIPPER

The objective proposed in this chapter was the design and implementation of a self-adaptive gripper, detailing the kinematic structure, adaptability to different shapes and weights of objects, electrical and software aspects, as well as the study of vibrations in the gripper system.

## 3.1. 3D design of the self-adaptive gripper

The kinematic structure of the self-adaptive gripper in Figure. 3.1 consists of several prehension fingers that are fixed on the same shaft.

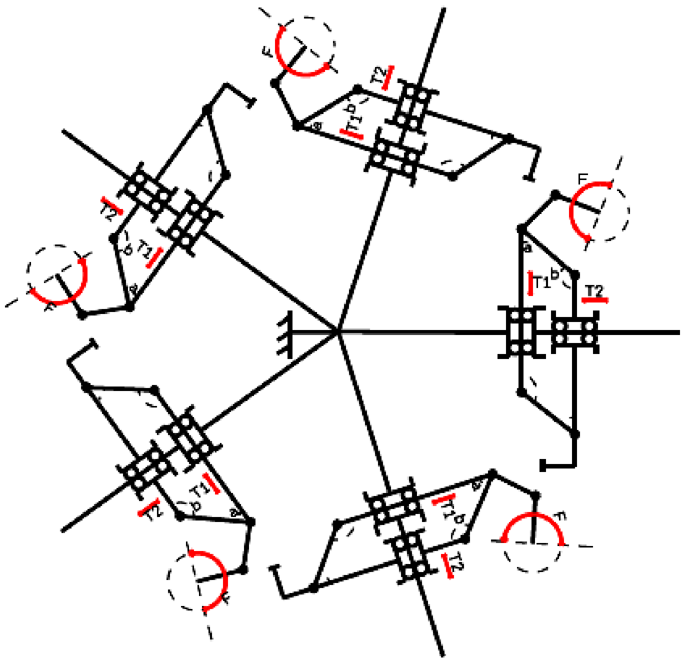


*Figure. 3.1. Kinematic diagram of the self-adaptive gripper with combined motions*

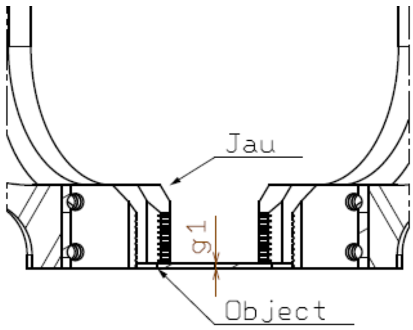


*Figure. 3.2. Detailed exemplification of a feature of the gripper*

The kinematic structure of the self-adaptive gripper demonstrates the mechanical independence of each individual module. By arranging the circular gripping elements, it covers all contact areas of the object, preventing it from moving [24].

The kinematic scheme represented in Figure. 3.1 demonstrates the mechanical particularities of a prehension system. This gripper is built with contact elements that perform the function of pins (Figure. 3.2), which take advantage of its particularity.

The gripper modules are secured to the rod (1) fixed in the bottom plate (16) by means of a clearance-free assembly with a cylindrical wedge (18) and countersunk set screw (17) secured from inside the actuator housing ( 2).

Following the implementation of the gripper modules, the gripper in the Figure was obtained. 3.3, where the marked plates are the support plates of the central rod and the modules.

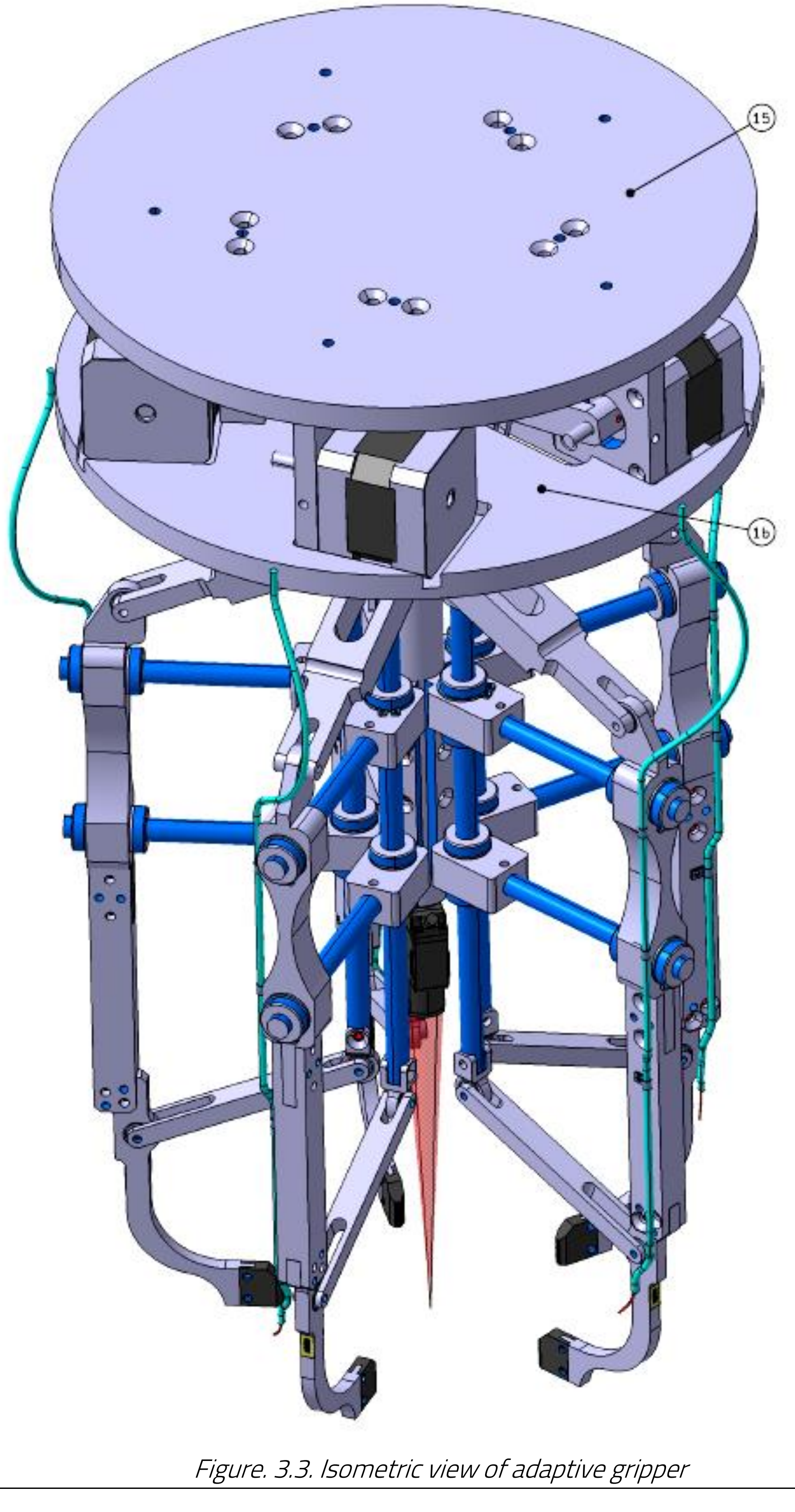


*Figure. 3.3. Isometric view of adaptive gripper*

Components or areas marked in blue are tolerated areas to ensure movements.

## 3.2. Study of the adaptability of the prehension system

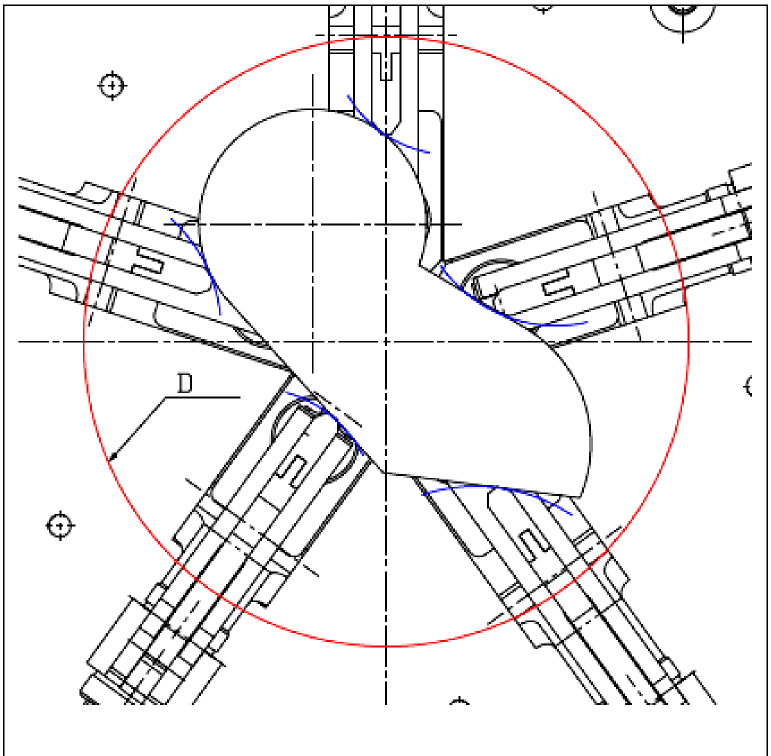


*Figura. 3.1. Adaptivitatea prehensorului*

Like any mechanical system, the structure of the self-adaptive gripper also has maximum limits for grasping objects, as can be seen in the Figure. 3.4, where it is highlighted with a red circle.

The self-adaptive grasping system has the ability to grasp objects of different sizes depending on the mechanical permittivity. This prehension system can be built in several versions with a different prehension gauge.

The larger the prehension system, the larger the active prehension area it can have. But there is also the possibility that it is dimensioned according to the weight of the objects, so that the large dimension of the gripper is the result of this.

The self-adaptive gripper can achieve effective prehension the more arms or fingers it has. By increasing the points or areas of contact with the object, the chances of it not slipping or being dropped from the docks are lower. The contact areas and the angles at which they fall with respect to the surface of the object are exemplified by a blue circle arc, according to the Figure. 3.4, where the angles of incidence between the jaws of the gripper and the object can be differentiated.

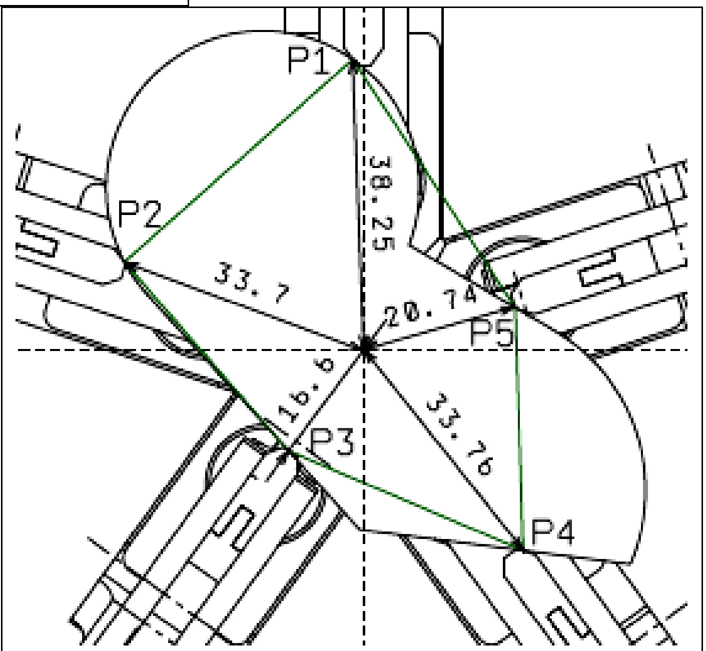


*Figura. 3.2. Deducerea geometrică a obiectelor*

Following the contacts between the jaws and the object, different geometric figures can be obtained through which we can deduce the shape of the grasped object, as shown in Figure. 3.5.

Through the angular contact of the jaws with the grasped object, it can generate moments of movement of the object in different directions. At first glance this may seem like a disadvantage, but the system can move in any direction and can also compensate for the angular difference generated during prehension.

This gripper is self-adaptive due to its particularities from a mechanical, electrical and software point of view. The three characteristics perfectly describe a mechatronic system that works simultaneously for each individual arm.Fiecare modul prehensor îşi realizează propriile sarcini şi generează la rândul lor informații legate de starea în care se află.

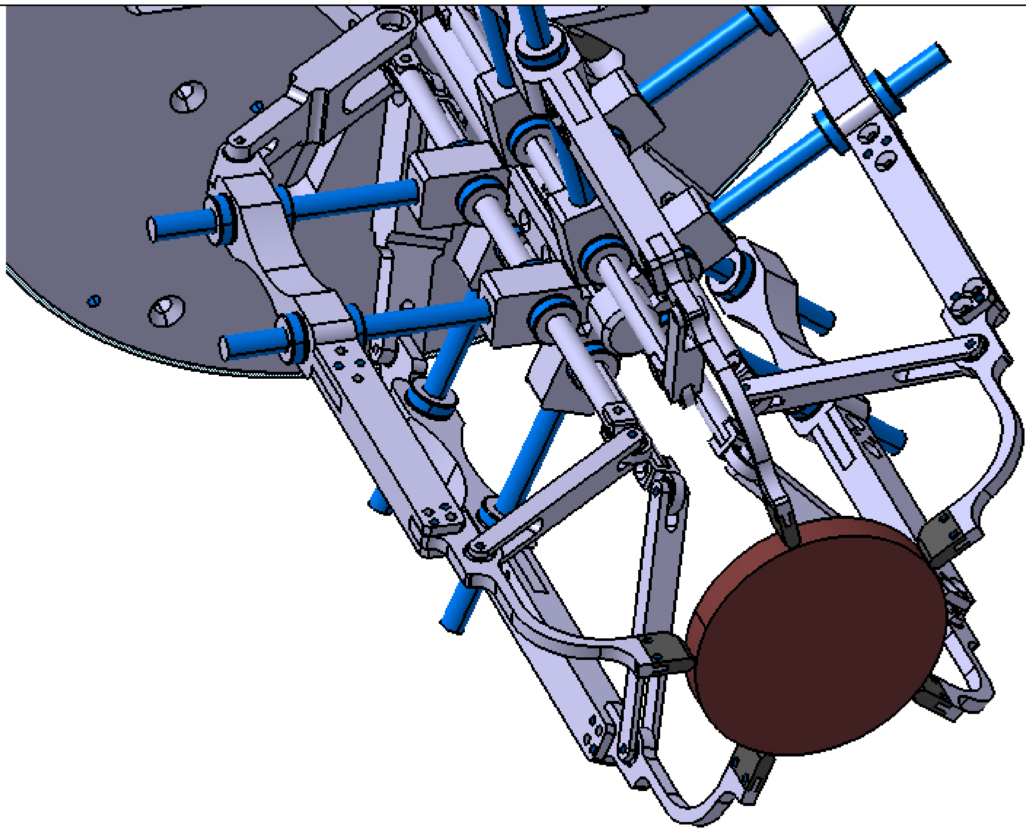

*Figure. 3.6. Adaptivity of the gripper to an object with a regular shape (bottom isometric view)*

Most grippers have the ability to grip regular objects, as seen in Figure. 3.6. The object is gripped evenly by all fingers, in the same position.

When the bins have touched the object, the actuator remains locked in its current position. To check the adaptivity, the gripper was implemented in the Kinematics Simulation module of the Catia program. The piece was declared fixed, and the states of the other pieces were set accordingly. Also, the type of couplings and the meaning of their movements were defined.

In a gripper module there is only one active coupler that generates the motion of the entire system, while the rest of the couplers are passive and are influenced by the first kinematic coupler [14].

To demonstrate adaptivity, simulations were also carried out on objects with an irregular shape, where the independent movements of each gripper module can be observed (Figure. 3.7 and Figure. 3.8).

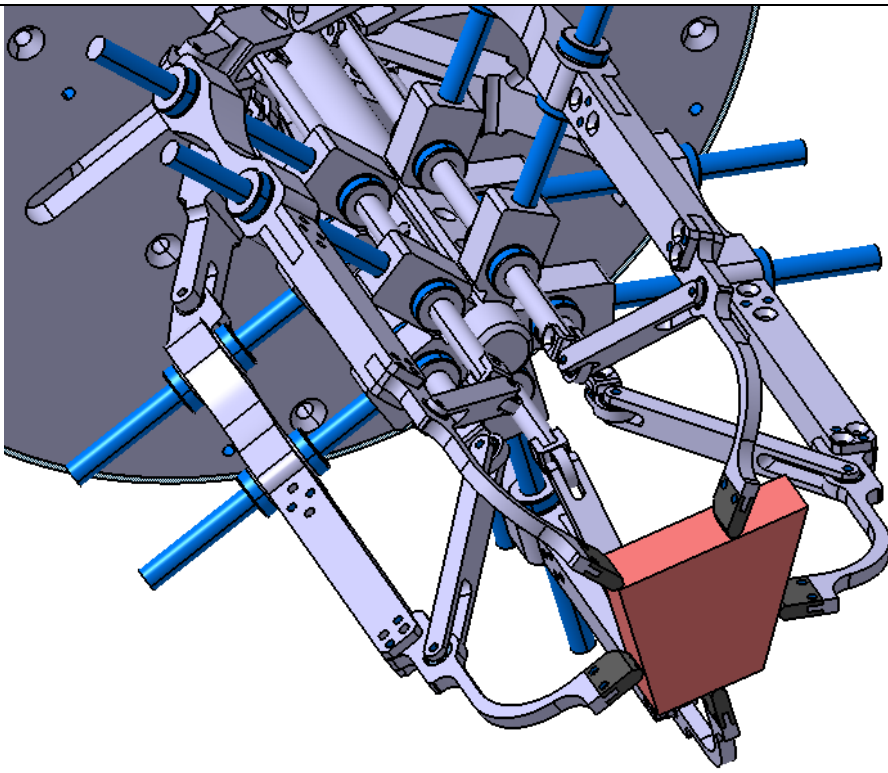

*Figure. 3.7. Gripper adaptivity for an irregularly shaped object*

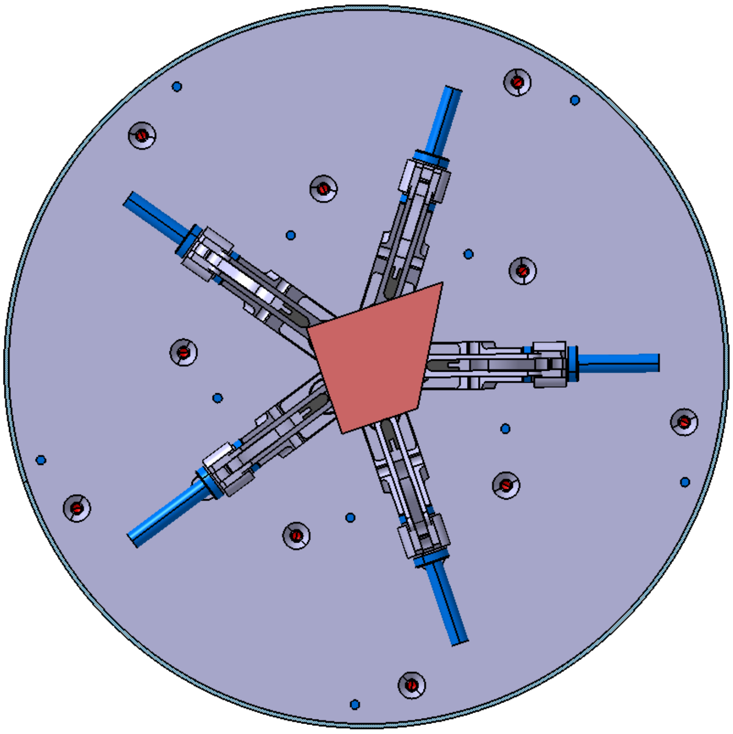

*Figure. 3.8. Bottom view of the gripper for an irregularly shaped object*

Following the simulation in Kinematics, the angular differences of each gripper module during prehension are observed. Different angular values demonstrate that the shape of the object is irregular (

To check the adaptivity of the gripper, a simulation was carried out on an object with a shape that is difficult to grasp (Figure 3.9)

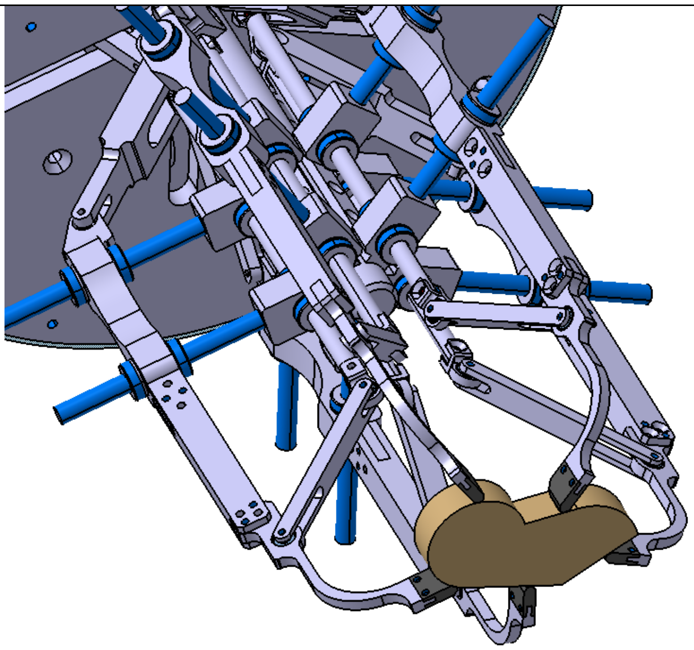

*Figure. 3.9. Adaptivity of the gripper for an irregularly shaped, hard-to-grasp object*

Following the simulation in Kinematics, the angular differences of each gripper module during prehension are observed. Different angular values demonstrate that the shape of the object is irregular

## 3.3. Constructive realization of the gripper

Following the assembly of the modules, several problems of non-respect of dimensions or tolerances were discovered. Failure to comply with the conditions imposed on the drawings resulted in gripper modules being seized in the translation areas. The physically realized gripper is represented in the Figure. 3.10.

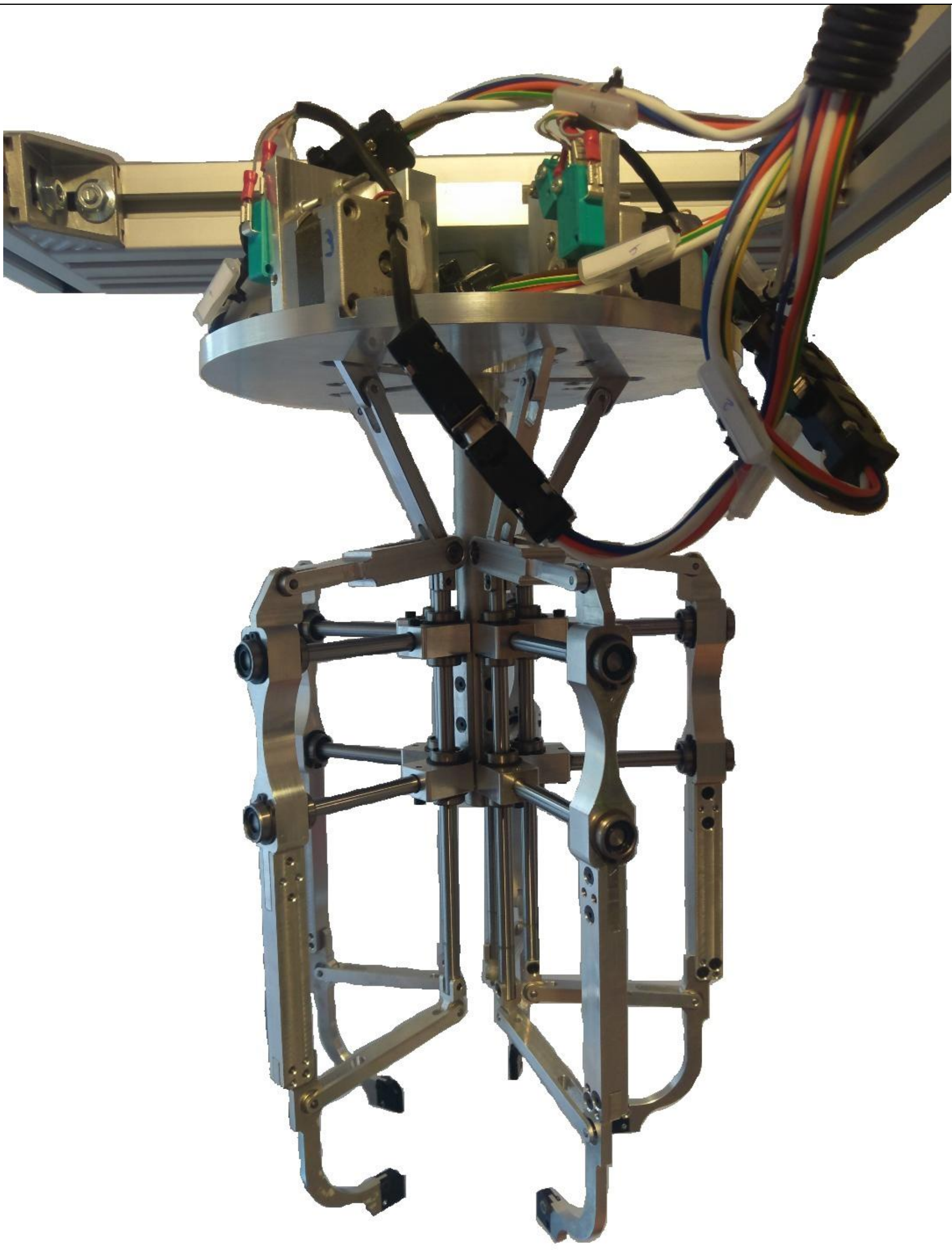

*Figure. 3.10. The practical realization of the adaptive gripper*

### 3.4. Realization and implementation of software in order to test the modules

```
#include <Stepper.h>
const int stepsPerRevolution = 150;
```

```
include <Stepper.h>
const int stepsPerRevolution = 150;
Stepper myStepper1(stepsPerRevolution, 22, 24, 26, 28);
Stepper myStepper2(stepsPerRevolution, 30, 32, 34, 36);
Stepper myStepper3(stepsPerRevolution, 38, 40, 42, 44);
Stepper myStepper4(stepsPerRevolution, 46, 48, 50, 52);
Stepper myStepper5(stepsPerRevolution, 23, 25, 27, 29);
```

*Figure. 3.11. Listing 1: Declaring the PWM control ports of the L298N type drivers*

```
int state = 0;
const int buttonPin1 = 2;
const int buttonPin2 = 3;
int buttonState1 = 0;
int buttonState2 = 0;

const int buttonPin19 = 19;
const int buttonPin18 = 18;
int buttonState19 = 0;
int buttonState18 = 0;

const int buttonPin17 = 17;
const int buttonPin16 = 16;
int buttonState17 = 0;
int buttonState16 = 0;

const int buttonPin15 = 15;
const int buttonPin14 = 14;
int buttonState15 = 0;
int buttonState14 = 0;

const int buttonPin21 = 21;
const int buttonPin20 = 20;
int buttonState21 = 0;
int buttonState20 = 0;

void setup()
{
Serial.begin(9400);
pinMode(buttonPin1, INPUT);
pinMode(buttonPin2, INPUT);

pinMode(buttonPin19, INPUT);
pinMode(buttonPin18, INPUT);

pinMode(buttonPin17, INPUT);
pinMode(buttonPin16, INPUT);

pinMode(buttonPin15, INPUT);
pinMode(buttonPin14, INPUT);

pinMode(buttonPin21, INPUT);
pinMode(buttonPin20, INPUT);
```

*Figure. 3.12. Listing 2: Declaring the travel limit sensors for each module*

```
if(Serial.available() > 0)
 { // Checks whether data is comming from the serial port
  state = Serial.read(); // Reads the data from the serial port   [21]
 }
buttonState1 = digitalRead(buttonPin1);
buttonState2 = digitalRead(buttonPin2);

buttonState19 = digitalRead(buttonPin19);
buttonState18 = digitalRead(buttonPin18);

buttonState17 = digitalRead(buttonPin17);
buttonState16 = digitalRead(buttonPin16);

buttonState15 = digitalRead(buttonPin15);
buttonState14 = digitalRead(buttonPin14);

buttonState21 = digitalRead(buttonPin21);
buttonState20 = digitalRead(buttonPin20);

    if ((state == 'j')&&(buttonState1 == HIGH)&&(buttonState2 == LOW))
          {
           myStepper1.setSpeed(300);
           myStepper1.step(-850);
            Serial.println("Brat 5 retras ");
          }

     if ((state == 'i')&&(buttonState1 == LOW)&&(buttonState2 == HIGH))
          {
           myStepper1.setSpeed(300);
           myStepper1.step(850);
            Serial.println("Brat 5 avans");
          }


       if ((state == 'c')&&(buttonState19 == LOW)&&(buttonState18 == HIGH))
          {
           myStepper2.setSpeed(300);
           myStepper2.step(-850);
            Serial.println("Brat 2 retras ");
          }
```

*Figure. 3.13. Listing 3: Declaring the commands for each module, each stepper motor is conditioned by the travel limiters and the drive command*

## 3.5. **Vibration study of coaxially driven modules**

The grasping process is determined by the degree of slippage of the grasped object. A considerable effect that can influence the degree of sliding is generated by the vibrations in the prehension system [25].

The vibration is generated by the moving elements during prehension. The amplitude of the vibrations is amplified by the number of moving parts moving at the same time [26].

According to the kinematic scheme in Figure. 3.14, the motor is positioned at point A, and for this type of coaxial drive, the gripper module generates vibration during movement and through the stepper motor step which is 1.6 .

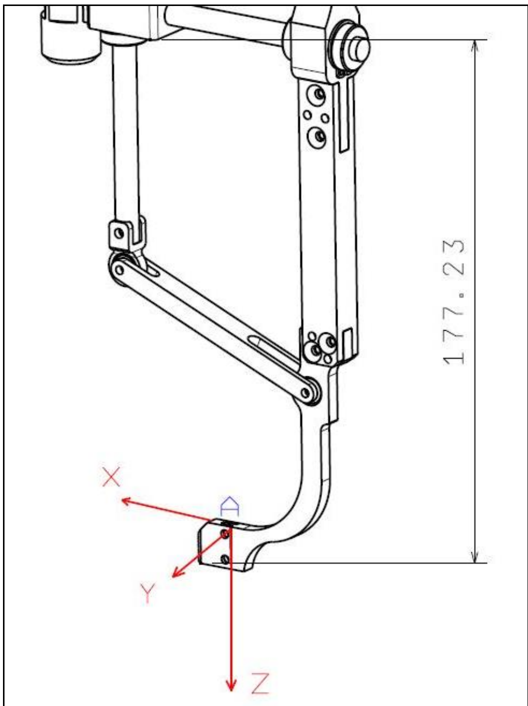


*Figure. 3.14. Placement and targeting of vibration sensors*

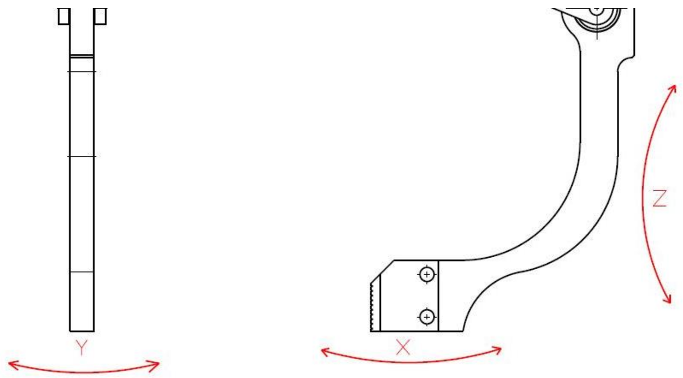


*Figure. 3.15. Directing vibrations on the 3 axes*

To determine the vibrations of a gripper module, SW-18010P type vibration sensors were placed in the x, y, z directions (Figure 3.14). This type of sensor can be used in various applications where vibration affects functionality.

The two sensor contacts are not connected in idle state. When the external force acts either on the movement of the gripper module or on the vibration generated by any other external generator, the two contact pins of the sensor are closed and open. When the force is removed, the sensor terminals return to open contacts [27], [28].

In Figure. 3.15 the vibration orientation of a gripper module is exemplified. The vibration sensor is located at the farthest point from a fixed point, which is 177 mm away. For each orientation of the sensor it is exemplified which vibration direction x, y, z is measured.

### 3.5.1. The vibrations obtained during the movement of the modules

*Table 3.1. Values obtained when measuring module movement*

| **Module 1 [Hz]** | | |
|---|---|---|
| **x** | **y** | **z** |
| 0 | 0 | 97 |
| 0 | 0 | 0 |
| 5503 | 0 | 478 |
| 7156 | 214456 | 549 |
| 139435 | 97289 | 259 |
| 68474 | 13610 | 7167 |
| 25117 | 1350 | 269 |
| 1445 | 3309 | 52226 |

In order to determine the vibrations of a gripper module as correctly as possible, it was necessary to measure each module separately. Through the particular testing of the module, the noises that can influence the measurements have been eliminated [29], [30].

Table 3.1 shows some of the input values determined by the vibration sensors during several forward and backward movements. This simulation was carried out in free movement of the gripper arms without it encountering an obstacle [31], [32].

The table shows some maximum values that were detected by the sensors during the movement.

| | | |
|---|---|---|
| 9271 | 11 | 58 |
| 0 | 14075 | 22569 |
| 53711 | 1588 | 19690 |
| 520 | 14990 | 26852 |
| 6352 | 5188 | 12879 |
| 354 | 24106 | 46558 |
| 350 | 6009 | 39535 |
| 186 | 1122 | 166 |
| 137 | 78 | 1226 |
| 1143 | 70 | 22935 |
| 352 | 1302 | 0 |
| 74 | 1096 | 3195 |
| 1076 | 1169 | 372 |
| 266 | 18148 | 125 |
| 36132 | 30709 | 300 |
| 345544 | 335426 | 950 |
| 42976 | 4843 | 2459 |
| 22356 | 52460 | 5054 |
| 33796 | 426 | 89 |
| 36684 | 79 | 36 |
| 2133 | 62 | 1420 |

### 3.5.2. Graphical representation and interpretation of data

According to the input data from the vibration sensors for all modules, a graph was made for each, showing the amplitude per cycle of advance/retraction by the gripper module as a function of time [33].

The forward and backward travel together achieves 102mm of travel. Vibration measurement in the 3 x, y, z directions was done independently to highlight the differences in vibrations.

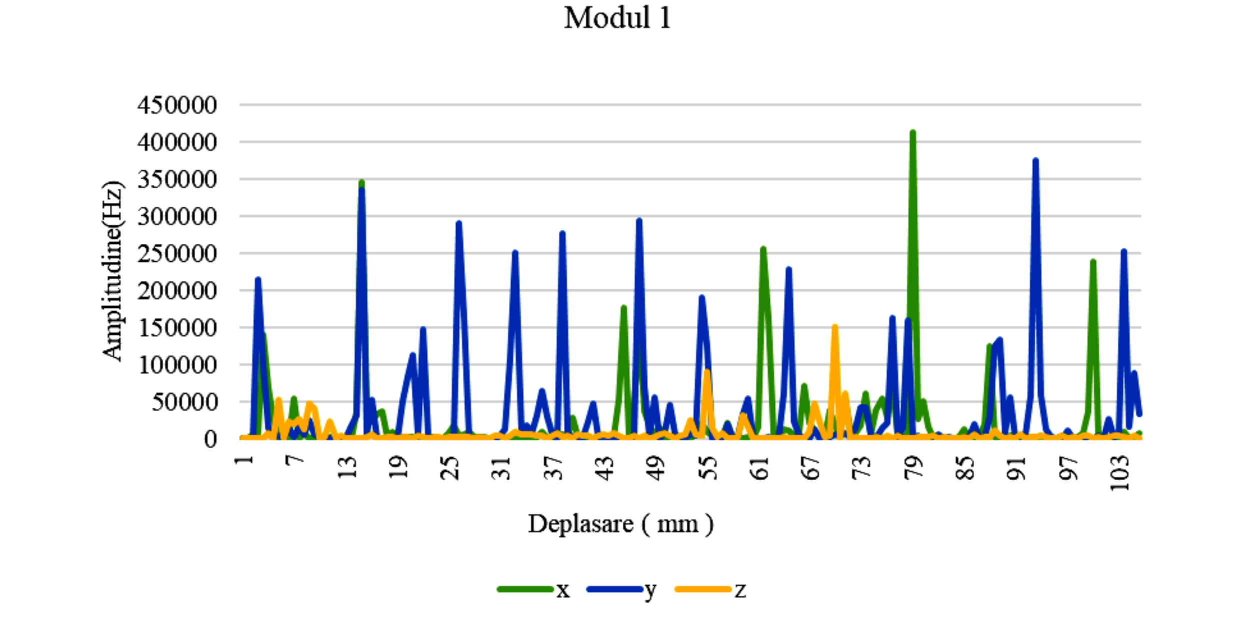


*Figure. 3.16. Amplitude measurement for module 1*

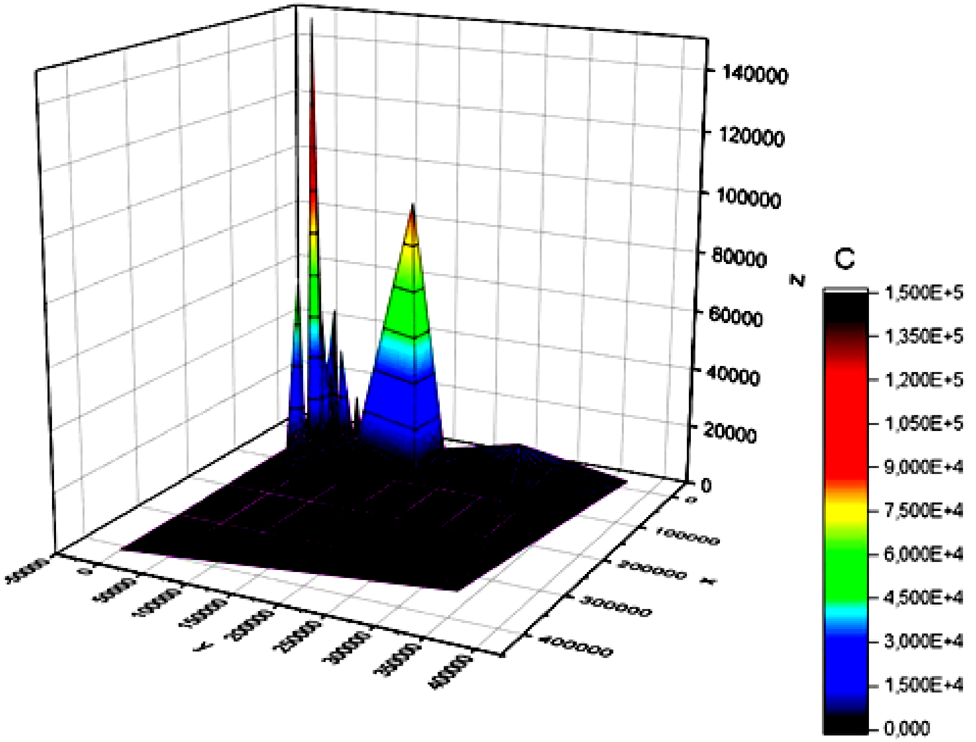


*Figure. 3.17. 3D graphical representation of the amplitude, for module 1*

Following the measured values for module 1, the graph in the Figure was created. 3.16, where the amplitude is represented over a displacement of 102 mm in one unit of time.

According to the data, it is observed that the displacement of the module generates large vibrations, exceeding the nominal values (0-1000), so the maximum value at point 131 reaches the value of 413593 in the X direction, followed by point 155 with the value of 375741 in the Y direction.

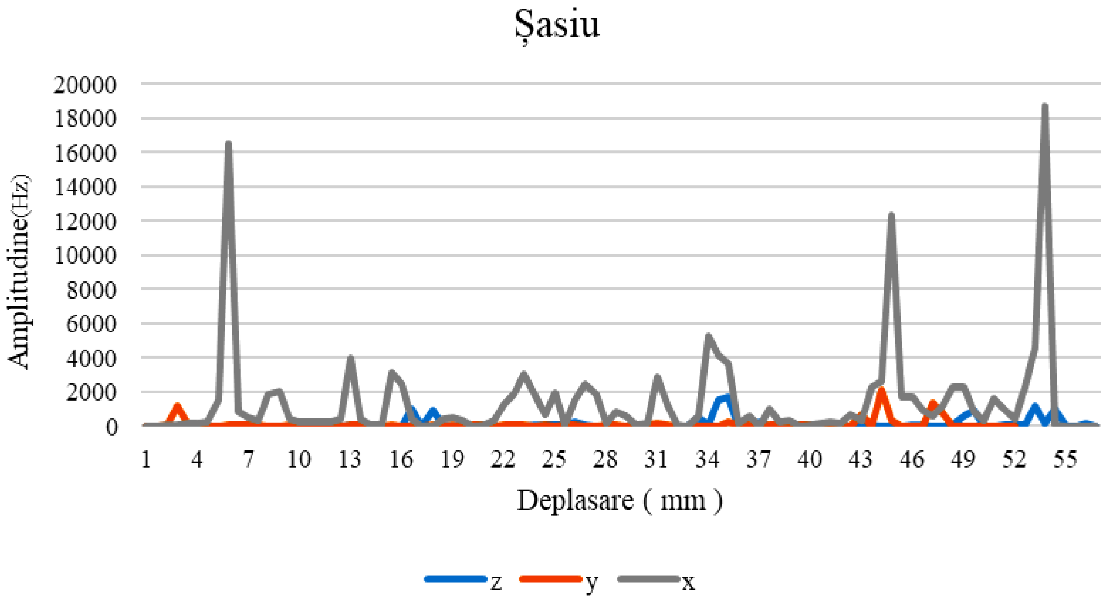


*Figure. 3.18. Amplitude measurement for gripper chassis arm*

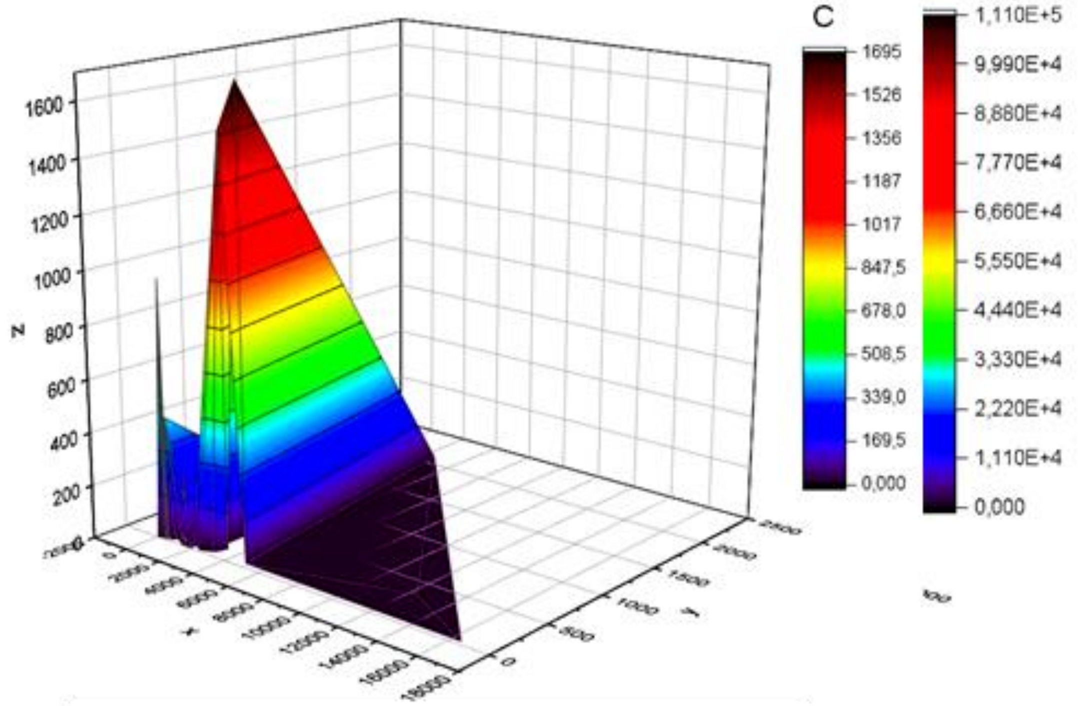


*Figure. 3.19. Amplitude of vibrations in the gripper chassis*

For the chassis, the Figura graphic was made. 3.18, where the amplitude over a 102 mm displacement of all arms, operated alternately and simultaneously, is represented.

According to the data it is observed that the movement of the arms generates high vibrations, exceeding the nominal values (0-500), where the maximum value in point 89 reaches the value of 18736 in the X direction, followed by point 73 with the value of 2103 in the Y direction and point 57 with the value 1541 in the Z direction.

As can be seen, the vibrations transmitted in the chassis have much lower values because it is close to the frame mounting area.

## 3.6. Conclusion

Following the measured values and analysis of the mechanical structure, very high vibration data was recorded. The measured vibrations with a very high amplitude are caused by the mechanical shocks generated by the gripper modules when advancing and retracting.

By rotating the stepper motor shaft, the system cannot control the stopping of these modules, nor can it brake them when the limit switch is detected, so they generate shocks in the system by hitting the central shaft.

The self-adaptive gripper is designed to ensure an efficient prehension of objects by using the prehension fingers fixed on the same axis. This design allows for mechanical adaptability and the ability to grasp objects of various shapes and sizes.

The study of the adaptivity of the system highlighted its ability to grasp both regular and irregular objects. Simulations in the Catia program demonstrated that the gripper can adjust movements and angles to adapt to varying object shapes, ensuring safe and effective prehension.

The implementation of the electrical and software system involved the use of specific components such as motor drivers, ATmega2056 controller, Bluetooth modules, etc. These components are crucial to the precise control of movements and to ensure correct and safe operation of the gripper.

Vibrations during prehension were investigated using SW-18010P sensors on three different axes (x, y, z). The results showed that the movements of the gripper arms generate significant vibrations, and their analysis is essential to optimize performance and reduce possible object slippage.

The self-adaptive gripper demonstrates robust operation and adaptability to various gripping conditions. However, to improve performance in terms of vibration reduction and motion optimization, continuous design improvements and the implementation of advanced control and monitoring strategies are required.

# 4. MODIFICATION AND STRUCTURAL IMPLEMENTATION OF THE GRIPPER MODULE FOLLOWING THE CONCLUSIONS

The objective proposed in this chapter was to improve the performance of the gripper by adapting the mechanical structure, reducing vibrations and optimizing the actuation with the help of a reducer, to ensure a precise and trouble-free handling of the objects.

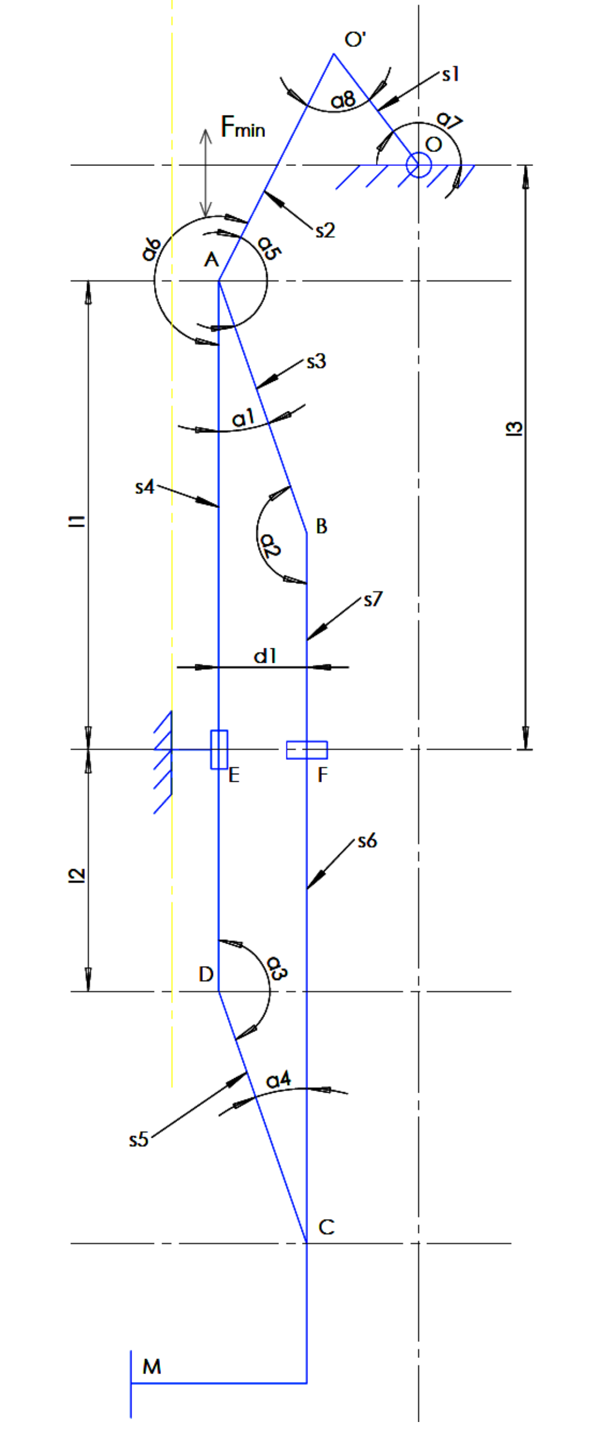


*Figure. 4.1. Initial kinematic scheme [1]*

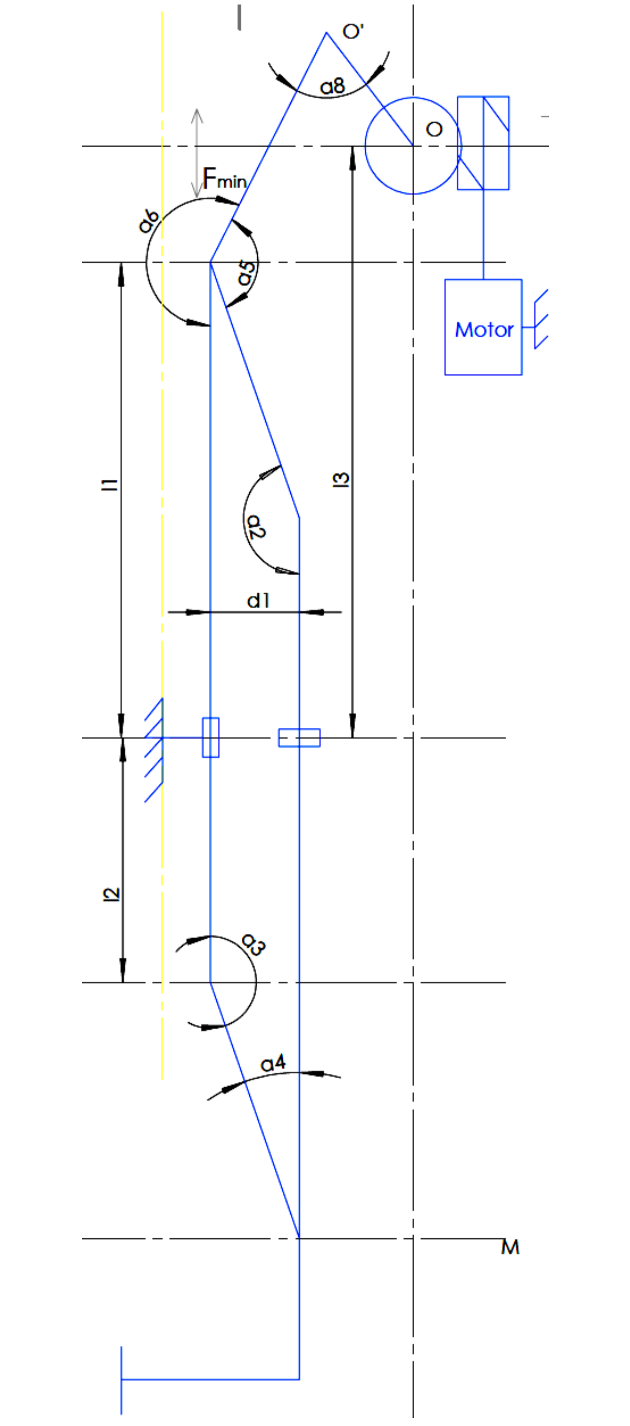


*Figure. 4.2. Updated kinematics*

## 4.1. Modification of the kinematic scheme

Following the vibration analyses, the initial mechanical structure was adapted (Figure 4.1) and an updated kinematic scheme was generated, according to the Figure. 4.2.

In the initial mechanical system, the gripper module is driven by a direct stepper motor, and the angular movement is made directly on the axis, point A in the Figure. 4.1 and Figure. 4.2. By turning the motor shaft step by step, the chain of angles is changed, generating the translational movement that changes the distance (d3).

Regardless of the drive system, the mobile system of the gripper module achieves a slightly accelerated movement. At the start of the grip for an angle reduced by 1.8o, the gripper jaw moves 0.5 mm, and at the end of travel for an angle of 1.8o, the jaw moves 3.8 mm.

In the case of the first actuation variant of the gripper module, at the end of the stroke making a greater displacement than the initial one (being driven directly by the motor shaft), it does not have enough braking space and generates a shock with the main shaft.

For this type of actuation, a table has been generated that exemplifies the displacement of the bar relative to the axis depending on the angle.

The stepper motor exerts a traction force of 39.97 Kg*m, which means it develops a torque of 3.92 Nm.

On the new mechanical structure, where the reducer was implemented, advantages in terms of torque and precision are obtained by eliminating the shocks generated by the old system.

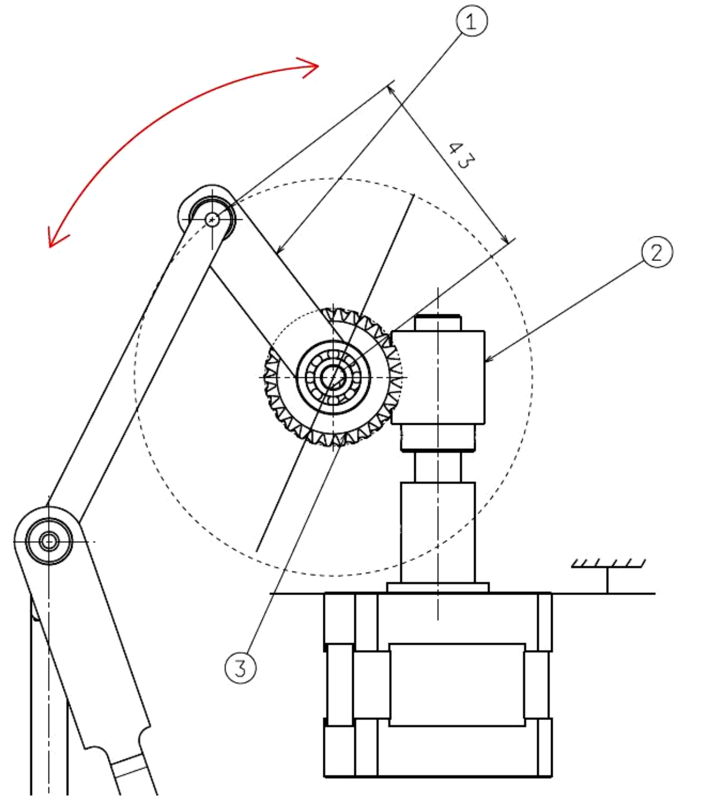


*Figure. 4.3. Actuation of the module through the reducer.*

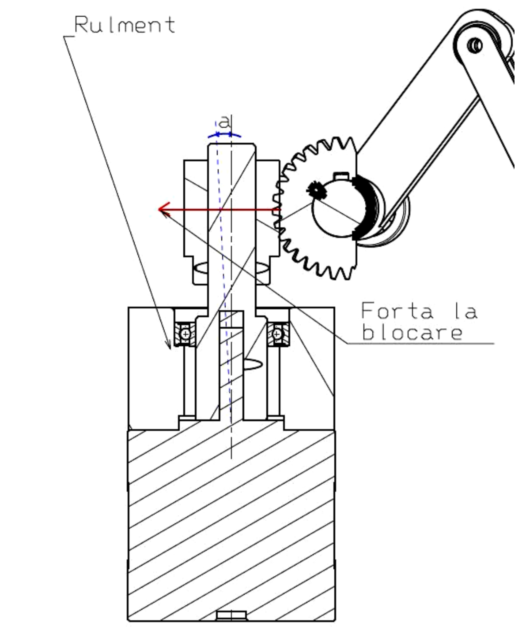


*Figure. 4.4. Section through engine and gear*

In the current drive system, the motor transmits the rotational motion to the worm gear (2), amplifying the torque and in turn transmitting the motion to a gear (3) with a module of 1.25.

On the gear wheel is the axis that generates the rotation movement and prints it in the arm (1).

The ratio is amplified R= 30:1, which means that: $F = F_m \cdot R;$ (4.1)

This system solves the vibration problem due to the fact that for the angle of 61.2º the stepper motor no longer makes the number of 35 steps.

A full rotation of the stepper motor is performed with a number of 200 steps, thus resulting in the fact that the tolerance of the system in 35 steps is very large.

Considering that 35 steps are required to achieve the angle of 61.2º, it follows that by implementing the reducer 833 steps are required, therefore the motor makes 3,675 complete revolutions.

Through the reduction system, the acceleration generated by the levers of the gripper module as well as its sensitivity can be easily controlled, regardless of the engine speed declared in the program. The angular step of the stepper motor is 1.8º, becoming at the output of the reduction a step of 0.06º, which leads to the increase of the precision of the system.Calculul matematic în vederea diminuării raportului de transmitere

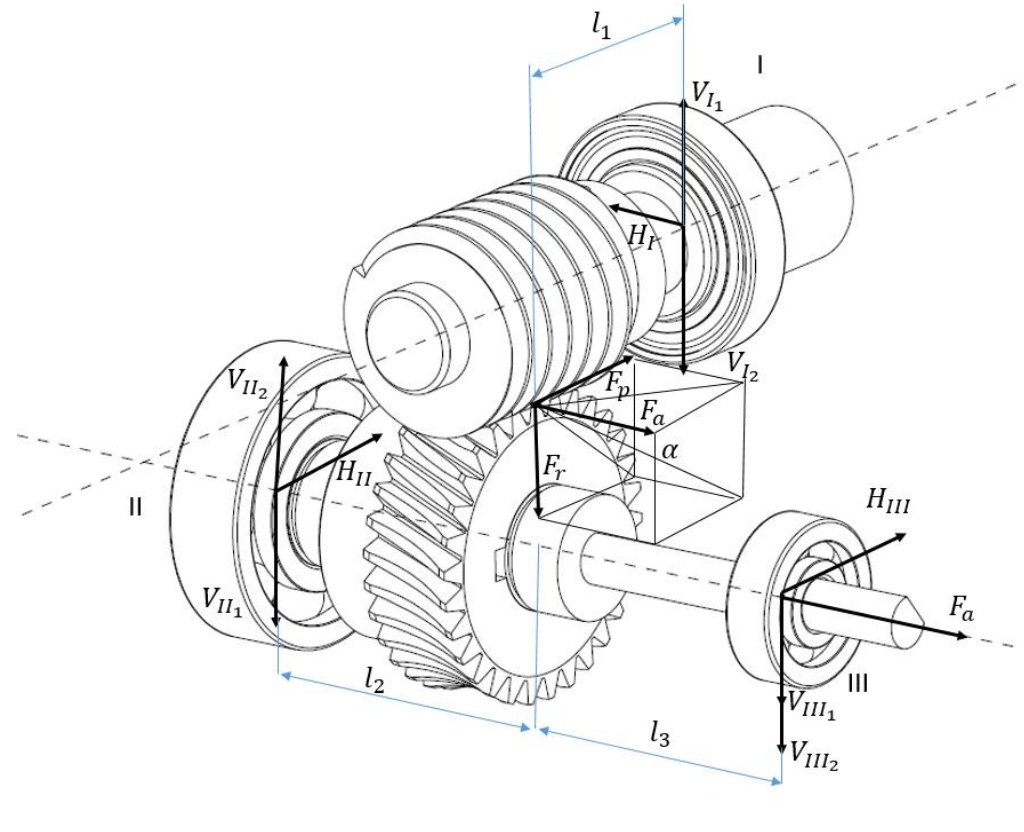


*Figure. 4.5. Forces in worm gear - worm gear*

Peripheral force $F_a$ for the snail is determined like the force $F_p$ for a spur gear:

$$F_a = \frac{2M_{t_{c1}}}{d_{r1}}. \tag{4.2}$$

Coefficient of friction for steel-bronze material couple, $\mu = 0{,}002 \div 0{,}03$

Axial force, $F_a$, is taken up by a single bearing at the worm shaft $F_{a1} = F_p$, for the gear shaft $F_{a_{II}} = F_p$ sau $F_{a_{III}} = F_p$.

$$F_r = F_a \cdot \frac{\sin\alpha}{\cos\alpha \cdot \sin\beta + \mu \cdot \cos\beta}. \tag{4.3}$$

$$F_p = F_a \cdot \frac{\cos\alpha \cdot \cos\beta - \mu \cdot \beta \cdot \sin\beta}{\cos\alpha \cdot \sin\beta + \mu \cdot \cos\beta}. \tag{4.4}$$

$$tg\beta = \frac{P_e}{2\pi \cdot r_{r1}} = \frac{S \cdot P_a}{2\pi \cdot r_{r1}}. \tag{4.5}$$

*Table 4.1. Reactions of forces in camps I, II, III*

| **Bearing I** | **Bearing II** | **Bearing III** |
|---|---|---|
| | Reactions due to force $F_a$: | |
| $H_I = F_a \frac{1}{l_1}$ | $H_{II} = F_a \frac{r_{r2}}{l_2 + l_3}$ | $H_{III} = F_a \frac{r_{r_2}}{l_2 + l_3}$ |
| | Reactions due to force $F_r$: | |
| $V_{I_1} = F_r \frac{1}{l_1}$ | $V_{II_1} = F_r \frac{1_3}{l_2 + l_3}$ | $V_{III_1} = F_r \frac{1_2}{l_2 + l_3}$ |
| | Reactions due to force $F_p$: | |
| $V_{I_2} = F_p \frac{r_{r1}}{l_1}$ | $V_{II_2} = F_p \frac{r_3}{l_2 + l_3}$ | $V_{III_2} = F_p \frac{l_2}{l_2 + l_3}$ |
| | The resultant load: | |
| $F_{r_I} = \sqrt{H_I^2 + (V_{I_2} - V_{I_1})^2}$ | $F_{r_{II}} = \sqrt{H_{II}^2 + (V_{II_1} - V_{II_2})^2}$ | $F_{r_{III}} = \sqrt{H_{III}^2 + (V_{III_1} - V_{III_2})^2}$ |

## 4.2. Analysis of the vibrations exerted on the modules after modifications

For module 1, the graph in the Figure was created. 4.6 following the changes, where the vibration amplitude is represented over a displacement of 176 mm.

According to the data, it is observed that the displacement of the module generates low-medium vibrations, exceeding the nominal values (0-1000), where the maximum value at point 119 reaches the value of 46415 in the X direction, followed by point 40 with the value of 25623 in the Y direction and point 112 with the value 19343 in the Z direction.

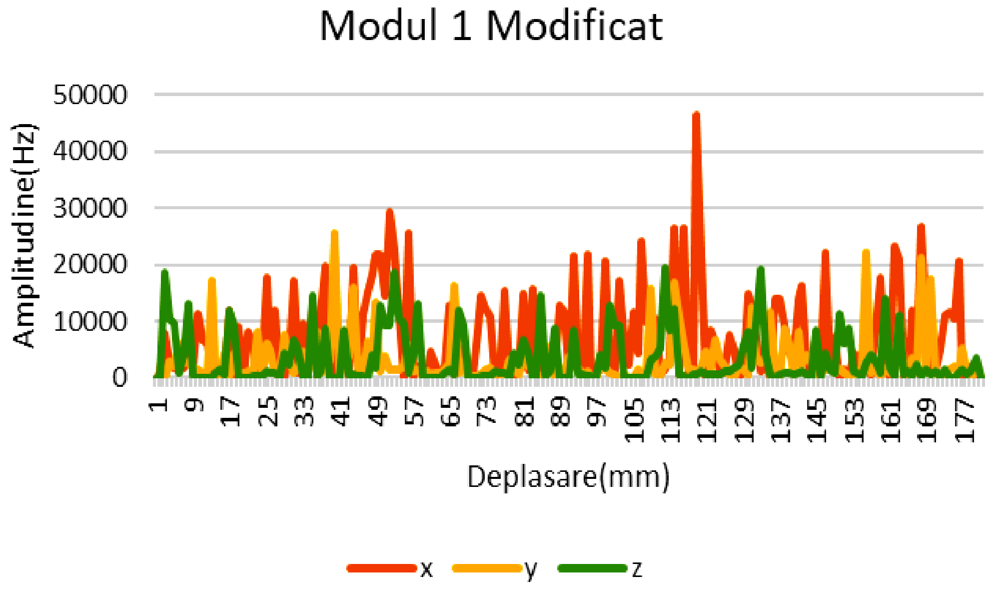


*Figure. 4.6. Amplitude measurement for module 1, following modifications*

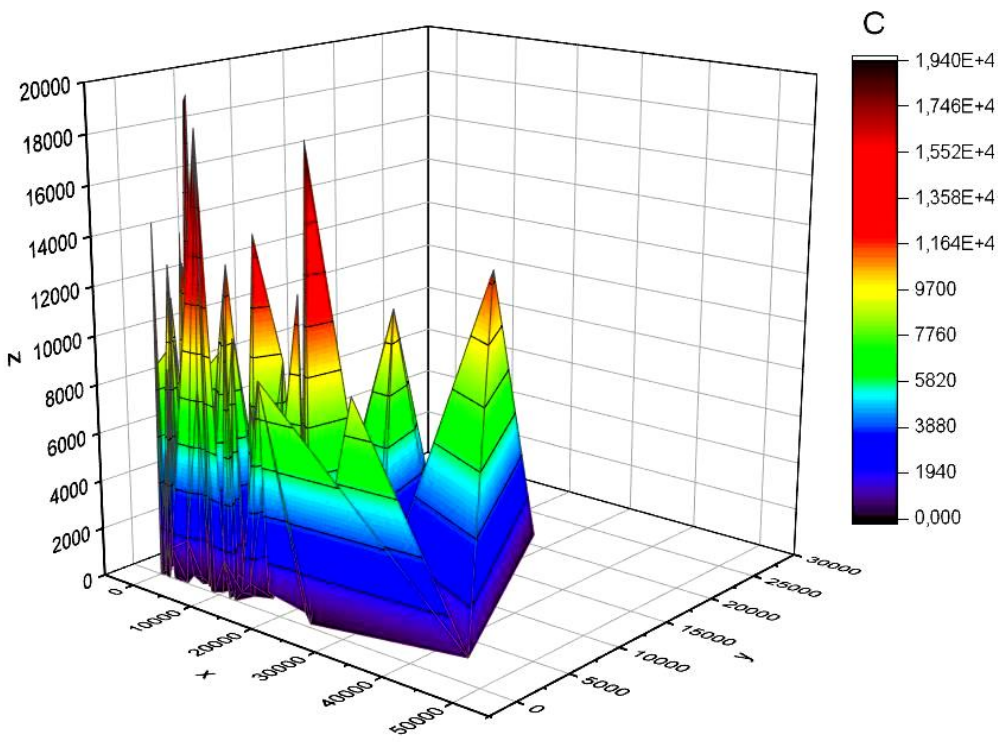


*Figure. 4.7. 3d representation of the vibration amplitude of the modified module 1.*

## 4.3. The differences of the amplitudes of the modules on the 3 measured directions.

After measuring the amplitudes after implementing the mechanical changes to the actuation of the gripper module, the graphs in Figure were made. 4.8, Figure. 4.9, Figure. 4.10, for module 1 which represents the major differences between the two systems.Diferemțele sunt:

- On the X axis, the old system has a maximum amplitude of 413953, and the new one 46415;
- On the Y axis, the old system has a maximum amplitude of 375471, and the new one 25623;
- On the Z axis, the old system has a maximum amplitude of 149650, and the new one 19343;

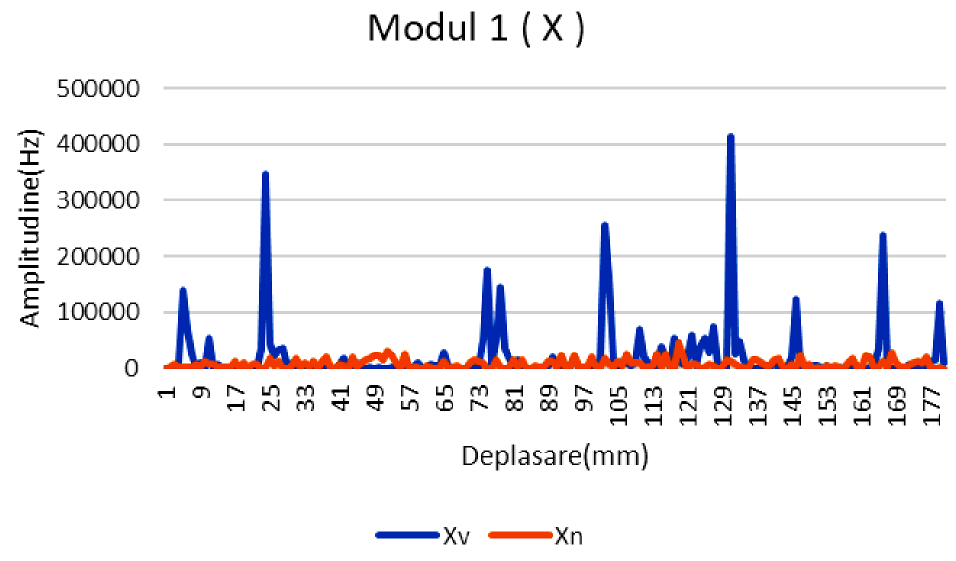


*Figure. 4.8. Differences in x-axis vibration amplitudes for mode 1.*

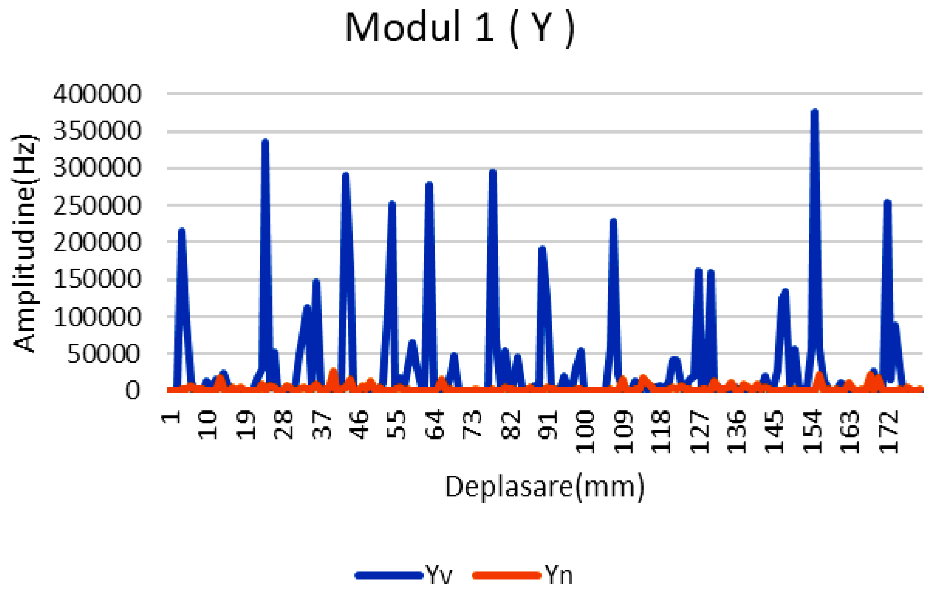


*Figure. 4.9. Y-axis amplitude differences for mode 1.*

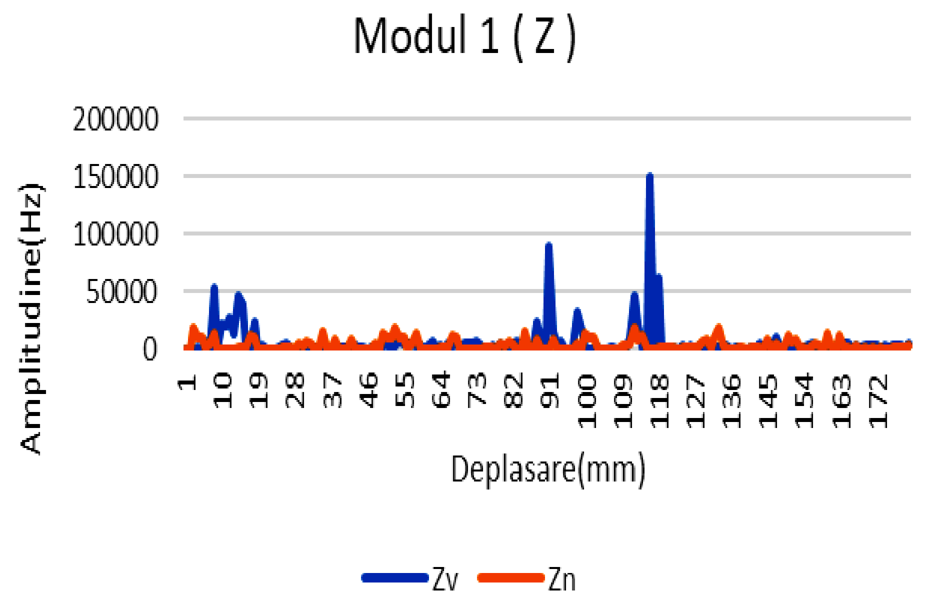


*Figure. 4.10. The differences of the amplitudes on the Z axis for the module 1.*

### 4.4. Conclusion

The implementation of the reducer led to a significant reduction in vibrations and improved movement accuracy. The adaptation of the mechanical structure allowed a better distribution of the forces and decreased the negative impact on the main axis following the movements of the prehension.

The gripper's acceleration and sensitivity control ability has been significantly improved by using the reducer, effectively adapting to different operating conditions.
The amplitudes measured for each component of the gripper indicated a significant decrease in vibration compared to the original configuration.

Detailed data analysis demonstrated that the structural modifications were effective in reducing vibration to acceptable levels, thereby improving gripper stability and reliability in practical operations.

# 5. DESIGN OF THE SENSORY GRIPPER SYSTEM

The proposed objective of this chapter was the development and implementation of an efficient and precise self-adaptive sensory grasping system for the manipulation of objects in an industrial environment.

## 5.1. Development of the logical architecture of the sensory system in order to achieve self-adaptivity

The logical architecture for each module is designed to perform grasping independently mechanically, electrically, and software-wise.
Self-adaptive grasping is done in 3 steps:

- Step 1 – In this step the states of the sensors in the retract position of the module are declared, if the module is in the forward position or another intermediate position, then the controller makes the decision to move to the forward position and will wait for the command to achieve a new grasp.
- Step 2 – At this stage, the advance command of the module has been received, and the sensor system is in the "ON" state permanently waiting for the collection of new states. This stage can be completed if the sensory system has fulfilled its software condition, namely:

1.The handle of the module came into contact with the object to be grasped.

2. After entering the contact, tightening is carried out until the force declared in the software is reached.

3. The object stops moving after the squeeze is done.

- Step 3 – After step 2 has been accomplished, the sensory system detects the non-compliance of condition “3” in step 2, which means that the grasped object slip has been detected and enters the retraction phase. If even after the subsequent tightening the sensory system detects movement, the tightening will be performed again, this work will be repeated until the sensory system reaches the maximum declared thresholds, namely:

- Strength exceeded maximum limits
- The slide has reached its maximum point

When one of the maximum limits, among the conditions above, has been reached, then the module will stop grasping.

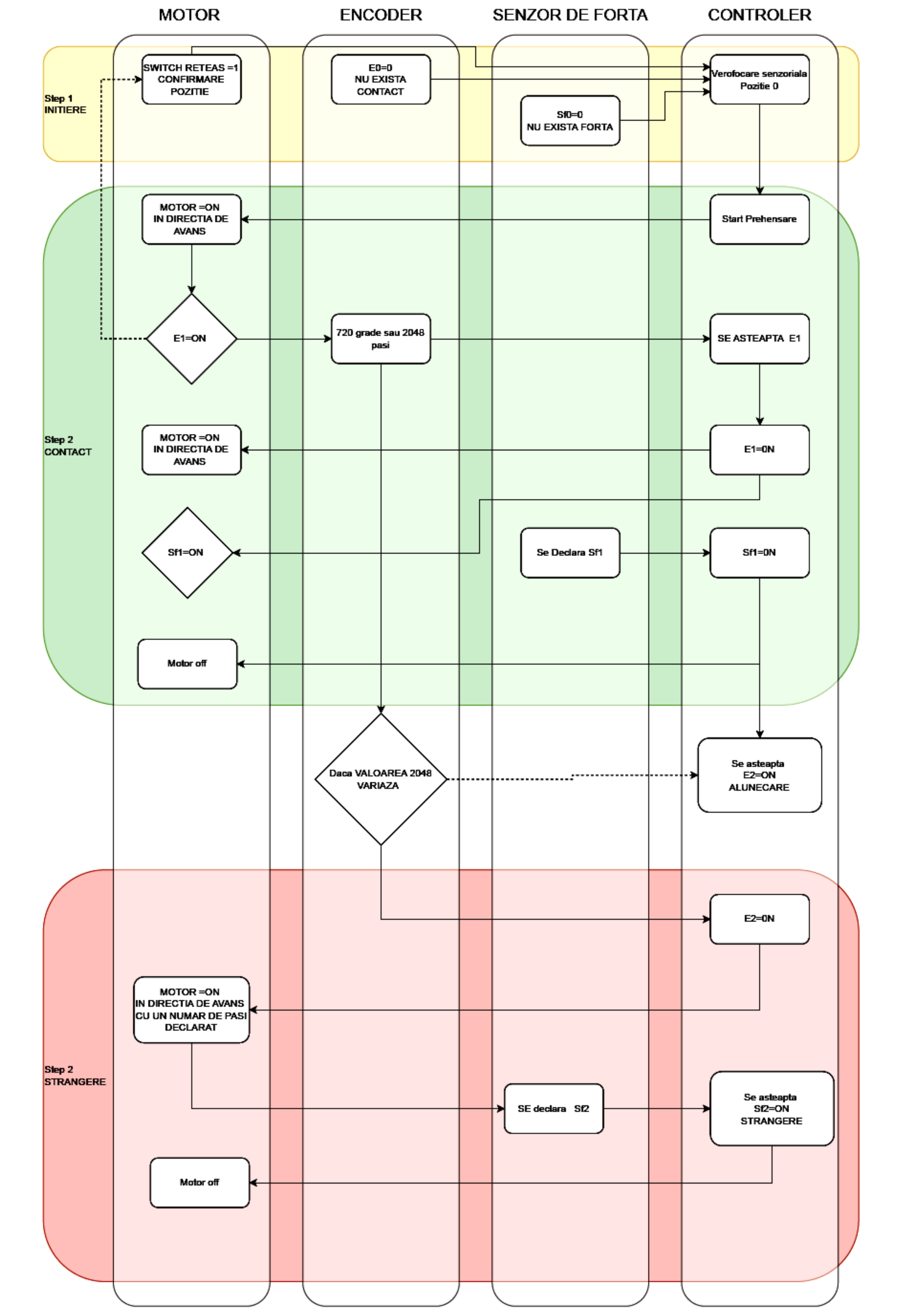


*Figure. 5.1. Logical architecture*

## 5.2. Presentation of the sensory system

The sensory system consists of a resistive encoder (1) that has a shaft that performs a rotational movement, and it generates values that are amplified by an electronic system so that they can be read. The encoder is actuated by means of an elastic belt (6) which achieves an amplified transmission between two drive wheels. The drive wheel (2) that transmits the movement to the encoder also has the role of tensioning the drive belt. Each value generated by the encoder correlates with the position of the stepper motor axis in real time to be able to make a decision if more or less force needs to be exerted on the product [34].

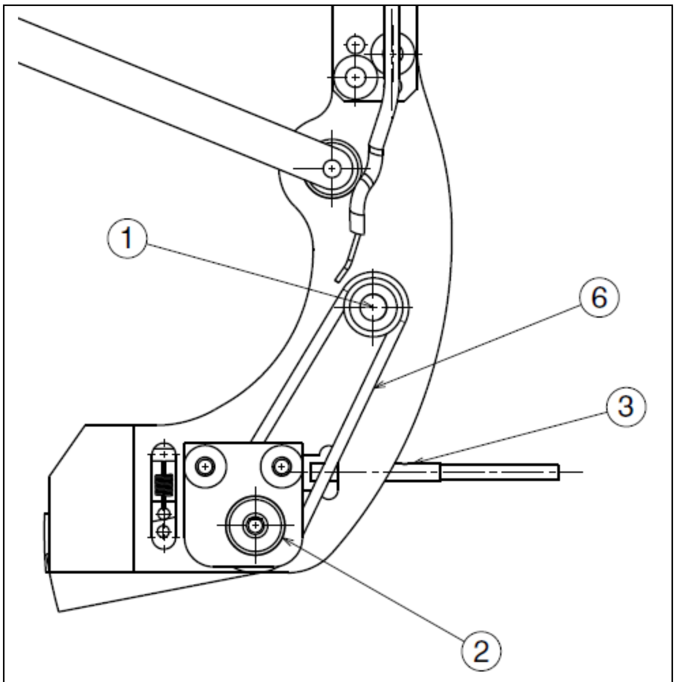

*Figure. 5.2. The handle of the self-adaptive gripper with the implemented sensory system*

The whole system is driven by a platband that forms a lever with the first rotation system, which at the same time also performs a translational movement relative to the system's horizontal. The platen that performs a translational movement does not exert any effort on the grasped product, and once it reaches the end of the stroke, the firm contact of the object is detected by an inductive sensor (3). All the sensory system is activated with the contact confirmation of the inductive sensor (Figure. 5.2)[35].

### 5.2.1. Description of the sensor tightening process

The 5-module adaptive gripper bay in which the interchangeable sliding sensor system is implemented. In the represented section, you can see the rotational movement it makes after contact with the object. The stages of grasping with sliding sensory systems are:

The step-by-step motor activates the gripper arm until the tray plate touches the product and confirms the inductive sensor;

After the presence sensor confirms, the motor tightens by a maximum of 5%;

If the product moves in the bins due to inertia or weight greater than the force exerted on it after it is grasped, then the platband makes a downward rotational movement, and in at the same time every 0.1o the stepper motor puts more pressure on the product until it stops moving.

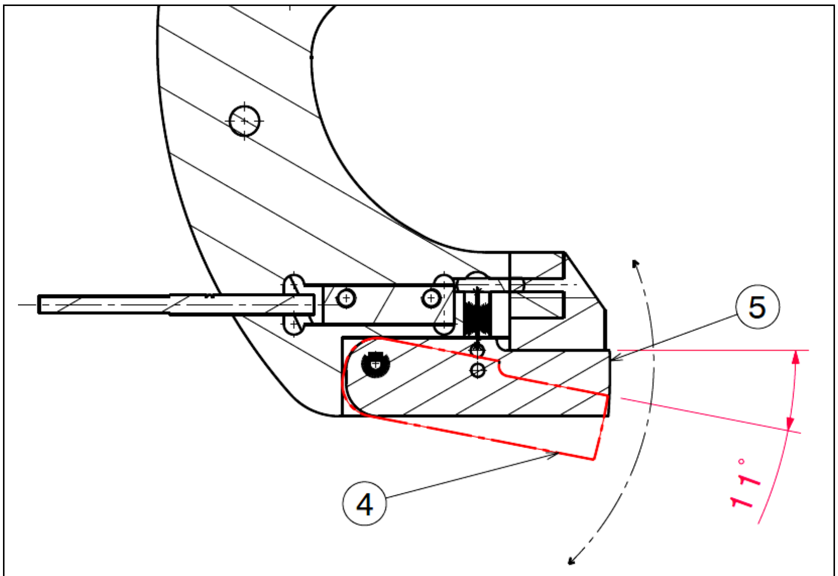

*Figure. 5.3. Deployed bar section*

Platbanda realizează mişcarea de rotație din pozitia (5) în poziția (4), astfel face o rotație maximă de 11°, iar după aceea ea revine în poziția inițială (5) cu ajutorul unui arc de tracțiune (**Eroare! Fără sursă de referință.**).

## 5.3. Conceptual testing of the slip sensor

### 5.3.1. Software realization of the sensory system.

The sensory system is a system in which several electrical values generated by the sensors are accumulated to finally make a momentary decision.

```
const int potPin = A0;

void setup() {
  // Începe comunicația serială la 9600 bps
  Serial.begin(9600);
}

void loop() {
  // Citeşte valoarea analogică de la potențiometru
  int potValue = analogRead(potPin);

  // Trimite valoarea citită pe Serial Monitor
  Serial.print("Valoarea citită: ");
  Serial.println(potValue);

  // O întârziere pentru a nu supraîncărca Serial Monitor-ul
  delay(100);
}
```

*Figure. 5.4. Resistive encoder data collection code*

The „potValue" function - this function reads the analog value (0 to 1023) from the pin the potentiometer is connected to, which indicates the current position of the potentiometer when the output voltage is divided. This function is used to control the position of the potentiometer more effectively and to decrease the degree of error.

### 5.3.2. Resistive encoder structure and generated signals

**5.3.3.** The encoder is a sensory system that generates electrical signals or parameter variations depending on the type of encoder chosen. In the sensory system of the adaptive gripper, a resistive type encoder is used that allows a 360° rotation[37].

It generates resistive variations to the programmer on its inputs. The signal read by the programmer is realized through an analog input with a read function, (val = analogRead(Ax)). The resistive variations of the encoder transform the output current of the encoder into a variable one with a linear characteristic, but also with a reading error. The read error is declared with the function (if ((val "read value" > previous+3) || (val "read value"< previous-3))), where the declared error 3 is the sensitivity threshold of the encoder. This declared threshold is important because there are times when at a certain mechanical position the encoder can generate lower or higher values even if it is at rest.
These error values are variable and must not further influence the mechanical system, and depending on the noise generated by the encoder at rest, the interval in which the encoder can generate variable currents is established. The encoder performs the rotation movement until it is stopped by the mechanical sliding component at the angle of 11o (Table 5.1)[38].

### 5.3.4. Mode of operation of the resistive slip sensor

The sensor system, in the present case, consists of a presence sensor and an encoder type sensor. The values are read from the encoder as long as the proximity sensor confirms the presence of the object by generating the signal (1 or true). In software, this type of proximity sensor is declared as a simple contactor (int digitalread x), where x is the chosen pin number. After declaring the connection between the sensor and the programmer, the type of connection (input) is declared, which is a very important parameter for stabilizing the system, taking into account the resolution declared in the step-by-step motor programming. For a stepper motor with a resolution of 150 declared in the form (stepresolution 150) it performs a step when the encoder error value is exceeded. To reposition the motor, the value generated permanently by the encoder is read in real time with the function (previous = val(current value)).

*Table 5.1. Encoder generated values on SerialMonitor*

| The angle made by the mechanical sliding component (˚) | The values of the electrical voltages on the serial monitor (V) | Error generated by the encoder |
|---|---|---|
| 0 | 0 | (-0.03 -- +0.03) V |
| 0.5 | 0.05 | (-0.03 -- +0.03) V |
| 1 | 0.07 | (-0.03 -- +0.03) V |
| 1.5 | 0.09 | (-0.03 -- +0.03) V |
| 2 | 0.11 | (-0.03 -- +0.03) V |
| 2.5 | 0.13 | (-0.03 -- +0.03) V |
| 3 | 0.15 | (-0.03 -- +0.03) V |
| 3.5 | 0.17 | (-0.03 -- +0.03) V |
| 4 | 0.19 | (-0.03 -- +0.03) V |
| 4.5 | 0.21 | (-0.03 -- +0.03) V |
| 5 | 0.23 | (-0.03 -- +0.03) V |
| 5.5 | 0.25 | (-0.03 -- +0.03) V |
| 6 | 0.27 | (-0.03 -- +0.03) V |
| 6.5 | 0.29 | (-0.03 -- +0.03) V |
| 7 | 0.31 | (-0.03 -- +0.03) V |
| 7.5 | 0.33 | (-0.03 -- +0.03) V |
| 8 | 0.35 | (-0.03 -- +0.03) V |
| 8.5 | 0.37 | (-0.03 -- +0.03) V |
| 9 | 0.39 | (-0.03 -- +0.03) V |
| 9.5 | 0.41 | (-0.03 -- +0.03) V |
| 10 | 0.43 | (-0.03 -- +0.03) V |

## 5.4. Representation of the gripper in the updated form with the sliding sensor system.

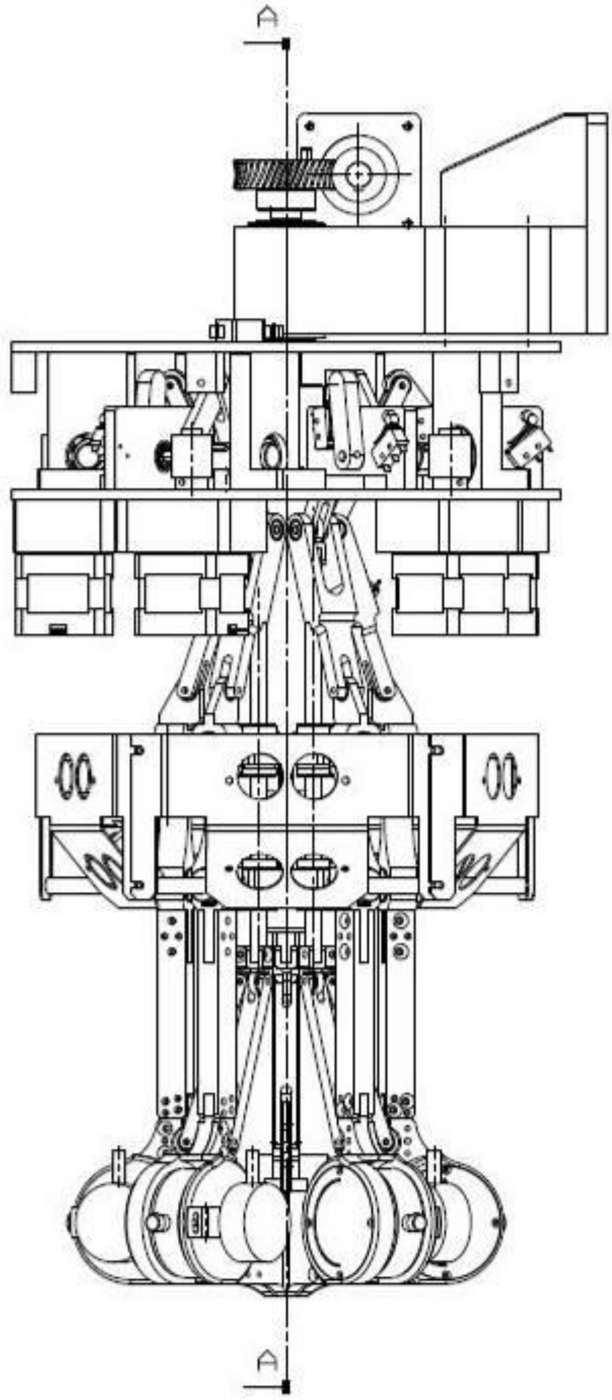


*Figure. 5.6. 2D front gripper view*

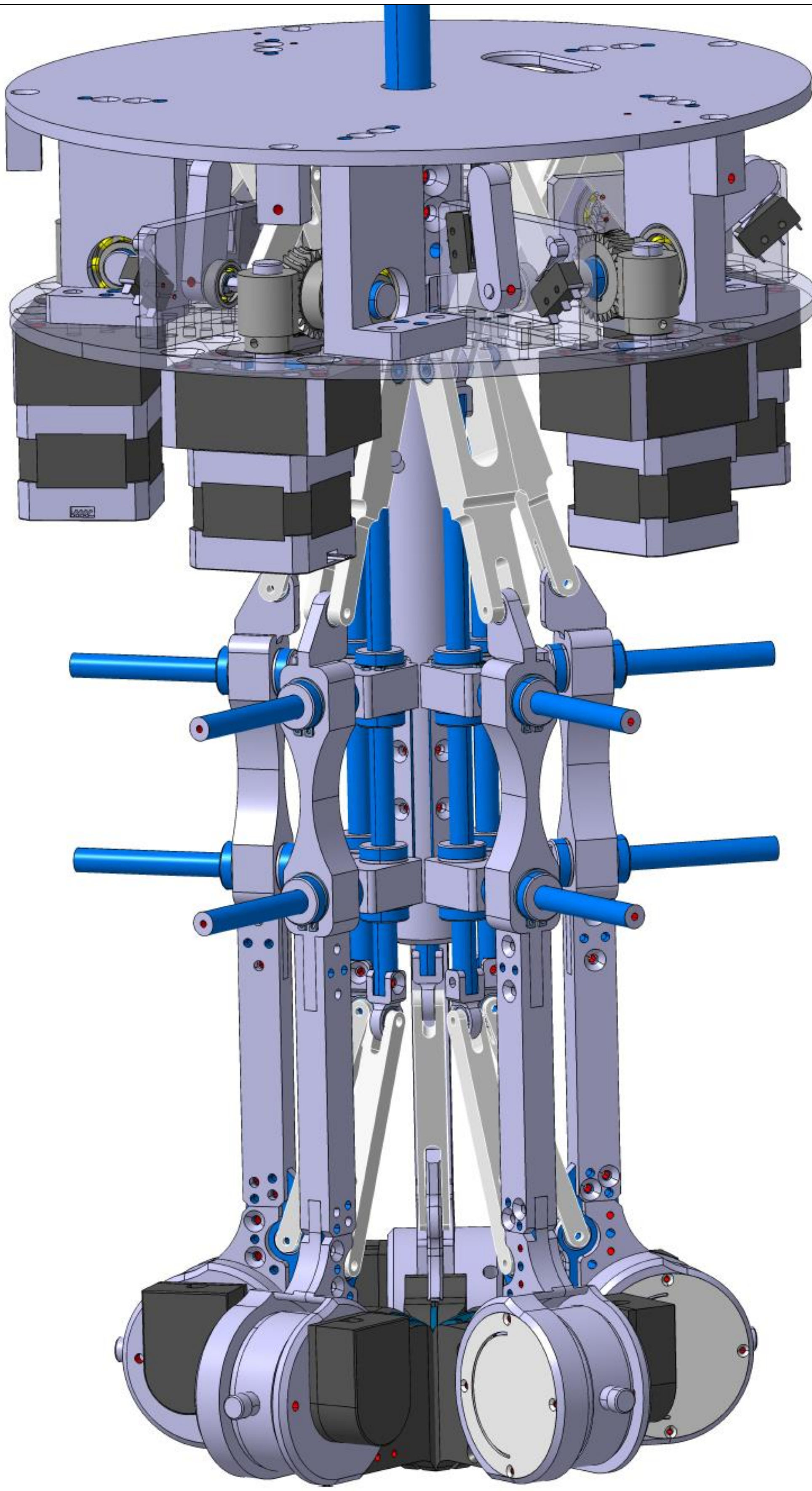

*Figure. 5.7. 3D gripper view*

## 5.5. Determining the positioning of the force sensor with the finite element method

To implement the force sensors it was necessary to determine the ideal position. To determine the position, the structure of the module was analyzed with the finite element method where a force of 1 kg was applied. The force was applied to the front of the boat.

For the purposes of the determinations, the material used in the execution of the module structure was declared to have the characteristics of Table 5.2.

*Table 5.2. Features of the material used in the structure*

| | |
|---|---|
| Material | Aluminium |
| Young's modulus | 7e+010N_m2 |
| Poisson's ratio | 0.346 |
| Density | 2710kg_m3 |
| Coefficient of thermal expansion | 2.36e-005_Kdeg |
| Yield strength | 9.5e+007N_m2 |

The analysis was done on the module structure without other added systems such as the slip sensor and other electronic elements.

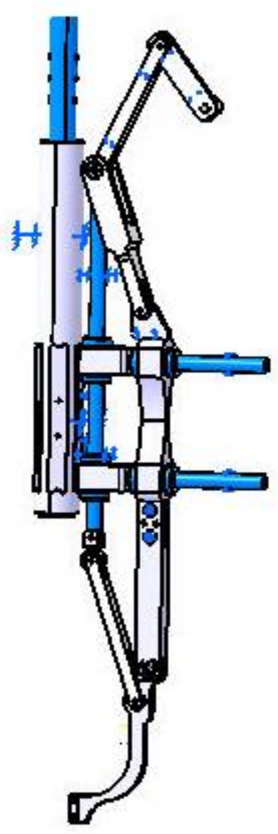

*Figure. 5.8. Decomposition of forces generated by Catia software*

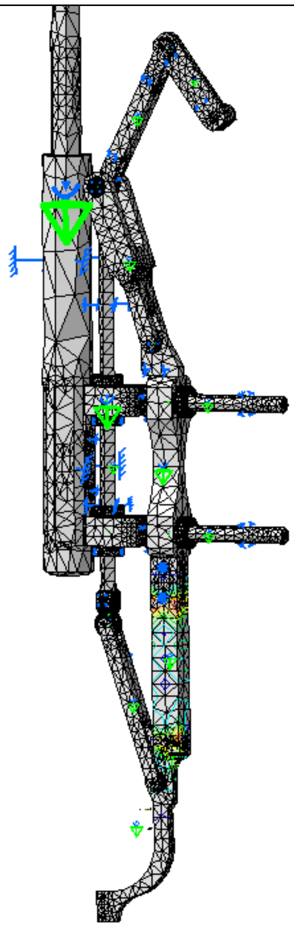

*Figure. 5.9. Stage I: analysis of the finite element method*

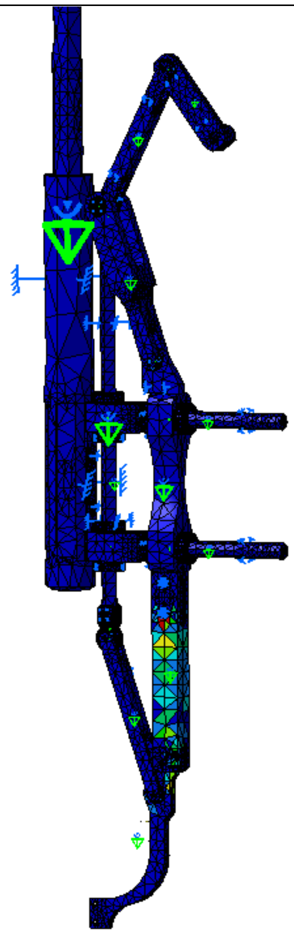

*Figure. 5.10. Stage II: analysis of the finite element method*

*Table 5.3. The values of the resultant forces and moments of the module*

| Components | Applied Forces | Reactions | Residual | Relative Magnitude Error |
|---|---|---|---|---|
| Fx (N) | -8.2718e-025 | 1.6360e-012 | 1.6360e-012 | 4.4804e-013 |
| Fy (N) | 1.0000e+000 | -1.0000e+000 | -9.8965e-013 | 2.7103e-013 |
| Fz (N) | -9.6240e-019 | 1.5066e-012 | 1.5066e-012 | 4.1260e-013 |
| Mx (Nxm) | 8.0314e-002 | -8.0314e-002 | 4.7726e-014 | 3.1647e-014 |
| My (Nxm) | 4.9534e-019 | -1.4732e-013 | -1.4732e-013 | 9.7690e-014 |
| Mz (Nxm) | -4.7208e-012 | 4.6514e-012 | -6.9400e-014 | 4.6019e-014 |

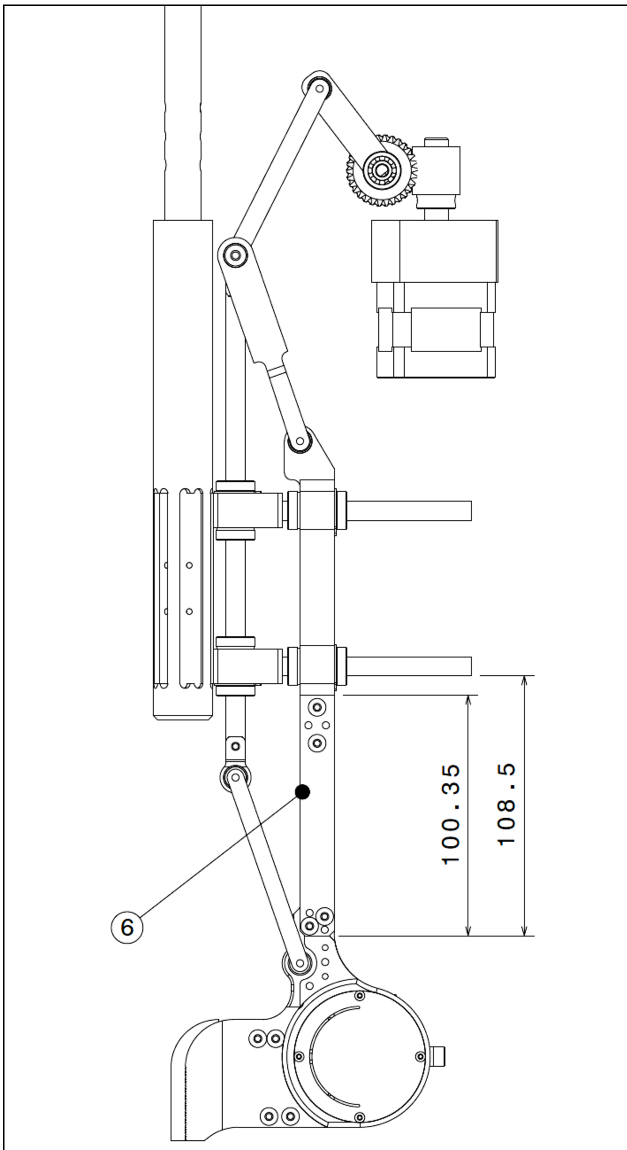


*Figure. 5.11. Initial sizing without force sensor*

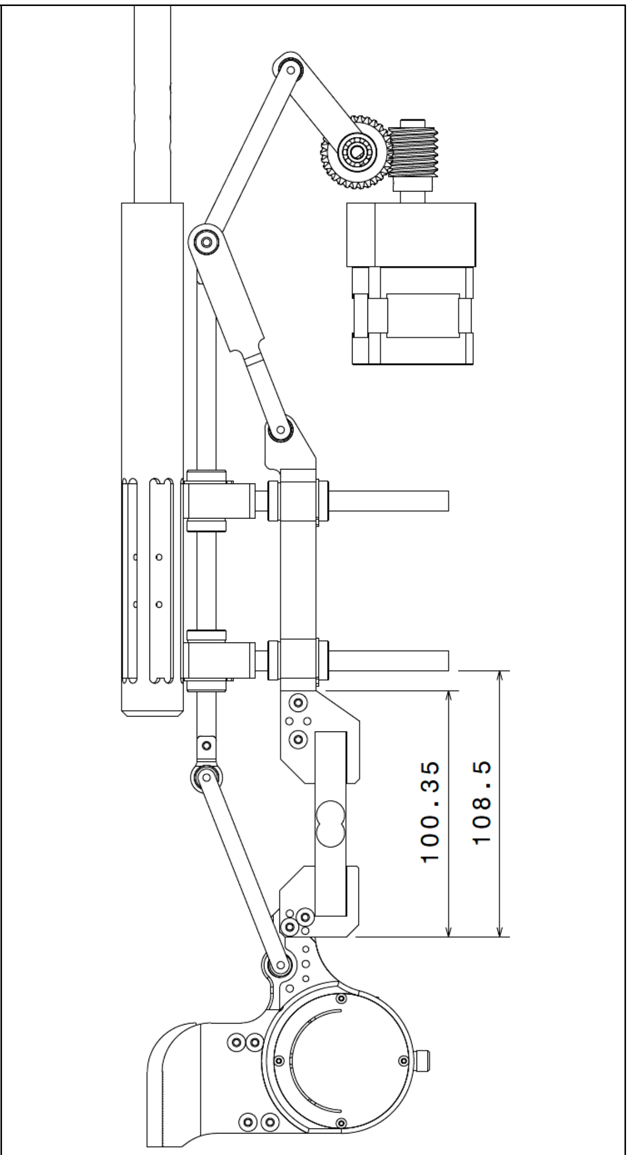


*Figure. 5.12. Updated sizing with force sensor*

Following the analysis, simulations were generated with the plastic and elastic deformations of the gripper module.

From the Figure. 5.9 and Figure. 5.10, the maximum deformation zones are observed which are marked in different colors. This area indicates where the force sensor should be placed for optimal results.

## 5.6. Structural integration of force sensors for self-adaptivity

Implementation of the force sensor in 3d following the kinematic scheme.

According to the analysis with the finite element method, the element with the most pronounced plastic deformations (6) was replaced by the force sensor respecting the existing structure.

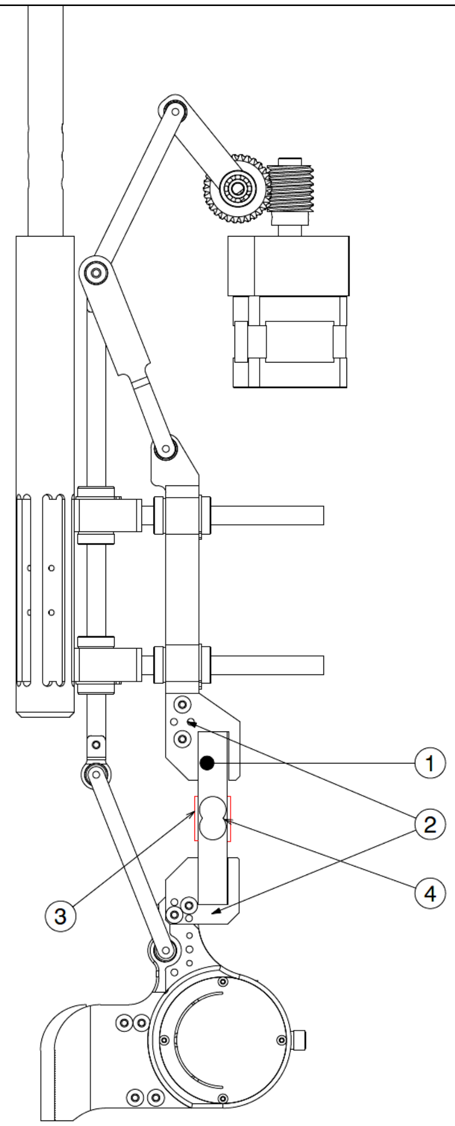


*Figure. 5.13. Subassembly detailing the mechanical elements of the force sensor*

The force sensor is designed from a non-ferrous material (aluminum) (1) and a wiston half-bridge that consists of two piezoresistive sensors (3) that are placed on one side and the other of the sensitive area (3) that was specially designed to increase sensitivity to deformation.

The adaptation of the 5 prehensor modules and the realization of the new final prehensor model.

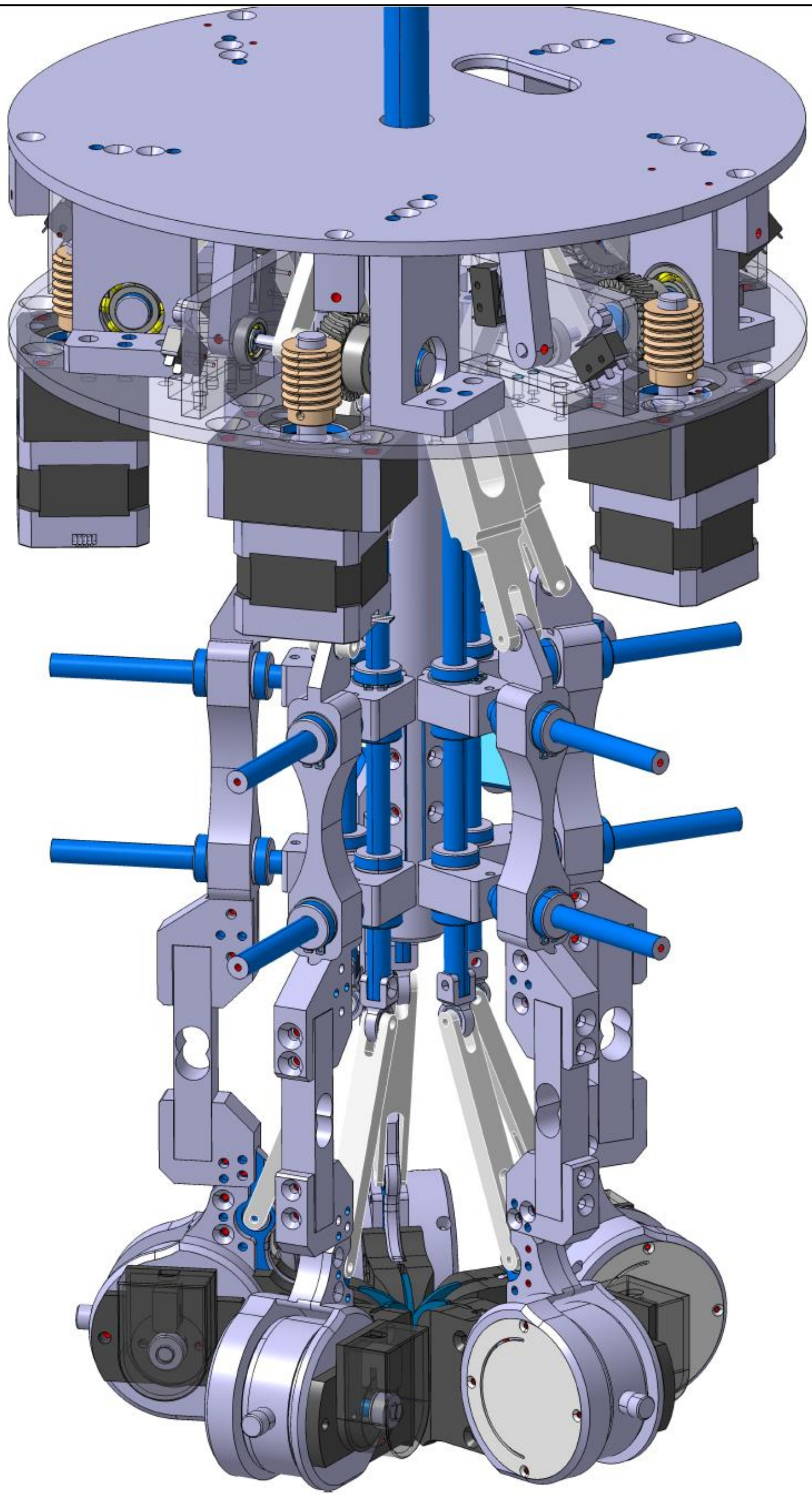

*Figure. 5.14. Self-adaptive gripper in forward position*

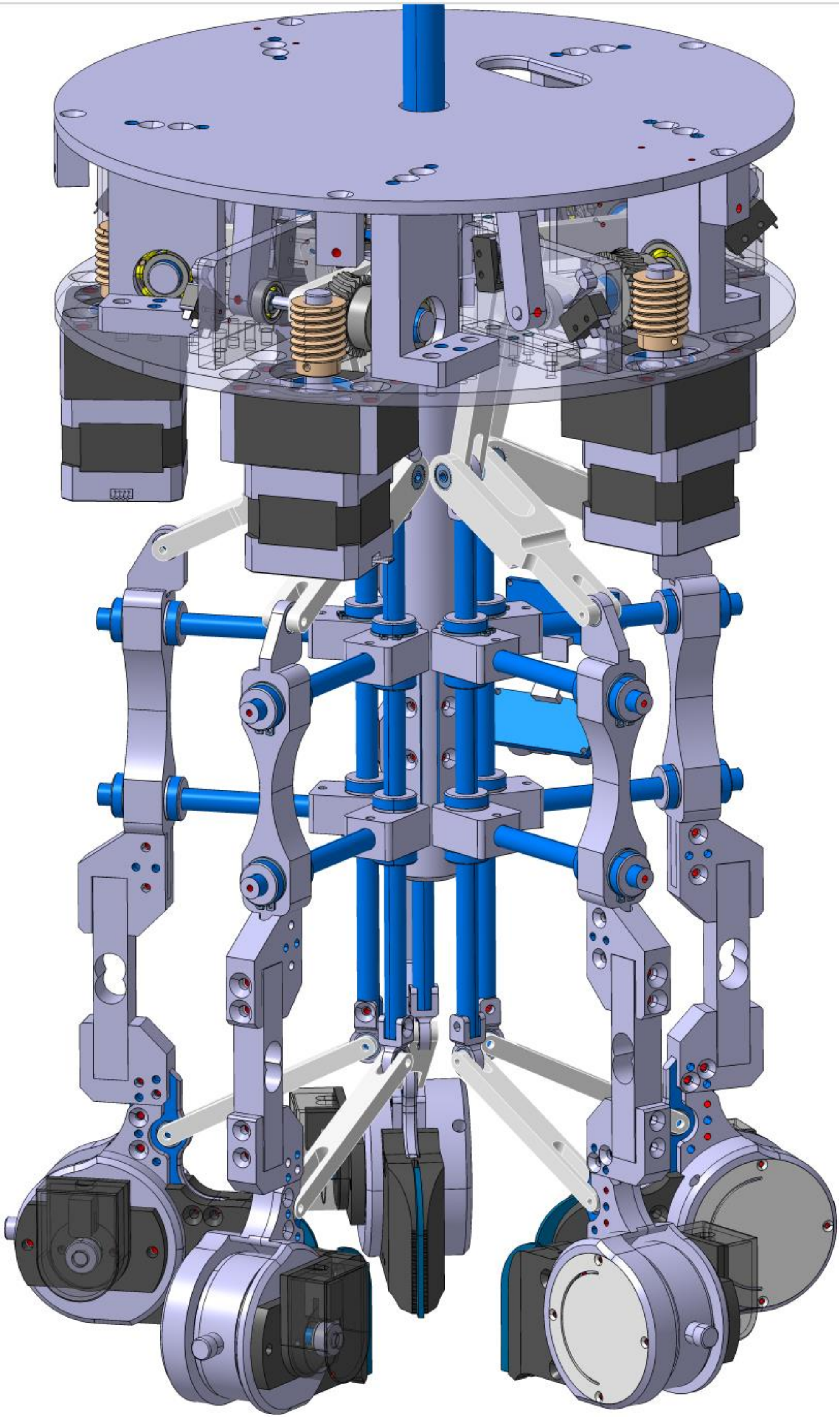

*Figure. 5.15. Self-adaptive gripper in retracted position*

## 5.7. The design of the electronic scheme on the module, according to the new architecture

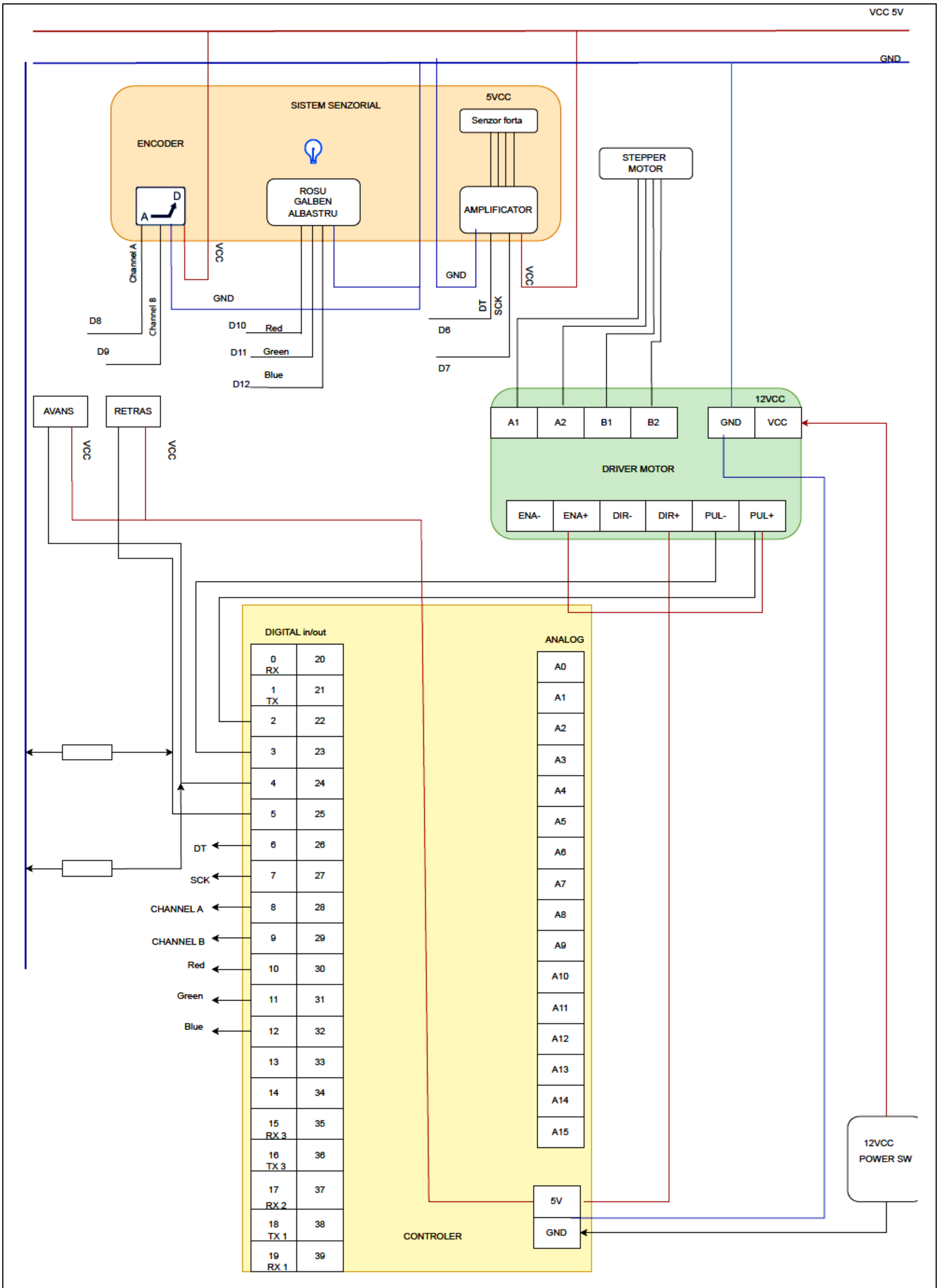


*Figure. 5.16. Final wiring diagram of a gripper module*

For the design of the electrical scheme, the logical structure and all the electronic parts implemented on each module were taken into account. The important elements that were taken into account are:

- Stepper motor with programmable driver;
- The incremental optical encoder;
- Force sensor with signal amplifier;
- The controller;
- Travel limit contactors;

*Figure. 5.17. Physical realization of the electrical panel*

## 5.8. Determination of clamping forces for self-adaptive grasping

- Study of the stages of parameterization and calibration of force sensors:

- The force sensors are piezo timing and a wiston half bridge is created (using only two sensors instead of 4).
- The values generated by each module are measured separately in 3 phases (Figure 5.18):
- • Phase 1 – the values measured at rest (here the noise/mechanical tension exerted in the sensor can be observed);
- • Phase 2 – the values measured at touch (the force is applied frontally to the trays, perpendicular to the force cell) according to the figure;
- • Phase 3 – values measured during tightening (the force is applied frontally to the bins, perpendicular to the force cell).

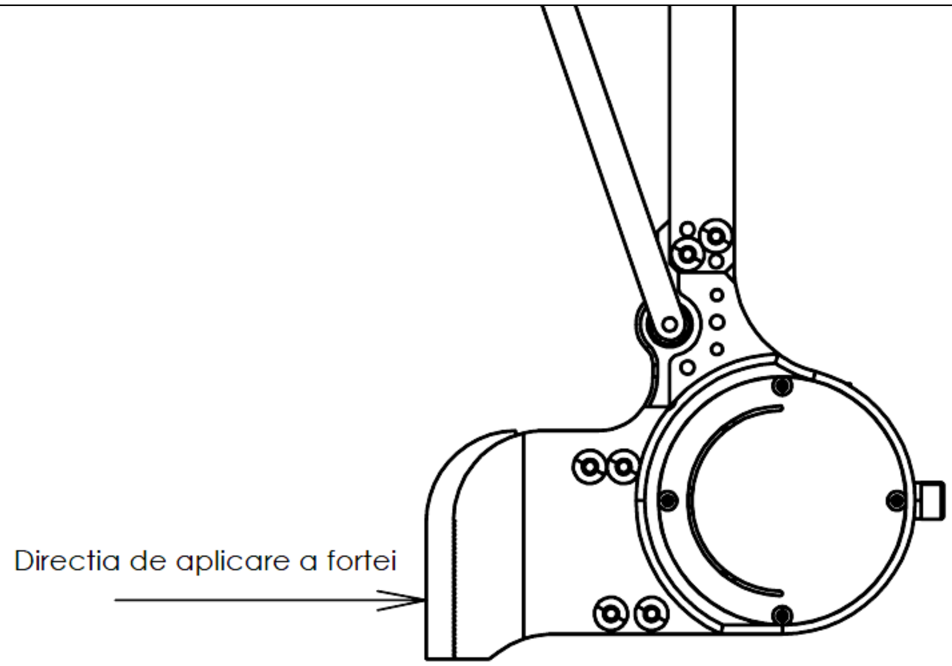


*Figure. 5.18. Direction of application of force*

To make the determinations, a signal amplifier of type HX711.h was implemented and a software was created for measuring the force cells for calibration.
Steps created in the software to perform the calibration:
**Step 1.** Declared the communication pins between the ATmega programmer and the HX711 amplifier as constants
"const int LOADCELL_DOUT_PIN = 6;"
"const int LOADCELL_SCK_PIN = 7;
**Step 2.** Initialized the serial communication and the frequency it works on
"Serial.begin(9600)"
"scale.begin(LOADCELL_DOUT_PIN, LOADCELL_SCK_PIN) // HX711 scale initialization"
" Serial.println("Calibration...")"
"Serial.println("In this phase there must not be any force applied to the sensor.")
"scale.hard(); // Reset scale to zero"
"Serial.println("Calibration complete!"
**Step 3.** Sensor calibration commands entered as:
"char temp = Serial.read(); - Reading the character from Serial (useful for commands
" if (temp == 't' || temp == 'T')"
" scale.hard(); // Recalibrate if 't' or 'T'" is sent
**Step 4.** Declared scaling mode and weight display mode

*Tabelul 5.1. Colectarea datelor afișate*

(scaledWeight) > 0.01) - Checking if the scaled weight is greater than a small threshold
Serial.print("Weight: ")
Serial.print(scaledWeight, 2) - Print the weight scaled to 2 decimal places
Serial.println(" units"); - The display mode will be displayed as units representing the weight

**Step 5.** Collect the data shown in Table 5.4.
All selected data will be filtered and separated into separate columns.
Data were collected for each module separately, taking into account the three phases previously specified.
The results for Module No. 1 over a one-minute interval. The measured units declared in the weight determination software are equivalent to grams (1 unit = 1 g). Made the final force sensor test software.

| Nr | Measurement details |
|---|---|
| 1 | 17:56:04.534 -> Greutate: -27.62 unități |
| 2 | 17:56:05.045 -> Greutate: -18.34 unități |
| 3 | 17:56:05.557 -> Greutate: -27.65 unități |
| 4 | 17:56:06.115 -> Greutate: -27.66 unități |
| 5 | 17:56:06.627 -> Greutate: -27.63 unități |
| 6 | 17:56:07.182 -> Greutate: -27.74 unități |
| 7 | 17:56:07.695 -> Greutate: -27.65 unități |
| 8 | 17:56:08.209 -> Greutate: -18.25 unități |
| 9 | 17:56:08.720 -> Greutate: -27.67 unități |
| 10 | 17:56:09.279 -> Greutate: -27.68 unități |
| 11 | 17:56:09.792 -> Greutate: -18.24 unități |
| 12 | 17:56:10.305 -> Greutate: -27.65 unități |
| 13 | 17:56:10.822 -> Greutate: -27.65 unități |
| 14 | 17:56:11.376 -> Greutate: -18.15 unități |
| 15 | 17:56:11.884 -> Greutate: -18.09 unități |

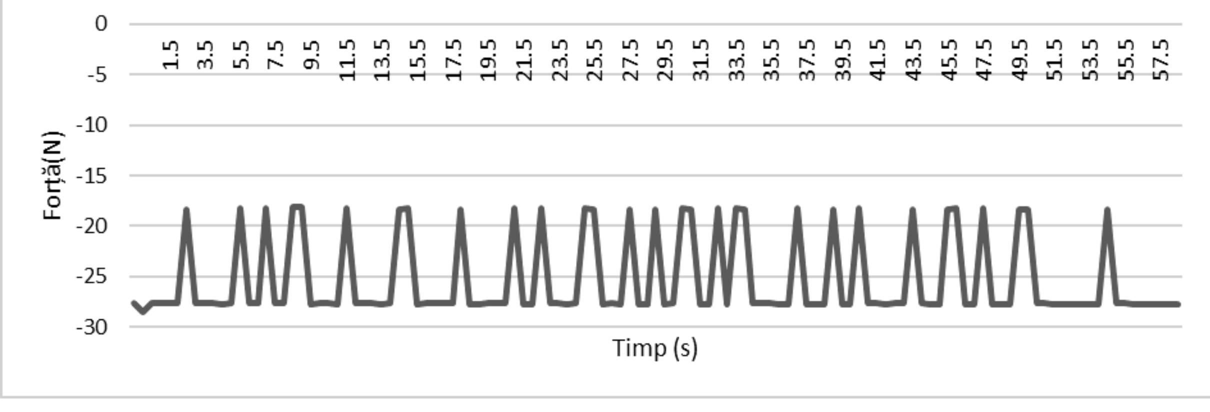


*Figure. 5.19. Module 1 noise per minute*

After separating the collected data, the graph was generated
Figure. 5.19, which represents the noise of module 1 over the interval of one minute without being influenced by any external force.

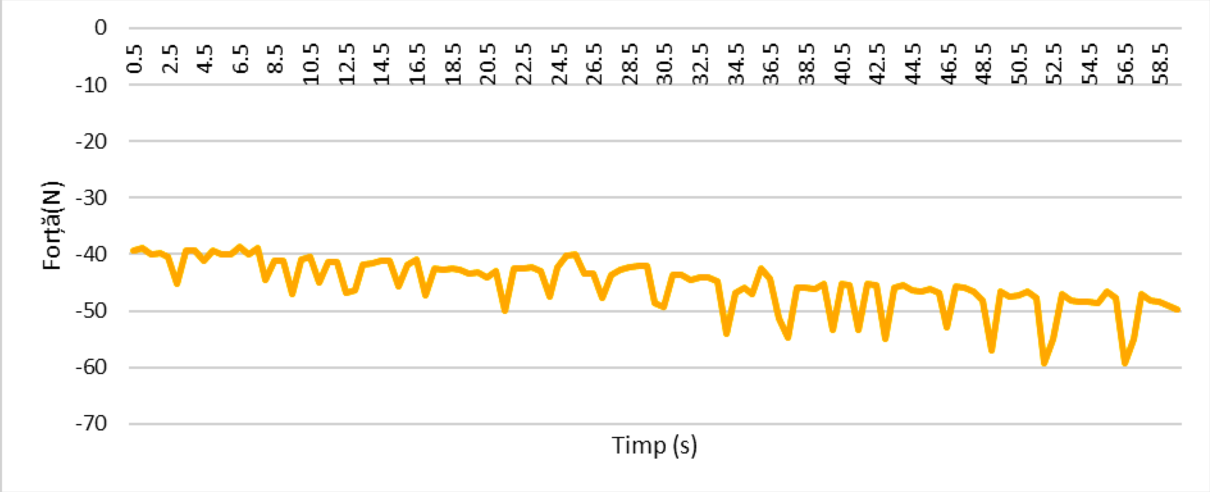


*Figure. 5.20. Result Module 1, phase 2*

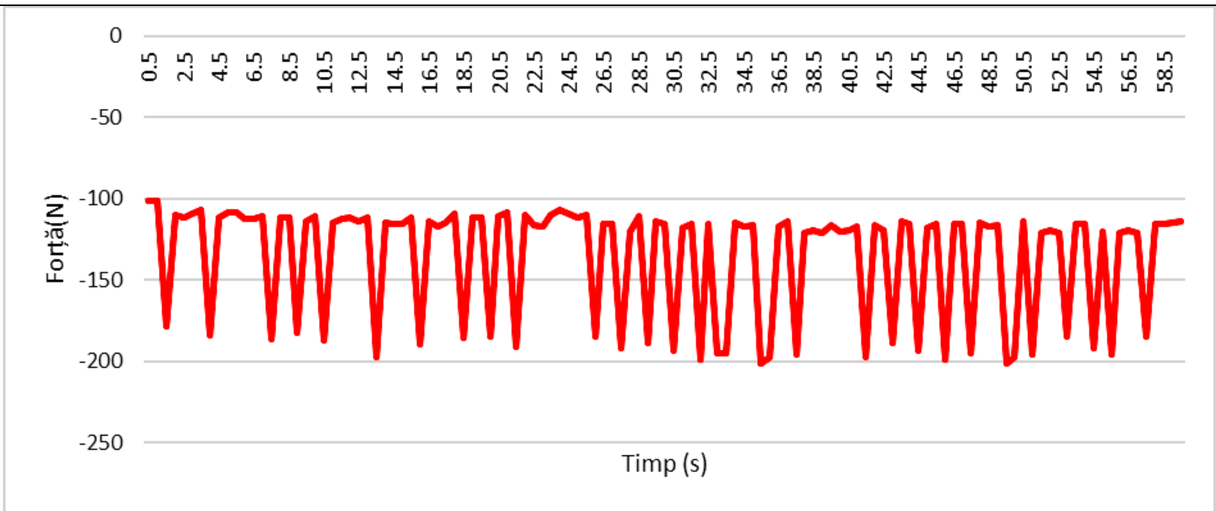


*Figures. 5.20. Result Module 1, phase 2*

## 5.9. Determining the angular values of the sliding sensor for self-adaptivityRealizarea software în scopul determinărilor unghiulare

To determine the angular values, a dedicated software was created for testing, which was installed on each module of the gripper.

```
const int channelA = 8;
const int channelB = 9;

volatile int position = 0;
volatile int lastEncoded = 0;

void setup() {
  Serial.begin(9600);
  pinMode(channelA, INPUT);
  pinMode(channelB, INPUT);
  attachInterrupt(digitalPinToInterrupt(channelA), updateEncoder, CHANGE);
  attachInterrupt(digitalPinToInterrupt(channelB), updateEncoder, CHANGE);
}

void loop() {
  Serial.print("Position: ");
  Serial.println(position);
  delay(100);
}

void updateEncoder() {
  int MSB = digitalRead(channelA);
  int LSB = digitalRead(channelB);

  int encoded = (MSB << 1) | LSB;
  int sum = (lastEncoded << 2) | encoded;

  if (sum == 0b1101 || sum == 0b0100 || sum == 0b0010 || sum == 0b1011) position++;
  if (sum == 0b1110 || sum == 0b0111 || sum == 0b0001 || sum == 0b1000) position--;

  lastEncoded = encoded;
}
```

*Figure. 5.22. Software for angular variation testing*

Each gripper module has a slip sensor that must be parameterized independently, as each has its own fault, either electrical or mechanical.

### a) Implementation and collection of read values

The values read by the software are done 10 / second to have a much higher angular displacement accuracy.

The slip sensor folds on the logic flow of the system and will measure in the steps made in the logic diagram.

To integrate the sensor within the sensor system, it is essential to collect data in various phases of the prehension process:

Sequence 1 - Evaluation of errors generated by the encoder before prehension for each module.

Sequence 2 - Measuring the angle made by the sensor probe until the gripped object touches the support.

Sequence 3 - Determination of the angular values that indicate the sliding of the grasped object, for each module.

Sequence 4- Determination of angular values for a complete slide sensor sequence.

**Determinarea erorilor pentru fiecare modul (Secvența 1)**

*Table 5.5. Sensor error generation over one second interval for Module 1*

| Time (s) | Angular position (°) |
|---|---|
| 0 | Position: 1 |
| 0.1 | Position: 1 |
| 0.2 | Position: 1 |
| 0.3 | Position: 1 |
| 0.4 | Position: 1 |

*Table 5.6. Sensor error generation on a one second interval for Module 2*

| Time(s) | Angular position (°) |
|---|---|
| 0 | Position: -2 |
| 0.1 | Position: -2 |
| 0.2 | Position: -2 |
| 0.3 | Position: -2 |
| 0.4 | Position: -2 |

| | |
|---|---|
| 0.5 | Position: 1 |
| 0.6 | Position: 1 |
| 0.7 | Position: 1 |
| 0.8 | Position: 1 |
| 0.9 | Position: 1 |
| 1 | Position: 1 |

| | |
|---|---|
| 0.5 | Position: -2 |
| 0.6 | Position: -2 |
| 0.7 | Position: -2 |
| 0.8 | Position: -2 |
| 0.9 | Position: -2 |

*Table 5.7. Sensor error generation on a one second interval for Module 3*

| Time (s) | Angular position (°) |
|---|---|
| 0 | Position: 7 |
| 0.1 | Position: 7 |
| 0.2 | Position: 7 |
| 0.3 | Position: 7 |
| 0.4 | Position: 7 |
| 0.5 | Position: 7 |
| 0.6 | Position: 7 |
| 0.7 | Position: 7 |
| 0.8 | Position: 7 |
| 0.9 | Position: 7 |

*Table 5.8. Sensor error generation over one second interval for Module 4*

| Time (s) | Angular position (°) |
|---|---|
| 0 | Position: -5 |
| 0.1 | Position: -5 |
| 0.2 | Position: -5 |
| 0.3 | Position: -5 |
| 0.4 | Position: -5 |
| 0.5 | Position: -5 |
| 0.6 | Position: -5 |
| 0.7 | Position: -5 |
| 0.8 | Position: -5 |
| 0.9 | Position: -5 |

**Contact angular determination for each module (Sequence 2)**

The measurements made by the sensor probe until the contact was established were repeated several times for the same sensor to define certain thresholds in the form of intervals. The simulations were performed over a period of 30 seconds.

The contact simulation for Module 1 corresponds to the graph data in Figure. 5.23.

*Table 5.9. Sensor error generation over a one second interval for Module 5*

| Time (s) | Angular position (°) |
|---|---|
| 0 | Position: -1 |
| 0.1 | Position: -1 |
| 0.2 | Position: -1 |
| 0.3 | Position: -1 |
| 0.4 | Position: -1 |
| 0.5 | Position: -1 |
| 0.6 | Position: -1 |
| 0.7 | Position: -1 |
| 0.8 | Position: -1 |
| 0.9 | Position: -1 |

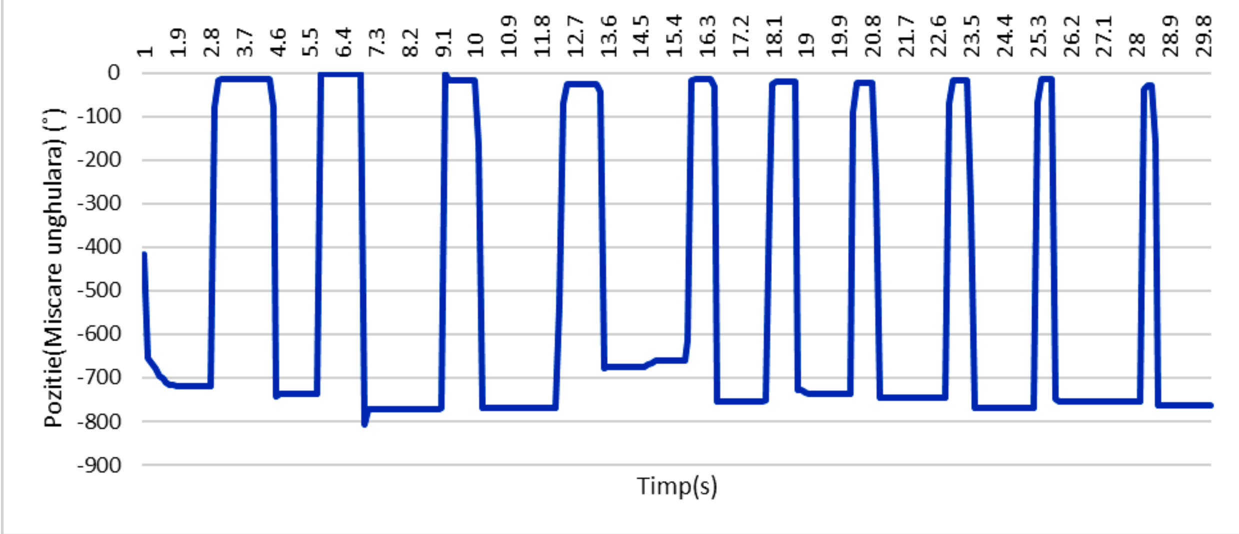


*Figure. 5.23. Contact angular determination in a time interval for Module 1*

In this data collection process the contact was repeated several times, according to the results, sensor 4 generates contact values between (600˚ and 750˚), and when released the values tend between (0 and -30˚).

As can be seen, the contact values are positive compared to the values generated by the other sensors. This will not affect, because only positive values will be declared in the software, even if they are generated as negative measurements.

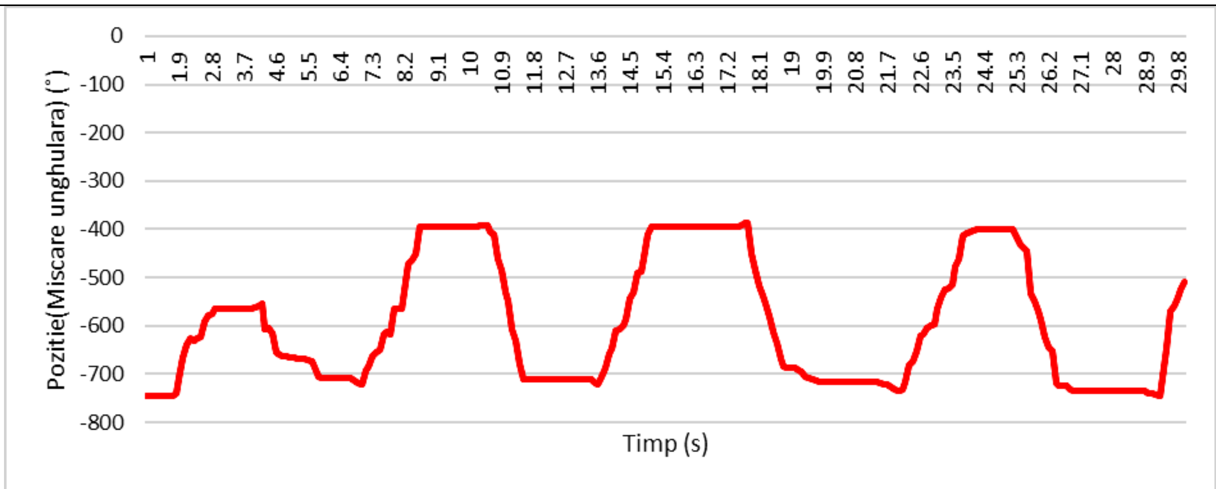


*Figure. 5.24. Angular determination of slip in a time interval for Module 1*

## Determination of angular values for a complete slide sensor sequence

In order to determine the complete sequences of the sliding sensor, complete cycles were performed by performing the 3 sequences (sequence 1, sequence 2 and sequence 3).

The measured values were obtained over a period of 30 seconds, during which several complete cycles were simulated to establish a specific interval in which slippage occurs for each gripper module

The simulation of the cycles of Module 1 corresponds to the data presented in the graph in the Figure. 5.25.

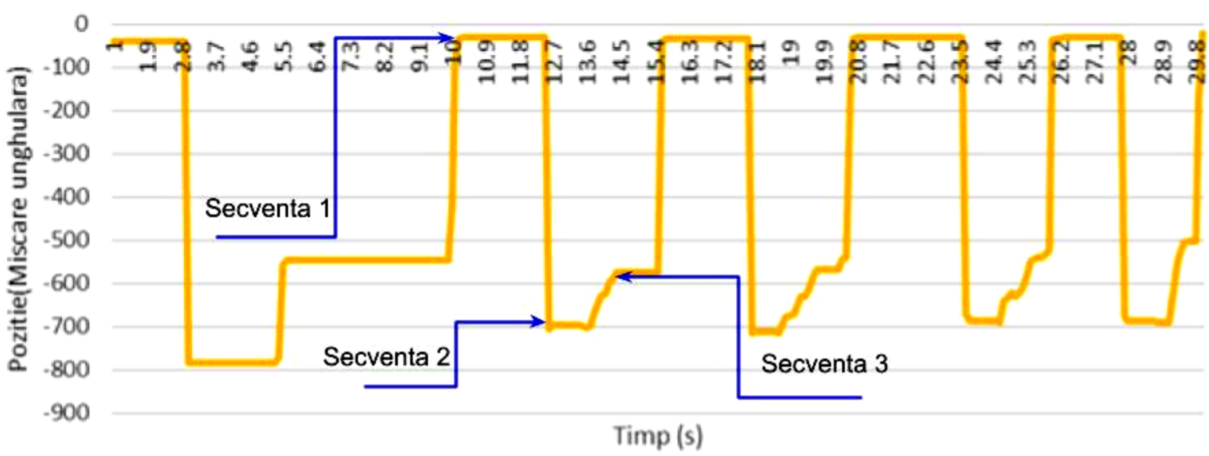


*Figure. 5.25. Determination of slip cycle values in a time interval for Module 1*

According to the data collected, the 3 sequences are observed for each cycle performed, the system starts collecting data when the sensor is for a short period of time (interval s9.8 - s12) in free state followed by a large angular value (-800˚) which represents the contact, in the contact position it was kept in balance for a short period of time (s12.1 – s13.5) after which there is a gradual angular decrease which represents the sliding (s13.5 - s15.3).

## 5.10. Conclusion

The logical architecture of the sensory system is designed to enable mechanically, electrically and software independent prehension. The implementation of three-step self-adaptive grasping ensures precise handling of objects, avoiding their sliding and deformation.

The sensor system implemented in the tail of the self-adaptive gripper uses a resistive encoder and a platen with translational and rotational motion for object detection and manipulation. It ensures an efficient and safe grip, minimizing the sliding and deformation of the gripped objects.

Software tests of the sensor system confirm the correct functionality of the resistive encoder in detecting position and small errors. However, the current encoder resolution is not high enough to detect slippage in a timely manner, suggesting the need for a redesign.

The need for a redesign is obvious to improve the accuracy and efficiency of the sensory system in detecting slip and manipulating objects. Implementation of a high-resolution optical incremental encoder and optimization of the translation and rotation mechanism are recommended to improve system performance and reliability.

The design of the advanced robotic gripper focused on the integration of a slip sensor to improve the ability to grasp and manipulate objects, highlighting the importance of geometric and material optimization for performance and durability.

Implementation and testing of the advanced robotic gripper demonstrated its efficiency and functionality under real-world conditions, confirming its ability to adapt and perform precise operations in various industrial and object handling applications.

# 6. DEVELOPING AND ACHIEVING GRIPPER ADAPTABILITY

The objective proposed in this chapter was the development and implementation of a self-adaptive gripper, based on a modular architecture and an efficient communication structure, to realize the prehension of various objects in a controlled and synchronized way.

## 6.1. Development of the logical architecture of the prehension system in order to achieve self-adaptivity

In order to make the gripper self-adaptive, it is necessary to control each module of the gripper independently, and for this purpose each module has its own controller that performs gripping independently of the other modules. This helps in controlling and decision making in processes much faster.

Having 5 controllers for each module, the sixth controller was implemented which was set as Master controller, and the other five set as Slave (Figure. 6.1).

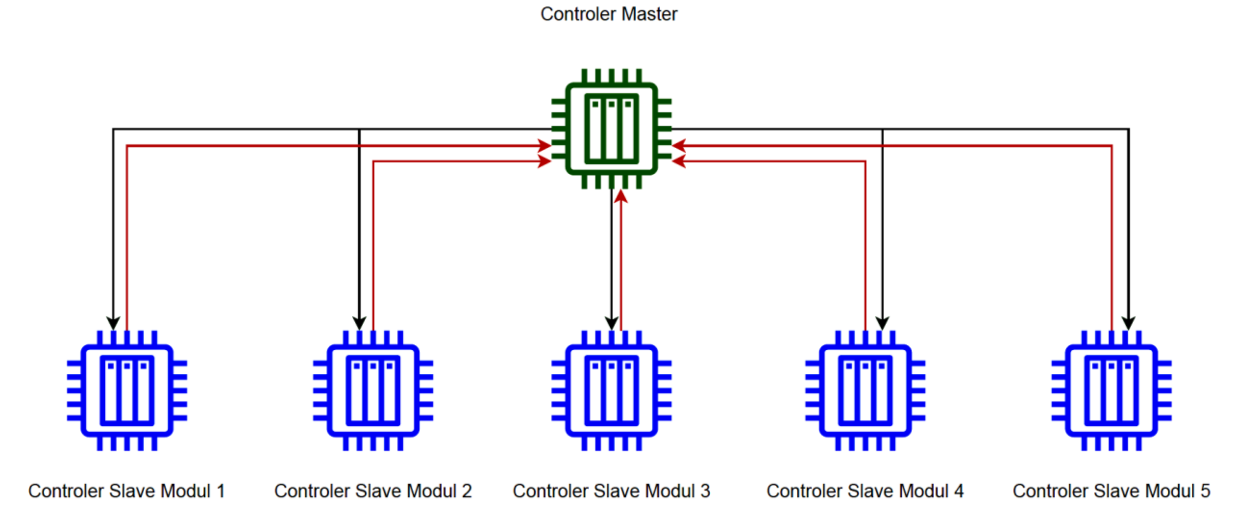


*Figure. 6.1. Master-Slave scheme*

## 6.2. Realization of the Master to Slave communication structure

The Master-Slave communication structure (Figure. 6.2) was implemented so that the Master controller executes commands simultaneously to the slaves. It collects data related to the prehension of objects from each module, making decisions regarding the time and necessity of reactivating the prehension processes for each individual module.

## 6.3. Master to Slave Binary Communication Logical Structure

On the communications declared according to the color code, on each of them logical information related to the grasp can be sent or received.
The logical communication is as follows:
Communication 1 (Module1) – if it is logical 1 – the Module is in advance position;

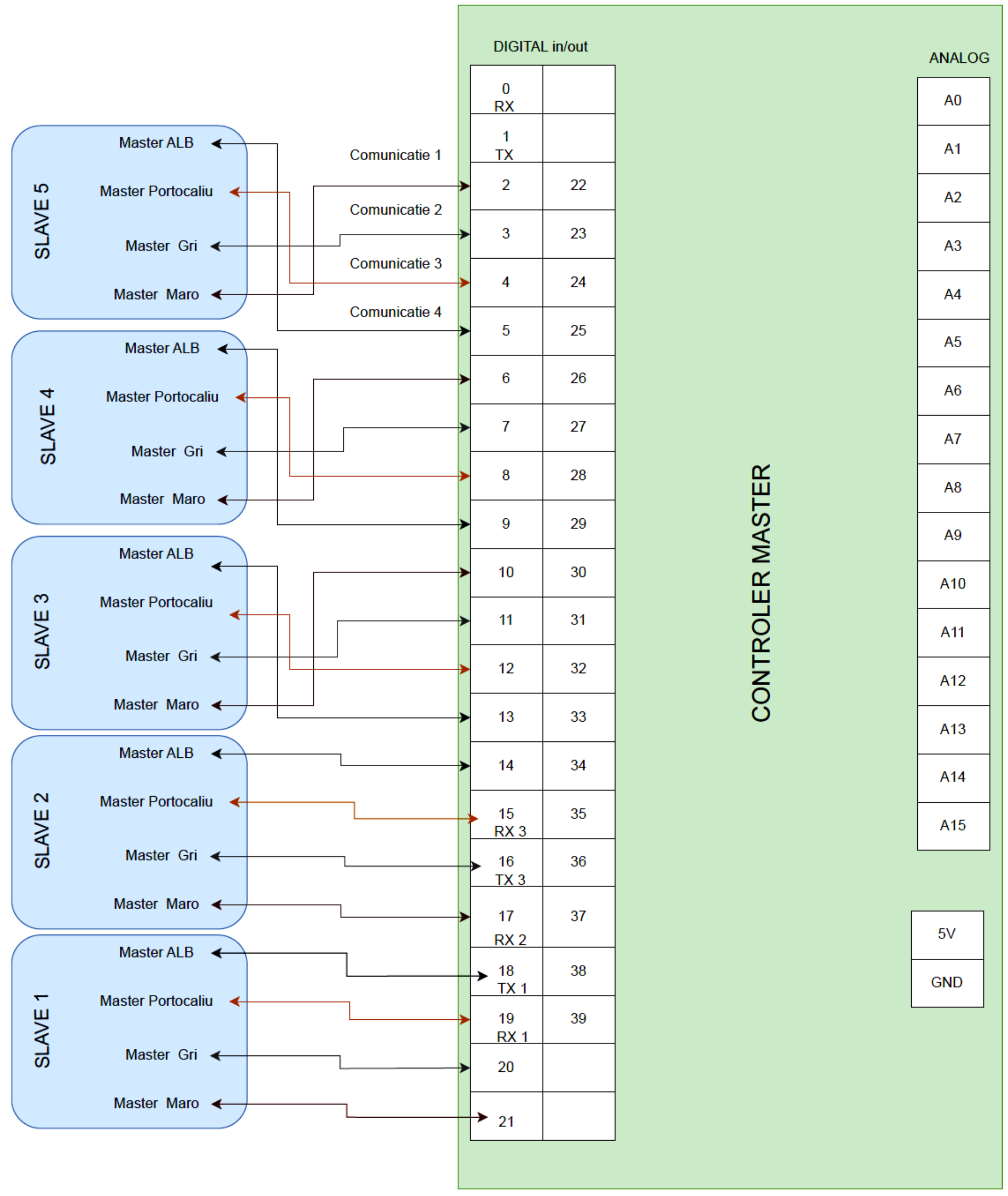


*Figure. 6.2. Master-Slave communication scheme*

All modules will have the same communications as the master controller, but on different digital ports.

The master controller, before grasping, requests the current status of the modules to decide whether to grasp or if repositioning is required for a new grasp.

The logic structure for grasp preparation is shown in Table 6.1, then the Master controller sends the grasp command (Table 6.2).

*Tabelul 6.1. Logica care arată poziția modulelor de avans*

| No. Modul | Communication 1 IN | Communication 2 IN | Communication 3 IN |
|---|---|---|---|
| 1 | 1 | 0 | 0 |
| 2 | 1 | 0 | 0 |
| 3 | 1 | 0 | 0 |
| 4 | 1 | 0 | 0 |
| 5 | 1 | 0 | 0 |

*Table 6.2. Logic command of STAR grasping*

| Communication 4 OUT |
|---|
| 1 |
| 1 |
| 1 |
| 1 |
| 1 |

In the situation where the Master controller requests the status from the Slave controllers and the status is of the following nature (Table 6.3), then it sends the logical repositioning command (1) for Module 2 (Table 6.4).

*Table 6.3. Logic showing position of advance modules less Module 2*

| No Modul | Communication 1 IN | Communication 2 IN | Communication 3 IN |
|---|---|---|---|
| 1 | 1 | 0 | 0 |
| 2 | 0 | 0 | 0 |
| 3 | 1 | 0 | 0 |
| 4 | 1 | 0 | 0 |
| 5 | 1 | 0 | 0 |

*Table 6.4. Reposition logic command for Module 2*

| Communication 4 OUT |
|---|
| 0 |
| 1 |
| 0 |
| 0 |
| 0 |

## 6.4. Design and execution of the control panel scheme

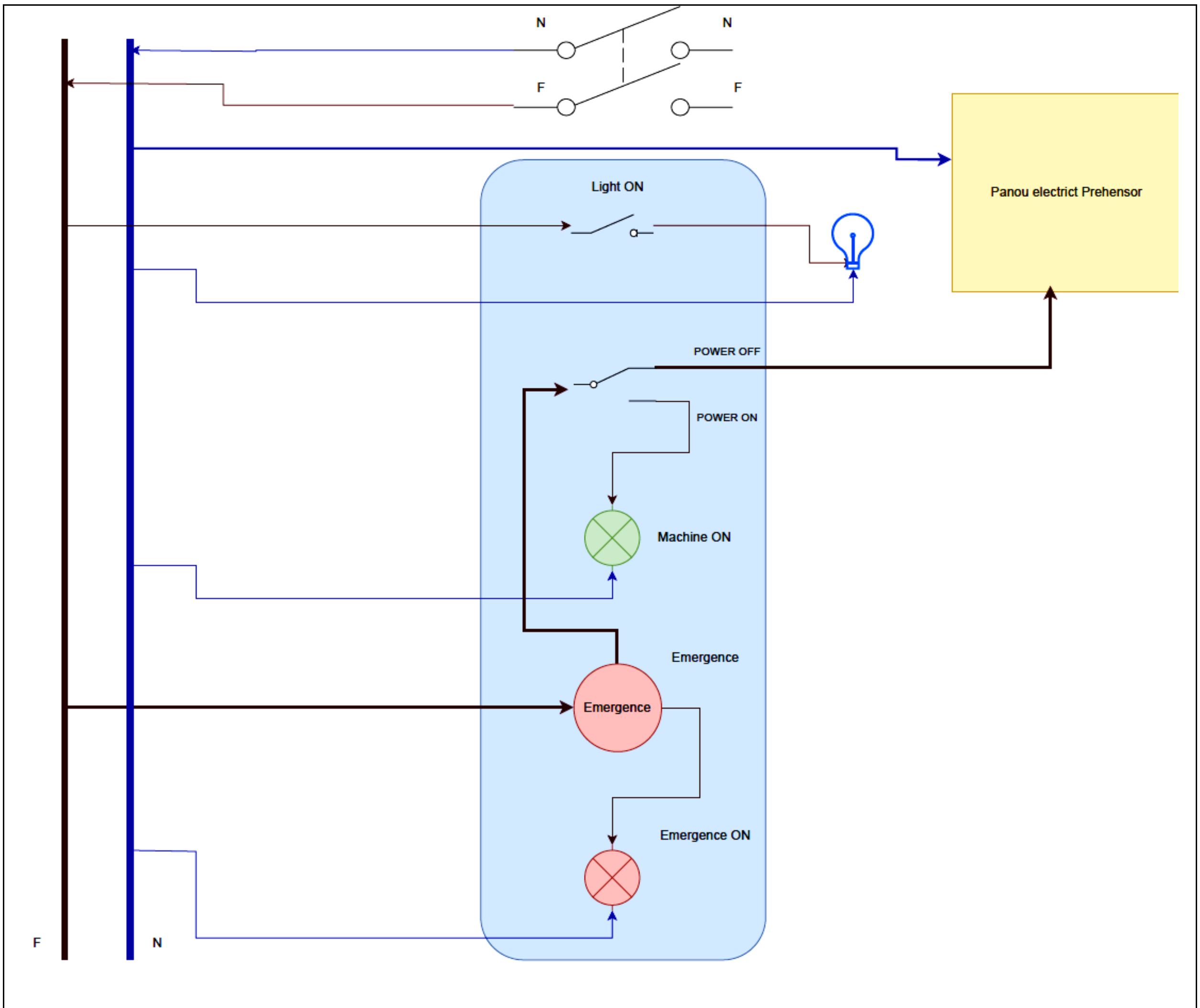


*Figure. 6.3. Electrical diagram of the control panel*

## 6.5. Gripper software development for self-adaptability

This development contains 3 software elements:
• Software development for each module of the gripper, this software is loaded on each controller;
• Software development on the Master control, it is designed to manage the modules according to the logical structure;
• Interface-type software application development.

### 6.5.1. Controller digital communications configuration

- Stepper motor
- Motor driver
- Force sensor
- Incremental optical sensor
- RGB LED for visual confirmation.

The configuration of the connections is as follows:
The driver is attached to digital pin 9 for PulPin+ and digital pin 8 for DIRPin+.

The Pul-, Ena- and Dir- lines are connected to GND.
The switches are connected as follows: the advance switch to digital pin 5 and the retreat switch to digital pin 4.
The encoder is connected with channel A to digital pin 2 and channel B to digital pin 3.
The force sensor is connected with DT to digital pin 6 and SCK to digital pin 7.
The RGB LED is connected with Red to digital pin 10, Green to digital pin 11 and Blue to digital pin 12.
A start/stop button for the grasping sequence is connected to digital pin 17.

```
#include <Stepper.h>

const int stepsPerRevolution = 200;


Stepper myStepper(stepsPerRevolution, 9, 8); // Pini pentru PUL+ și DIR+

const int switchAvans = 5;
const int switchRetras = 4;
const int pinEncoderA = 2;
const int pinEncoderB = 3;
const int pinDT = 6;
const int pinSCK = 7;
const int buttonStartStop = 17;

const int redPin = 10;
const int greenPin = 11;
const int bluePin = 12;

volatile int encoderValue = 0;
volatile int lastEncoded = 0;

void setup() {
  pinMode(switchAvans, INPUT);
  pinMode(switchRetras, INPUT);
  pinMode(pinEncoderA, INPUT);
  pinMode(pinEncoderB, INPUT);
  pinMode(pinDT, INPUT);
  pinMode(pinSCK, OUTPUT);
  pinMode(buttonStartStop, INPUT);
  pinMode(redPin, OUTPUT);
  pinMode(greenPin, OUTPUT);
  pinMode(bluePin, OUTPUT);
```

*Figure. 6.4. Declaring electronic components in software*

### 6.5.2. Establishing sensory parameters

Determinarea paramentrilor comuni ai senzorilor de forță pentru cele trei faze de prehensare.
Determinarea valorilor Fazei 1 (**Eroare! Fără sursă de referință.**). Valorile comune declarate în software pentru Faza 1 sunt cuprinse în intervalul -35 si +30 de unități.

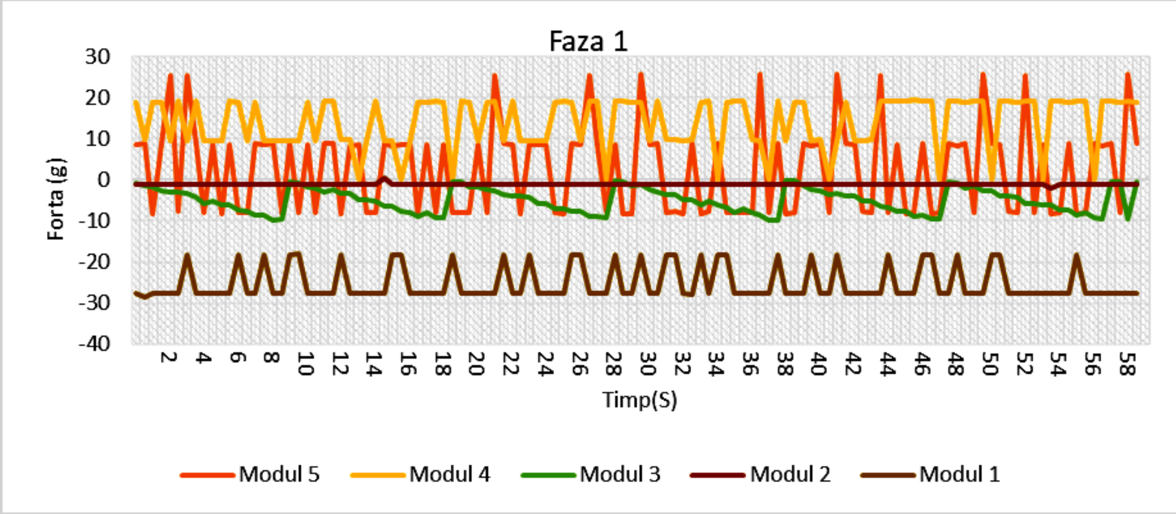


*Figure. 6.5. Parameters of the 5 modules in Phase 1*

Determination of angular values related to Sequence 1 (Figure. 6.6):
Common angular values declared in the software for Sequence 1 (the contact sequence) are between -550 and -900 units.

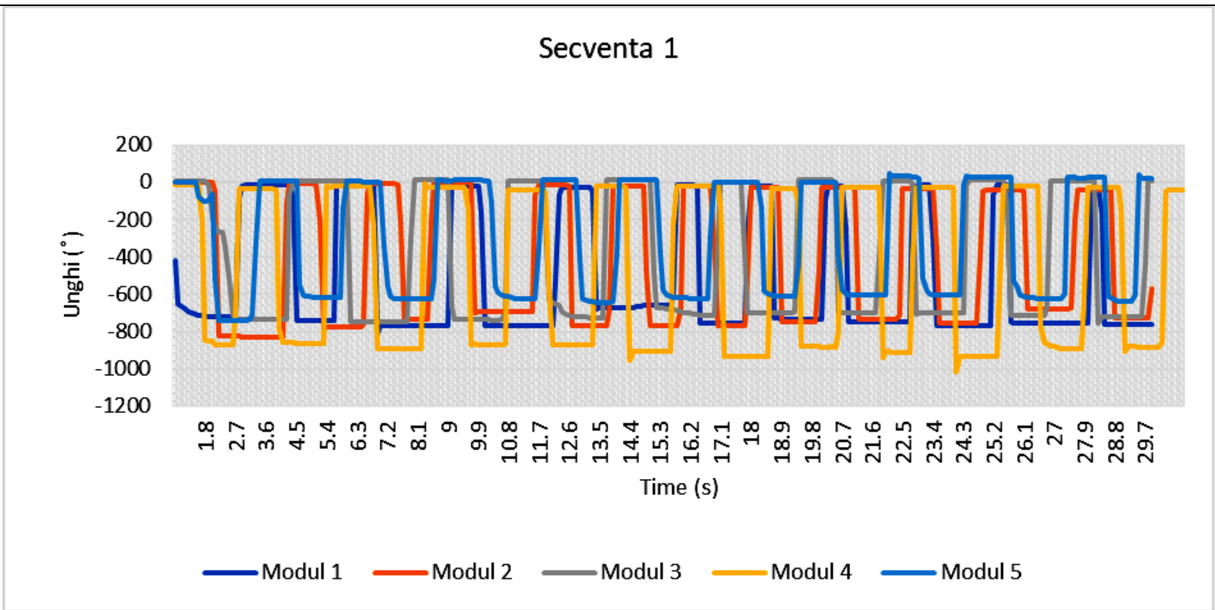


*Figure. 6.6. The angular values for the 5 modules in Sequence 1*

### 6.5.3. Realization of self-adaptive software

At this stage, a program was developed and implemented to manage the following operations and conditions according to the logical architecture, taking into account the previously collected sensor values:

**Condition 1:**

This is an initialization stage.

1. If digital button 17 is disabled (equal to 0), the motor will downshift until the retract switch is activated.

2. If the digital button 17 is activated, the grasping action will be initiated: grasping:

```
void loop() {
  if (digitalRead(buttonStartStop) == HIGH) {
    prehensare();
  } else {
    retragere();
  }
}
```

*Figure. 6.7. Initialization code*

**Condition 2:**

The stepper motor will advance until the advance switch is activated and retract until the retract switch is activated. This function is one of safety in order to protect the mechanical structure.

```
if (forwardState == HIGH) {
  digitalWrite(DIRPin, HIGH);  // Setează direcţia înainte
  continuousStep();
} else if (backwardState == HIGH) {
  digitalWrite(DIRPin, LOW);  // Setează direcţia înapoi
  continuousStep();
} else {
  stopMotor();
}
```

*Figure. 6.8. Safety function*

**Condition 3:**

Management Led

1. As long as the force sensor does not register values between +30 and -30, the LED will be blue.
2. As long as the encoder does not exceed the angular values of +20 and -20, the LED will remain blue.

```
void manageLED(int force, int encoder) {
  if (force > 30 || force < -30 || encoder > 20 || encoder < -20) {
    setColor(0, 0, 255); // Setează LED-ul pe albastru dacă forţa sau unghiul sunt în limite
  } else if (force >= 200 && force < 300) {
    setColor(255, 0, 0); // Setează LED-ul pe roşu dacă forţa este între -200 şi -300
  } else if (force >= 300 && force < 400) {
    setColor(255, 0, 0); // Setează LED-ul pe roşu dacă forţa este între -300 şi -400
  } else if (force >= 400) {
    setColor(0, 255, 0); // Setează LED-ul pe verde dacă forţa este stabilă la -400
  }
}
```

*Figure. 6.9. LED management functions*

1. If the values remain stable from the encoder (not fluctuating more than 10 units after the tightening stage), the LED will turn green.
2. If after tightening, the encoder value exceeds 10 units (represents slippage), the LED will turn red during this period and turn green again if the value stabilizes and the encoder does not indicate further decrease.

```
// Continuă să adaugi codul pentru gestionarea acțiunilor descrise
void prehensare() {
  // Verifică switch-ul de avans și deplasează motorul în direcția de avans
  while (!digitalRead(switchAvans) && digitalRead(buttonStartStop) == HIGH) {
    myStepper.step(1); // Avansează motorul cu un pas
    int force = analogRead(pinDT); // Citește valoarea senzorului de forță
    manageLED(force, encoderValue); // Actualizează starea LED-ului

    if (encoderValue >= -950 && encoderValue <= -550) {
      break; // Întrerupe bucla dacă encoderul ajunge în intervalul dorit
    }
  }

  // Verifică valoarea forței și ajustează dacă este necesar
  while (analogRead(pinDT) < 200) {
    myStepper.step(1); // Continuă să avansezi motorul
    int force = analogRead(pinDT);
    manageLED(force, encoderValue); // Actualizează starea LED-ului
  }
}

void retragere() {
  while (!digitalRead(switchRetras) && digitalRead(buttonStartStop) == LOW) {
    myStepper.step(-1); // Retrage motorul cu un pas
    int force = analogRead(pinDT); // Citește valoarea senzorului de forță
    manageLED(force, encoderValue); // Actualizează starea LED-ului
  }
}
```

*Figure. 6.10. The function of grasping and implementing sensor values*

**Condition 4:**

Prehension

1. The motor will advance until the encoder registers angular values between -550 and -950. Once this value is reached, the motor will continue to advance until the force sensor reaches -200.
2. If the force sensor value drops more than 20 units from -200, the motor will continue to advance until the sensor reads -300.
3. If the force sensor reading drops more than 20 units from -300 again, the motor will continue to advance until the sensor reads -400.
4. If at any point in the process the button on digital 17 becomes 0, the motor will downshift until the retract switch is activated.Dezvoltarea aplicației Android pentru intrefațarea panoului de comandă

Pentru a putea comunica şi controla sistemul de prehensiune este necesar un panou de control, unde se poate comuta modul de funcționare (manual, automat şi reset). În lipsa panoului de comandă s-a creat o aplicație Android ce comunică cu modulul Bluetooth implementat în panoul electric de test al prehensorului adaptiv.

To create an application that uses the internal communication system of the device (phone, tablet, etc.) a function is needed that calls on the internal programming library (Figure 6.11) [39].

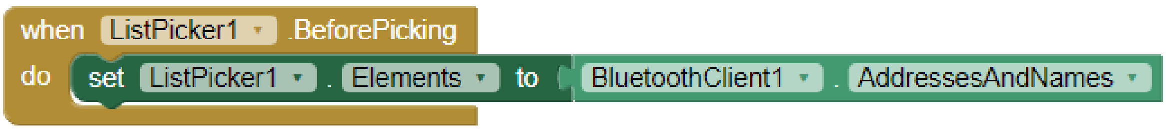


*Figure. 6.11. Bluetooth implementation function*

After the Bluetooth implementation function has been declared it is necessary to establish the connection with the bluetooth module of the gripper. To establish the connection, a device search function and a search trigger button are implemented (Figure 6.12).

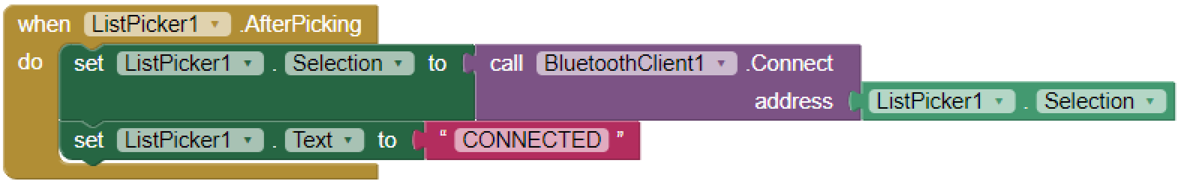


*Figure. 6.12. Bluetooth search function*

Commands passed to the controller on (serialRead) are numeric or alphanumeric, and each digit implemented in the function is passed to the controller. To be able to transmit (0) a button is needed to generate this "code" (Figure. 6.12).

After completing the functions that generate command "codes", they can be accessed with an Android interface containing the buttons and their explanations.

*Figure. 6.13. Object 1 with irregular shape*

*Figure. 6.14. Object 2 with irregular shape*

*Figure. 6.15. Object 3 with irregular shape*

The "PREHENSOR" command is used to search for Bluetooth devices, followed by selecting the desired device.

In this interface there is no access to the code behind it, where are the functions that send characters to the gripper (Figure. 6.16).Simularea reală a autoadaptivitații

For real self-adaptivity testing and simulation, several solid objects with irregular shapes were taken and the gripper's self-adaptivity was tested.

In Figure. 6.13 object number 1 is rendered in order to actually simulate self-adaptivity. The object was held by the hand until the grasper achieved grasping of the object, in Figure. 6.17 showing its holding position.

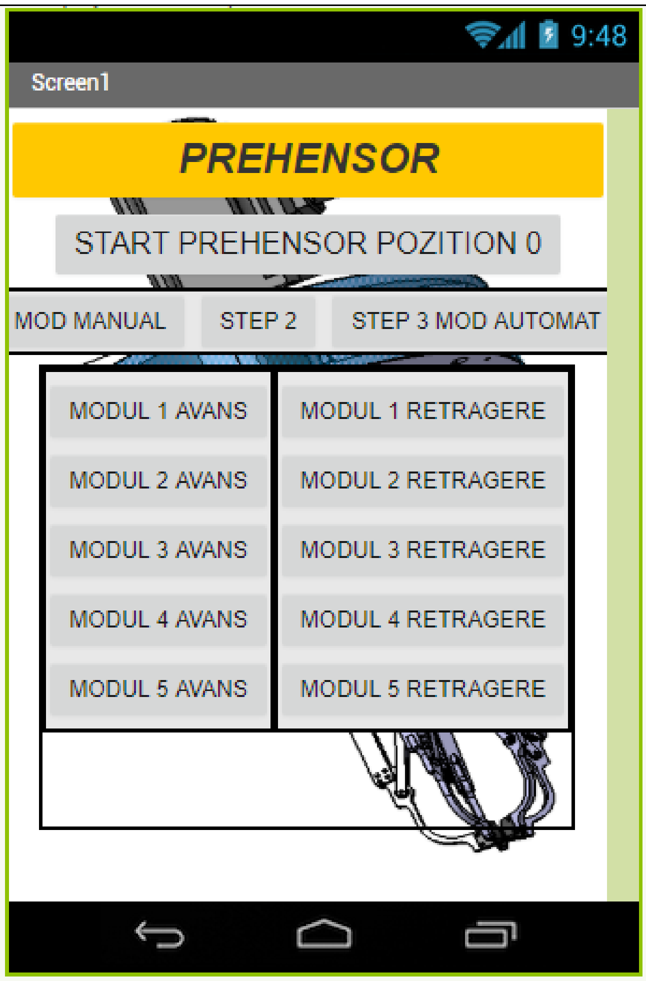


*Figure. 6.16. Android interface*

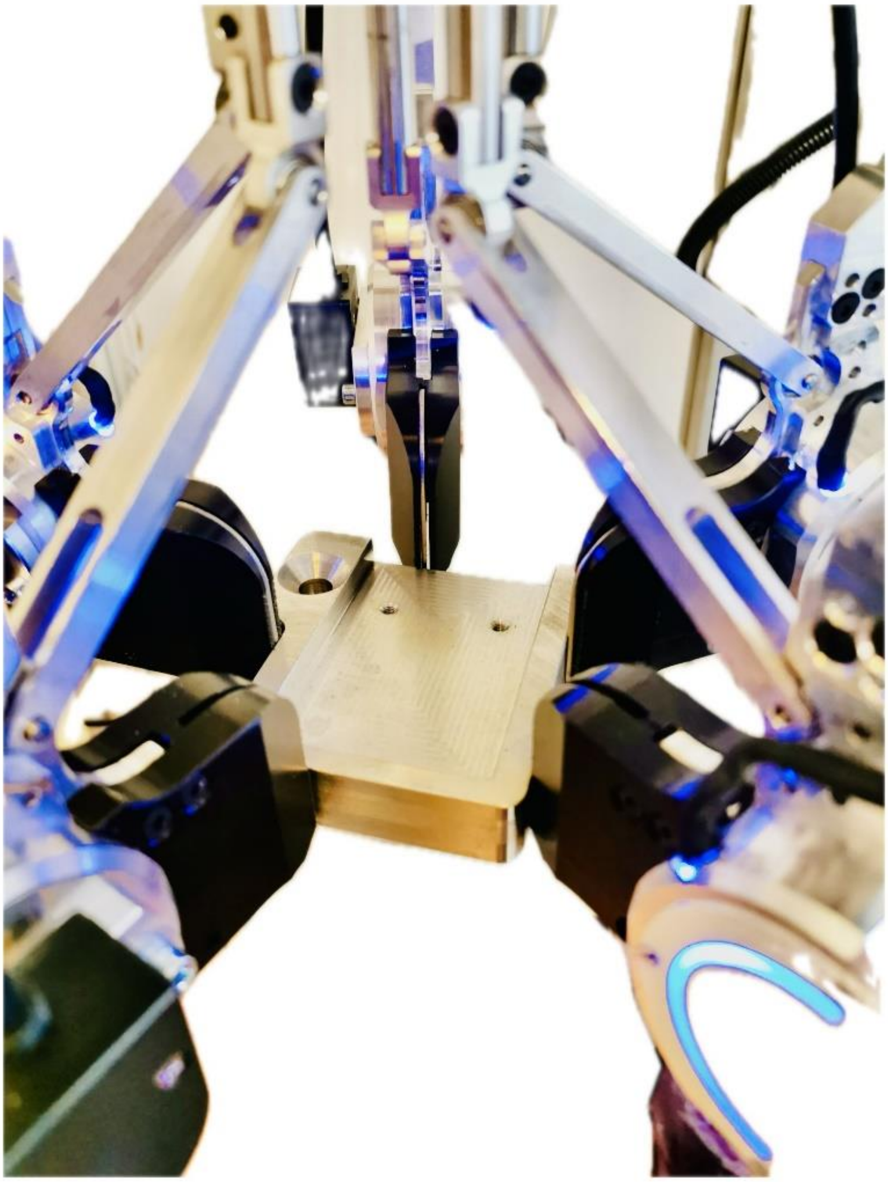

*Figure. 6.17. Top view of grasping object number 1*

In Figure. 6.14 the object number 2 is rendered in order to actually simulate the self-adaptivity. The object was held by the hand until the grasper achieved grasping of the object, in Figure. 6.18, showing its holding position.

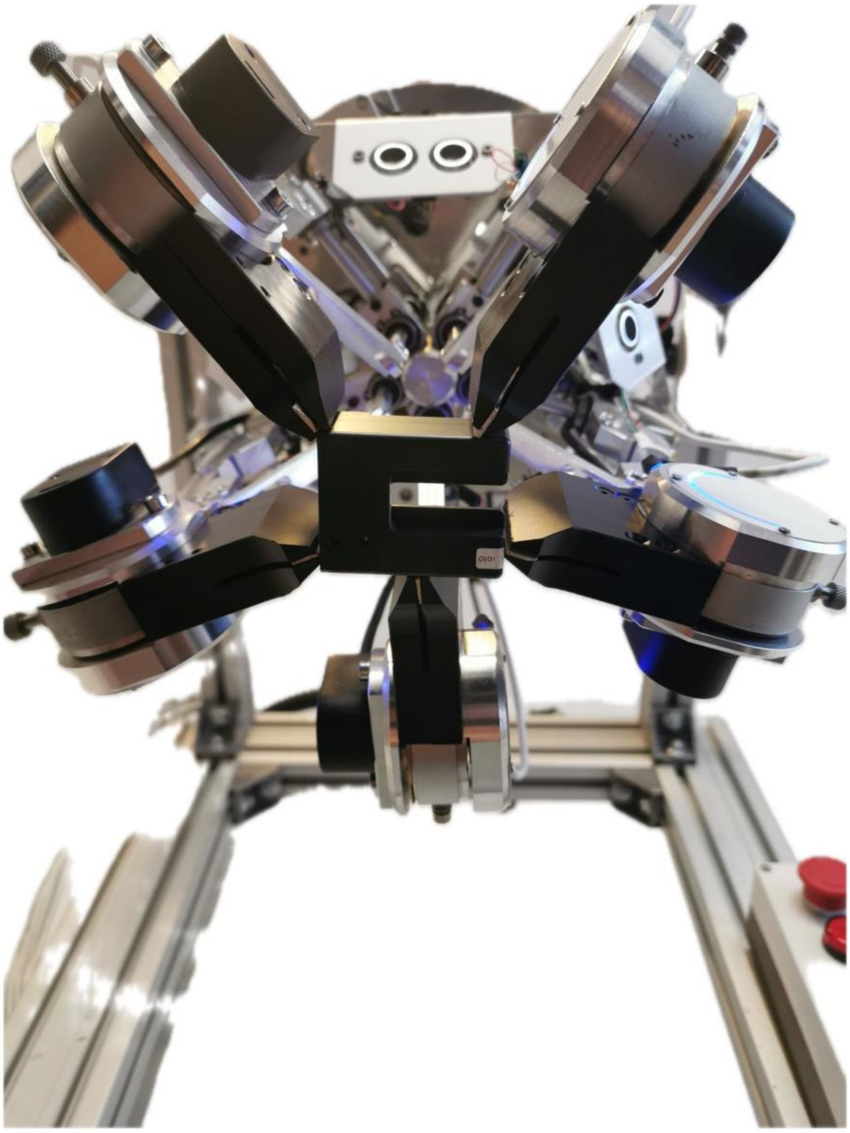

*Figure. 6.18. Bottom view of grasping object number 2*

In Figure. 6.15 object number 3 is rendered in order to simulate the real self-adaptivity. The object was held by the hand until the grasper achieved grasping the object, in

Figure. 6.19 and Figure. 6.20 showing its attachment positions.

## 6.6. Conclusions

The gripper was successfully performed, with each module of the gripper operating independently and correctly.

It is necessary to optimize each individual module, a process that involves adjustments to the software specific to each module, depending on the data from its sensors. This optimization will help to improve the prehension process.

All tests were performed without the gripper performing additional movements that would introduce inertial forces on the object or modules.

Creating a well-defined logical architecture, with independent controllers for each module of the gripper, facilitated the implementation of self-adaptivity. The individual control of the modules and the quick decisions made by the Master controller contributed to the adaptability and reliability of the gripper in various prehension conditions.

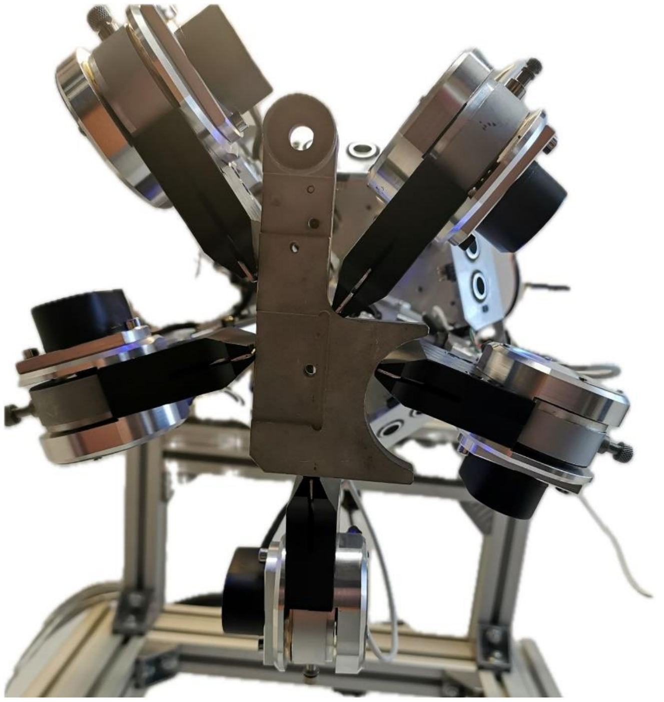

*Figure. 6.19. Bottom view of grasping object number 3*

The implementation of an effective communication structure between the Master controller and the Slave modules allowed a precise and synchronized coordination of the prehension process. The ability to transmit simultaneous commands and collect critical data about the status of each module contributed significantly to the overall performance of the gripper.

The implementation of a Master-Slave scheme in the gripper communication enables centralized control of the gripper, ensuring efficient management of each module according to its specific status and requirements. This logical structure facilitates quick and accurate decisions during prehension processes, contributing to the adaptability and efficiency of the system.

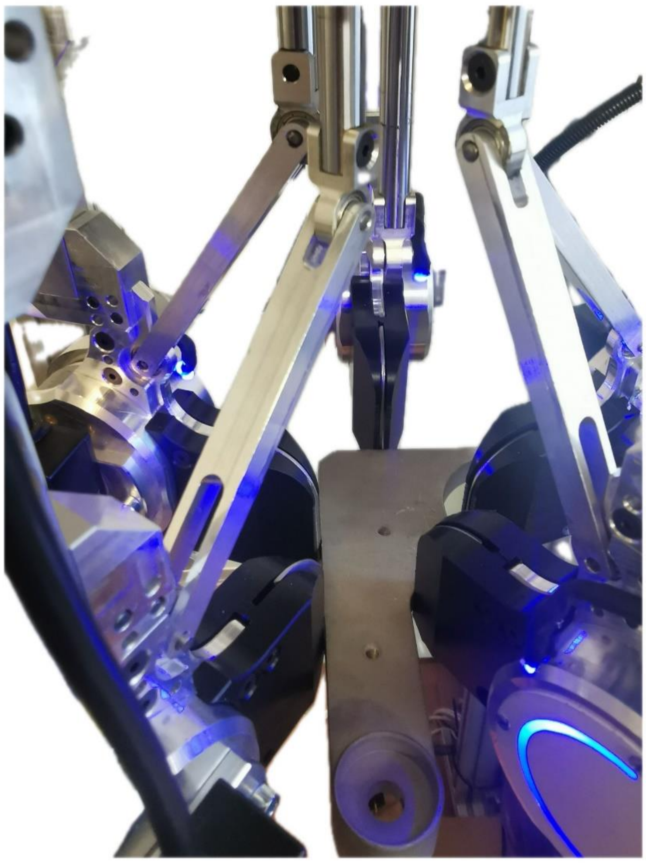

*Figure. 6.20. Top view of grasping object number 3*

The design and implementation of the control panel scheme facilitated precise control of the gripper, including initiation, monitoring and adjustment of the gripper according to the requirements of each object. This electrical and software integration ensured an efficient interaction between the operator and the gripper system, significantly contributing to the achievement of the goals of adaptability and correct operation of the gripper.

# 7. GENERAL CONCLUSIONS. PERSONAL CONTRIBUTIONS. DISSEMINATION OF RESULTS. FUTURE DIRECTIONS OF RESEARCH

## 7.1. General conclusions

In the case of the doctoral thesis entitled "Self-adaptive prehension system for solid parts with irregular shapes", studies carried out by the author were presented, regarding:

1. Fundamental analysis methods used in robotics have highlighted the importance of mathematical models and simulations for the design and evaluation of robotic systems. The integration of these methods allowed the optimization of gripper performance and reliability for a variety of applications.
2. Perception technologies and strategies used in robotics have emphasized the essential role of sensors in data collection and interpretation. The integration of advanced perception systems has significantly contributed to the gripper's autonomy and adaptability for various operational contexts.
3. Advanced control techniques and algorithms used in robotics have highlighted the importance of implementing accurate and efficient systems for handling and navigating robots in a safe and efficient manner. The integration of these methods enabled the optimization of gripper performance and adaptability in complex applications.
4. Technologies and strategies used for advanced manipulation in robotics highlighted the evolution and applicability of solutions for precise object manipulation in varied environments. The implementation of these techniques has improved the operational efficiency and flexibility of the grasping system in industrial and research applications.
5. Object grasping concepts and applications focused on the design, implementation and evaluation of grippers for handling complex objects in industrial contexts. The integration of innovative solutions in robotic prehension has significantly contributed to the increase of operational efficiency and reliability.

## 7.2. Personal contributions

1) Existing prehension systems in the global industry were studied.

2) The types of sensors used in prehension systems were researched and it was concluded that the most used are force sensors, proximity sensors, encoders for displacement verification.

3) An innovative kinematic configuration for the gripper with five independent fingers has been developed, based on a parallelogram-type architecture, which provides flexibility and precision in gripper movements.

4) A set of algorithms have been developed to control the movements of the gripper, ensuring that it can quickly and accurately adapt finger positions to handle objects of various shapes and sizes.

5) Detailed 3D modeling of the gripper was carried out using Catia CAD software, integrating the proposed kinematic configuration to ensure its geometric accuracy and functionality.

6) Different materials of the 3D model were implemented and tested, to identify the optimal solutions that provide durability and high performance in the use of the gripper.

7) Kinematic simulations were performed to evaluate the dynamic performance of the gripper, adjusting the design according to the results obtained to improve the adaptability and precision of the movements.S-a efectuat o analiză structurală detaliată folosind software de analiză prin elemente finite (FEA), evaluând rezistența și durabilitatea prehensorului sub diferite condiții de încărcare și utilizare.

8) The modularity of the gripper was designed and analyzed, ensuring that each module can work independently and assembled, without affecting the rest of the system.

9) Advanced simulations were performed to evaluate the strength and durability of the gripper components in various object handling scenarios.

10) An advanced object shape recognition algorithm was developed and implemented, used to automatically determine the optimal prehension mode based on the geometry and dimensions of the object.

11) Adaptive control strategies have been proposed and implemented that allow the grasper to automatically adjust the pressure and positioning of the grasping fingers according to the characteristics of the sensed object.

12) Optimized the wiring diagram to minimize interference and ensure operational stability in various environmental conditions.

13) Designed and implemented an efficient power supply system to support the power requirements of the gripper, considering power consumption and battery life in practical applications.S-a dezvoltat interfața de control utilizator (UI) pentru a permite operatorului să interacționeze eficient cu prehensorul, inclusiv setarea parametrilor de operare și monitorizarea stării sistemului în timp real.

14) Optimized the control algorithms to ensure accurate and fast gripper movements, adapting them to quickly respond to changes in the operating environment and object handling requirements.

15) Mathematical models were developed and advanced simulations were performed to evaluate and control the structural vibrations of the gripper during operations.

16) Integrated the reducer into the gripper system, evaluating its impact on overall performance and vibration reduction.

17) Mathematical calculation was performed to determine the optimal reduction ratio according to torque and precision requirements.

18) The performance of the reducer was experimentally analyzed in terms of reducing vibrations and improving control over movements.

19) A logical architecture has been designed and implemented that allows independent handling from mechanical, electrical and software points of view, ensuring the correct integration of each module into the overall system.

20) The components of the sensory system were detailed, including the resistive encoder, the plate for translation and rotation movement, and the inductive sensor, highlighting the role of each component in ensuring the functionality of the system.

21) Algorithms were proposed and implemented to optimize corrections in real time according to the variability of the parameters generated by the sensors during movement, ensuring the adaptability of the system to the prehension conditions specific to each object.

22) The functionality of the sensory system was integrated and tested on classic prehension systems, demonstrating the maximum performance of the self-adaptive prehension system compared to traditional variants.S-a testat și validat funcționalitatea sistemului, demonstrând eficiența și precizia acestuia în manipularea obiectelor fără a le deforma sau a le amprenta.

23) The Master-Slave communication scheme has been designed in detail, ensuring an efficient and synchronized interaction between the Master controller and the Slave modules. This involved defining the communication protocol, assigning responsibilities and implementing synchronization mechanisms.

24) An advanced control algorithm has been developed and implemented for the Master controller, which allows quick decision-making based on the feedback received from the Slave modules. This algorithm optimizes the reaction time of the gripper in the prehension process, helping to improve the efficiency and accuracy of the system.

25) Integrated the Master-Slave communication protocol within the gripper and tested it to ensure correct and secure data transmission between the Master controller and the Slave modules. This also involved the development of complex test scenarios to validate communication performance.

## 7.3. Dissemination of results

Part of the results obtained from the study carried out during the doctoral internship were disseminated through the publication of several scientific articles, as first author and co-author, presented at international conferences or published in specialized journals, as follows:

[1] **C. Frincu**, I. Stroe, and I. Staretu, 'Constructive Optimization of an Adaptive Mechanical Gripper Based on Vibration Level', 2023. doi: 10.1109/EMES58375.2023.10171726.

[2] **C. I. Frincu**, I. Stroe, and I. Staretu, 'Innovative self-adaptive gripper design, functional simulation, and testing prototype', *Int. J. Adv. Robot. Syst.*, vol. 19, no. 4, pp. 1–16, 2022, doi: 10.1177/17298806221119345.

[3] **I. C. Frincu** and I. Stroe, 'The state of stress and deformation by the finite element method of the mechanical structure for a self-adaptive prehensor', IOP Conf. Ser. Mater. Sci. Eng., vol. 568, no. 1, 2019, doi: 10.1088/1757-899X/568/1/012088.

[4] **C. Frincu** and I. Stroe, 'The state of the modular element structure of a prehensor through virtual prototyping', *IOP Conf. Ser. Mater. Sci. Eng.*, vol. 514, no. 1, 2019, doi: 10.1088/1757-899X/514/1/012024.

[5] **C. Frincu** and I. Stroe, 'Mechanical Geometry of a Self-Adaptive Prehensor with 2 or more Fingers', *Int. J. Control Syst. Robot.*, vol. 4, pp. 33–36, 2019.

[6] **C. Frincu** and I. Stroe, 'The structure of a sliding sensory system for a self-adaptive prehensor', *IOP Conf. Ser. Mater. Sci. Eng.*, vol. 568, no. 1, 2019, doi: 10.1088/1757-899X/568/1/012071

## 7.4. Future research directions

This PhD thesis makes significant contributions to the efficiency and shortening of handling processes in the industrial sector. In order to increase the attractiveness of the proposed process for manufacturers in this field, a considerable improvement of the procedure is essential.
In this direction, the following research directions can be explored for the industry:
1. Software optimization to improve grip.
2. Integration of an optical sensor to measure the distance between the gripper and the work table.
3. Applying the gripper to a KUKA industrial robot to obtain the following information:

- Analysis of plastic and elastic deformations of the gripper under conditions of rectilinear, circular and oscillatory motion at different speeds.Evaluarea vibrațiilor exercitate asupra bacurilor în condiții diverse de mișcare.

o Calculation of the inertial forces generated by a gripper handling an object weighing 1 kg.

o Determining the grip forces needed to manipulate objects.Perfecționarea structurii prehensorului.

2. 2. Updating the software with the parameters obtained from the research.
3. 3. Integration of a 3D camera to optimize the grasping process.
4. 4. Implementation of artificial intelligence through the development of an automatic learning algorithm (Machine Learning).

## BIBLIOGRAPHY


[1] 'Zoo.ro'. http://www.zoo.ro/

[2] M. Manz, S. Bartsch, M. Simnofske, and F. Kirchner, 'Development of a self-adaptive gripper and implementation of a gripping reflex to increase the dynamic payload capacity', *47th Int. Symp. Robot. ISR 2016*, no. June, pp. 56–62, 2016.

[3] D. ŢÂRLIMAN, 'Cercetări privind sistemele de prehensiune ale roboţilor industriali acţionate cu ajutorul muşchilor pneumatici Research concerning the gripper systems of industrial robots actuated by pneumatic muscles', Şcoala Doctorală Interdisciplinară, Brasov, 2014.

[4] S. Jonathan Monteiro, 'Adaptive Gripping Technology Development of a gripper interface for SCHUNK Dextrous Hand', 2010.

[5] S. Ionel, N. Mircea, and A. N, *Mâini mecanice. Mecanisme antropomorfe de prehensiune pentru protezare şi roboţi*. Brasov, 2001.

[6] U. Fischer, *Mechanical and metal trades handbook*. Tabellenbuch Metall, 2008.

[7] I. Staretu, *Prehensoare mecanice reconfigurabile cu trei şi patru degete pentru roboţi (II)*.

[8] I. Staretu, *Sisteme de prehensiune (Ediția I)*. Brasov, 1996.

[9] I. Staretu, *Sisteme de prehensiune (Editia II)*. 2010.

[10] 'Start Production Faster - Robotiq'. https://robotiq.com/

[11] 'Tehnologie de automatizare si solutii de instruire tehnica | Festo RO'. https://www.festo.com/ro/ro/

[12] T. Ortmaier and G. Hirzinger, 'Cartesian Control of Robots with Working-Position Dependent Dynamics', *IFAC Proc. Vol.*, vol. 33, no. 27, pp. 617–621, 2000, doi: 10.1016/s1474-6670(17)37999-5.

[13] X. Han and R. J. Richards, 'Variable structure control of robot manipulators in cartesian space with efficient computation', *IFAC Proc. Vol.*, vol. 27, no. 14, pp. 109–114, 1994, doi: 10.1016/s1474-6670(17)47302-2.

[14] S. Ionel, 'PREHENSOARE ANTROPOMORFE CU BARE ARTICULATE SAU CU FIRE ŞI ROLE PENTRU ROBOŢI INDUSTRIALI – SINTEZĂ, ANALIZĂ', no. 1, 2009.

[15] G. Castelli, E. Ottaviano, and P. Rea, 'A Cartesian Cable-Suspended Robot for improving end-users' mobility in an urban environment', *Robot. Comput. Integr. Manuf.*, vol. 30, no. 3, pp. 335–343, 2014, doi: 10.1016/j.rcim.2013.11.001.

[16] M. A. Arteaga, A. Castillo-Sánchez, and V. Parra-Vega, 'Cartesian control of robots without dynamic model and observer design', *Automatica*, vol. 42, no. 3, pp. 473–480, 2006, doi: 10.1016/j.automatica.2005.11.004.

[17] V. Lippiello and F. Ruggiero, *Cartesian impedance control of a UAV with a robotic Arm*, vol. 10, no. PART 1. IFAC, 2012. doi: 10.3182/20120905-3-HR-2030.00158.

[18] V. Parra-Vega, R. García-Rodríguez, and F. Ruiz-Sanchez, 'Cartesian sliding PD force-position control for constrained robots under jacobian uncertainty', *IFAC Proc. Vol.*, vol. 38, no. 1, pp. 145–150, 2005, doi: 10.3182/20050703-6-cz-1902.01294.

[19] H. Celikag, N. D. Sims, and E. Ozturk, 'Cartesian stiffness optimization for serial arm robots', *Procedia CIRP*, vol. 77, no. Hpc, pp. 566–569, 2018, doi: 10.1016/j.procir.2018.08.222.

[20] A. Wahrburg, B. Matthias, and H. Ding, 'Cartesian contact force estimation for robotic manipulators - A fault isolation perspective', *IFAC-PapersOnLine*, vol. 28, no. 21, pp. 1232–1237, 2015, doi: 10.1016/j.ifacol.2015.09.694.

[21] A. Catalin, *Simularea pe calculator a sistemelor mecanice articulate*. Brasov, Romania: Lux Libris, 2000.

[22] A. Catalin, *Softuare Platform for Analyzing and Optimizing the Mechanical System*. Brașov, Romania: Springer Sience&Business Media, 2009.

[23] 'PowerGripper | Festo CA'. https://www.festo.com/ca/en/e/about-festo/research-and-development/bionic-learning-network/highlights-from-2010-to-2012/powergripper-id_33664/

[24] C. Stăncescu, S. I., and M. Bolboe, 'Aspects Concerning the Systematization of Gripping Device with Jaws', in *The 9 th International Conference of Mechanisms and Mechanical Transmissions*,

2004, pp. 729–734.

[25] Y. S. Fan and G. T. Zheng, 'Research of high-resolution vibration signal detection technique and application to mechanical fault diagnosis', *Mech. Syst. Signal Process.*, vol. 21, no. 2, pp. 678–687, Feb. 2007, doi: 10.1016/J.YMSSP.2005.10.001.

[26] F. Beltrán-Carbajal, G. Silva-Navarro, F. Beltrán-Carbajal, and G. Silva-Navarro, 'Active vibration control in Duffing mechanical systems using dynamic vibration absorbers', *JSV*, vol. 333, no. 14, pp. 3019–3030, 2014, doi: 10.1016/J.JSV.2014.03.002.

[27] S. Electronics, 'Vibration Sensor SW-18010P'. https://www.sunrom.com/p/vibration-sensor-sw-18010p

[28] F. J. Blaauw *et al.*, 'Let's get Physiqual – An intuitive and generic method to combine sensor technology with ecological momentary assessments', *J. Biomed. Inform.*, vol. 63, pp. 141–149, Oct. 2016, doi: 10.1016/J.JBI.2016.08.001.

[29] L. Dal Bo, P. Gardonio, and E. Turco, 'Analysis and scaling study of vibration energy harvesting with reactive electromagnetic and piezoelectric transducers', *J. Sound Vib.*, vol. 484, p. 115510, 2020, doi: 10.1016/j.jsv.2020.115510.

[30] R. S. Langley, 'On the statistical mechanics of structural vibration', *J. Sound Vib.*, vol. 466, p. 115034, 2020, doi: 10.1016/j.jsv.2019.115034.

[31] F. Li, H. Wu, and P. Wu, 'Vibration fatigue dynamic stress simulation under non-stationary state', *Mech. Syst. Signal Process.*, vol. 146, p. 107006, 2021, doi: 10.1016/j.ymssp.2020.107006.

[32] F. J. Badesa, R. Morales, N. Garcia-Aracil, J. M. Sabater, A. Casals, and L. Zollo, 'Auto-adaptive robot-aided therapy using machine learning techniques', *Comput. Methods Programs Biomed.*, vol. 116, no. 2, pp. 123–130, 2014, doi: 10.1016/j.cmpb.2013.09.011.

[33] Z. Gosiewski and A. P. Koszewnik, 'Fast prototyping method for the active vibration damping system of mechanical structures', *Mech. Syst. Signal Process.*, vol. 36, no. 1, pp. 136–151, 2013, doi: 10.1016/j.ymssp.2011.12.011.

[34] H. B. M. GmbH, 'Strain Gauges.' doi: 10.5040/9781501365072.15711.

[35] S. Aurel Cornle, *Senzori si traductoare*. Editura Universității Transilvania Brașov, 2015.

[36] S. Ioan, *Senzori si traductoare pentruroboti industriali*. 2000.

[37] 'E5 | US Digital'. https://www.usdigital.com/products/encoders/incremental/kit/e5/

[38] 'Encoder rotativ Arduino'. https://www.robofun.ro/mecanice/encoder-rotativ-arduino.html

[39] 'MIT App Inventor'. https://appinventor.mit.edu/

# ANNEX

## Appendix 1. Measured vibration values for each module of the gripper

### Appendix 1.1. Vibrations in module 1

| Module 1 Frequency (Hz) | | |
|---|---|---|
| x | y | z |
| 0 | 0 | 97 |
| 0 | 0 | 0 |
| 5503 | 0 | 478 |
| 7156 | 214456 | 549 |
| 139435 | 97289 | 259 |
| 68474 | 13610 | 7167 |
| 25117 | 1350 | 269 |
| 1445 | 3309 | 52226 |
| 9271 | 11 | 58 |
| 0 | 14075 | 22569 |
| 53711 | 1588 | 19690 |
| 520 | 14990 | 26852 |
| 6352 | 5188 | 12879 |
| 354 | 24106 | 46558 |
| 350 | 6009 | 39535 |
| 186 | 1122 | 166 |
| 137 | 78 | 1226 |
| 1143 | 70 | 22935 |
| 352 | 1302 | 0 |
| 74 | 1096 | 3195 |
| 1076 | 1169 | 372 |
| 266 | 18148 | 125 |
| 36132 | 30709 | 300 |
| 345544 | 335426 | 950 |
| 42976 | 4843 | 2459 |
| 22356 | 52460 | 5054 |
| 33796 | 426 | 89 |
| 36684 | 79 | 36 |
| 2133 | 62 | 1420 |
| 8809 | 183 | 1401 |
| 1941 | 237 | 100 |
| 2335 | 49541 | 1982 |
| 1391 | 83252 | 1346 |
| 1054 | 111806 | 204 |
| 143 | 3361 | 3308 |
| 133 | 147274 | 1238 |
| 295 | 2133 | 0 |
| 1543 | 1259 | 2097 |
| 699 | 42 | 1192 |
| 79 | 164 | 531 |
| 6994 | 332 | 1958 |

| Module 1 Frequency (Hz) | | |
|---|---|---|
| x | y | z |
| 17155 | 870 | 1596 |
| 3256 | 290618 | 2512 |
| 5583 | 163894 | 2098 |
| 9422 | 946 | 1753 |
| 2216 | 29 | 46 |
| 552 | 1124 | 2164 |
| 1529 | 407 | 602 |
| 99 | 29 | 0 |
| 718 | 955 | 3755 |
| 454 | 2885 | 3990 |
| 245 | 11519 | 422 |
| 742 | 107392 | 3650 |
| 1096 | 250657 | 8962 |
| 1353 | 6716 | 5147 |
| 392 | 17186 | 5109 |
| 94 | 7450 | 4734 |
| 2638 | 30699 | 2744 |
| 8939 | 63947 | 3880 |
| 243 | 30275 | 233 |
| 356 | 5218 | 3568 |
| 6085 | 176 | 7123 |
| 4556 | 276398 | 2191 |
| 3842 | 7278 | 3398 |
| 27398 | 1190 | 399 |
| 2201 | 1012 | 4622 |
| 362 | 2278 | 3263 |
| 1246 | 23315 | 3990 |
| 16 | 46830 | 621 |
| 4 | 1104 | 4187 |
| 29 | 575 | 4738 |
| 4280 | 371 | 4174 |
| 1659 | 160 | 7125 |
| 52144 | 336 | 3310 |
| 176792 | 423 | 205 |
| 2931 | 220 | 0 |
| 48852 | 653 | 3823 |
| 144640 | 294015 | 149 |
| 36568 | 70684 | 4099 |
| 16752 | 2135 | 0 |
| 4958 | 55071 | 2447 |
| 13989 | 809 | 5475 |

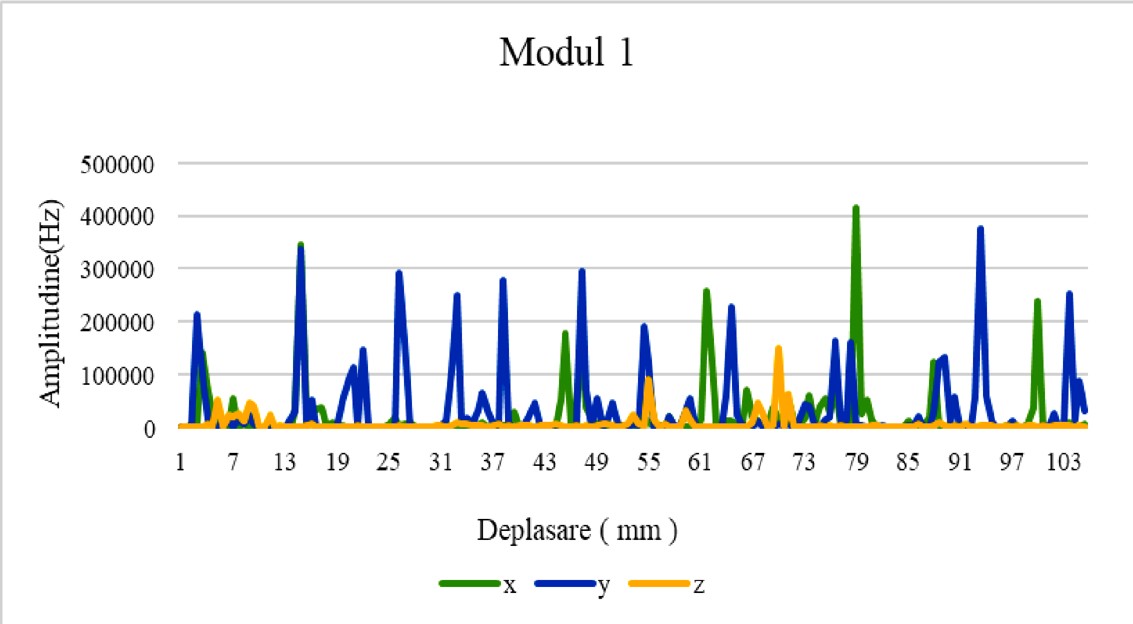


**Appendix 2. Vibration values measured on the 3 axes of the chassis on which the 5 gripper modules are attached**

| Chassis (Hz) | | | Chassis (Hz) | | |
|---|---|---|---|---|---|
| z | y | x | z | y | x |
| 0 | 0 | **0** | 0 | 76 | 3105 |
| 2 | 0 | 0 | 3 | 11 | 2434 |
| 3 | 75 | 21 | 980 | 0 | 421 |
| 8 | 1149 | 74 | 2 | 7 | 0 |
| 2 | 110 | 104 | 918 | 38 | 0 |
| 2 | 14 | 109 | 37 | 13 | 424 |
| 0 | 8 | 197 | 11 | 21 | 514 |
| 2 | 3 | 1474 | 2 | 7 | 342 |
| 2 | 30 | 16472 | 2 | 30 | 0 |
| 0 | 50 | 810 | 2 | 18 | 93 |
| 2 | 38 | 450 | 0 | 14 | 278 |
| 2 | 30 | 273 | 4 | 18 | 1244 |
| 0 | 3 | 1861 | 3 | 30 | 1845 |
| 0 | 7 | 2006 | 4 | 38 | 3036 |
| 2 | 18 | 435 | 38 | 7 | 1764 |
| 2 | 17 | 223 | 38 | 68 | 623 |
| 0 | 50 | 209 | 38 | 8 | 1933 |
| 28 | 38 | 187 | 37 | 18 | 67 |
| 37 | 38 | 254 | 267 | 27 | 1519 |
| 6 | 8 | 428 | 31 | 12 | 2403 |
| 35 | 38 | 3939 | 4 | 7 | 1853 |
| 2 | 38 | 424 | 0 | 21 | 108 |
| 37 | 31 | 86 | 2 | 43 | 823 |
| 0 | 7 | 55 | 2 | 7 | 528 |

| Chassis (Hz) | | |
|---|---|---|
| z | y | x |
| 3 | 89 | 72 |
| 2 | 101 | 119 |
| 5 | 121 | 2879 |
| 0 | 67 | 1242 |
| 0 | 0 | 43 |
| 2 | 0 | 0 |
| 478 | 0 | 546 |
| 18 | 0 | 5265 |
| 1541 | 0 | 4149 |
| 1695 | 208 | 3651 |
| 0 | 17 | 124 |
| 0 | 101 | 610 |
| 252 | 7 | 0 |
| 3 | 38 | 1025 |
| 0 | 17 | 204 |
| 2 | 38 | 311 |

| Chassis (Hz) | | |
|---|---|---|
| z | y | x |
| 2 | 38 | 0 |
| 0 | 17 | 87 |
| 3 | 38 | 166 |
| 28 | 38 | 192 |
| 38 | 20 | 157 |
| 2 | 12 | 648 |
| 37 | 692 | 335 |
| 33 | 0 | 2258 |
| 2 | 2103 | 2571 |
| 0 | 343 | 12353 |
| 0 | 2 | 1650 |
| 38 | 7 | 1715 |
| 40 | 13 | 907 |
| 0 | 1359 | 556 |
| 3 | 740 | 1152 |

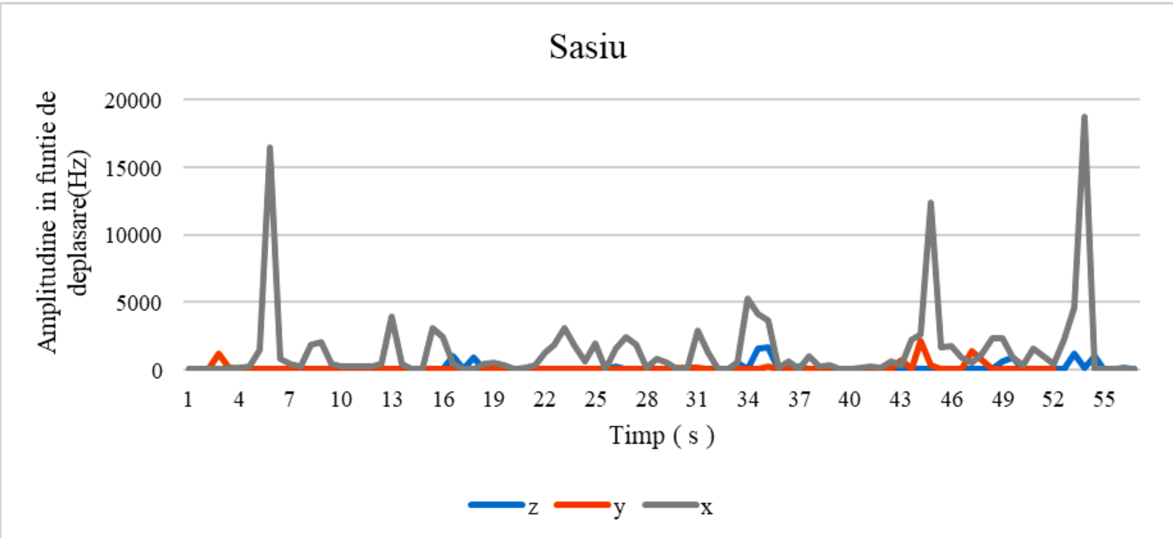


## Appendix 3. Collected force phase data for each gripper module

### Appendix 3.1. Module 1 – Phase 1

| Values mode 1 (free noise) |
|---|
| 17:56:01.365 -> Greutate: -18.07 unități |
| 17:56:01.876 -> Greutate: -27.65 unități |
| 17:56:02.433 -> Greutate: -28.47 unități |
| 17:56:02.949 -> Greutate: -27.63 unități |
| 17:56:03.463 -> Greutate: -27.66 unități |
| 17:56:03.975 -> Greutate: -27.62 unități |
| 17:56:04.534 -> Greutate: -27.62 unități |
| 17:56:05.045 -> Greutate: -18.34 unități |

| Values mode 1 (free noise) |
|---|
| 17:56:05.557 -> Greutate: -27.65 unități |
| 17:56:06.115 -> Greutate: -27.66 unități |
| 17:56:06.627 -> Greutate: -27.63 unități |
| 17:56:07.182 -> Greutate: -27.74 unități |
| 17:56:07.695 -> Greutate: -27.65 unități |
| 17:56:08.209 -> Greutate: -18.25 unități |
| 17:56:08.720 -> Greutate: -27.67 unități |
| 17:56:09.279 -> Greutate: -27.68 unități |

| Values mode 1 (free noise) |
|---|
| 17:56:09.792 -> Greutate: -18.24 unități |
| 17:56:10.305 -> Greutate: -27.65 unități |
| 17:56:10.822 -> Greutate: -27.65 unități |
| 17:56:11.376 -> Greutate: -18.15 unități |
| 17:56:11.884 -> Greutate: -18.09 unități |
| 17:56:12.396 -> Greutate: -27.71 unități |
| 17:56:12.906 -> Greutate: -27.70 unități |
| 17:56:13.463 -> Greutate: -27.64 unități |
| 17:56:13.975 -> Greutate: -27.74 unități |
| 17:56:14.490 -> Greutate: -18.21 unități |
| 17:56:15.049 -> Greutate: -27.70 unități |
| 17:56:15.565 -> Greutate: -27.60 unități |
| 17:56:16.078 -> Greutate: -27.63 unități |
| 17:56:16.590 -> Greutate: -27.71 unități |
| 17:56:17.104 -> Greutate: -27.69 unități |
| 17:56:17.663 -> Greutate: -18.37 unități |
| 17:56:18.174 -> Greutate: -18.27 unități |
| 17:56:18.733 -> Greutate: -27.71 unități |
| 17:56:19.250 -> Greutate: -27.62 unități |
| 17:56:19.808 -> Greutate: -27.68 unități |
| 17:56:20.321 -> Greutate: -27.64 unități |
| 17:56:20.835 -> Greutate: -27.66 unități |
| 17:56:21.345 -> Greutate: -18.40 unități |
| 17:56:21.904 -> Greutate: -27.71 unități |
| 17:56:22.419 -> Greutate: -27.71 unități |
| 17:56:22.940 -> Greutate: -27.69 unități |
| 17:56:23.460 -> Greutate: -27.67 unități |
| 17:56:23.977 -> Greutate: -27.62 unități |
| 17:56:24.497 -> Greutate: -18.23 unități |

| Values mode 1 (free noise) |
|---|
| 17:56:33.975 -> Greutate: -27.69 unități |
| 17:56:34.492 -> Greutate: -18.27 unități |
| 17:56:35.051 -> Greutate: -132.19 unități |
| 17:56:35.563 -> Greutate: -27.74 unități |
| 17:56:36.075 -> Greutate: -27.83 unități |
| 17:56:36.636 -> Greutate: -18.25 unități |
| 17:56:37.150 -> Greutate: -27.77 unități |
| 17:56:37.662 -> Greutate: -18.26 unități |
| 17:56:38.223 -> Greutate: -18.38 unități |
| 17:56:38.739 -> Greutate: -27.70 unități |
| 17:56:39.299 -> Greutate: -27.66 unități |
| 17:56:39.813 -> Greutate: -27.69 unități |
| 17:56:40.322 -> Greutate: -27.76 unități |
| 17:56:40.836 -> Greutate: -27.73 unități |
| 17:56:41.349 -> Greutate: -18.22 unități |
| 17:56:41.909 -> Greutate: -27.71 unități |
| 17:56:42.469 -> Greutate: -27.76 unități |
| 17:56:42.981 -> Greutate: -27.71 unități |
| 17:56:43.492 -> Greutate: -18.36 unități |
| 17:56:44.006 -> Greutate: -27.72 unități |
| 17:56:44.520 -> Greutate: -27.71 unități |
| 17:56:45.082 -> Greutate: -18.25 unități |
| 17:56:45.595 -> Greutate: -27.66 unități |
| 17:56:46.110 -> Greutate: -27.70 unități |
| 17:56:46.619 -> Greutate: -27.74 unități |
| 17:56:47.177 -> Greutate: -27.70 unități |
| 17:56:47.692 -> Greutate: -27.66 unități |
| 17:56:48.205 -> Greutate: -18.32 unități |
| 17:56:48.716 -> Greutate: -27.68 unități |

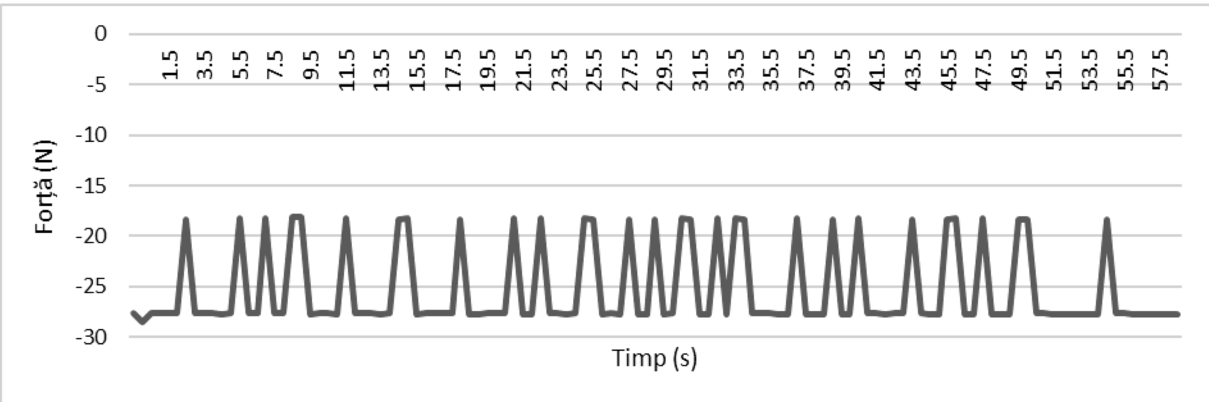

## Appendix 4. Data collected for the angular stages of each gripper module

### Appendix 4.1. Module 1 – stage 1

| Angular determination for contact |
|---|
| 09:41:48.289 -> Position: -417 |
| 09:41:48.381 -> Position: -654 |
| 09:41:48.428 -> Position: -666 |
| 09:41:48.473 -> Position: -678 |
| 09:41:48.566 -> Position: -695 |
| 09:41:48.611 -> Position: -702 |
| 09:41:48.749 -> Position: -710 |
| 09:41:48.842 -> Position: -715 |
| 09:41:48.889 -> Position: -717 |
| 09:41:49.029 -> Position: -718 |
| 09:41:49.121 -> Position: -719 |
| 09:41:49.214 -> Position: -719 |
| 09:41:49.306 -> Position: -720 |
| 09:41:49.492 -> Position: -720 |
| 09:41:49.631 -> Position: -720 |
| 09:41:49.814 -> Position: -720 |
| 09:41:49.953 -> Position: -720 |
| 09:41:50.094 -> Position: -720 |
| 09:41:50.280 -> Position: -720 |
| 09:41:50.372 -> Position: -80 |
| 09:41:50.418 -> Position: -18 |
| 09:41:50.512 -> Position: -15 |
| 09:41:50.606 -> Position: -15 |
| 09:41:50.699 -> Position: -15 |
| 09:41:50.792 -> Position: -14 |
| 09:41:50.931 -> Position: -14 |
| 09:41:51.024 -> Position: -14 |
| 09:41:51.117 -> Position: -14 |
| 09:41:51.211 -> Position: -14 |
| 09:41:51.303 -> Position: -14 |
| 09:41:51.395 -> Position: -14 |
| 09:41:51.535 -> Position: -14 |
| 09:41:51.629 -> Position: -14 |
| 09:41:51.722 -> Position: -14 |
| 09:41:51.814 -> Position: -14 |
| 09:41:51.906 -> Position: -79 |
| 09:41:52.000 -> Position: -743 |
| 09:41:52.093 -> Position: -738 |
| 09:41:52.279 -> Position: -738 |
| 09:41:52.416 -> Position: -738 |

| Angular determination for contact |
|---|
| 09:41:52.600 -> Position: -738 |
| 09:41:52.739 -> Position: -738 |
| 09:41:52.924 -> Position: -738 |
| 09:41:53.063 -> Position: -738 |
| 09:41:53.203 -> Position: -738 |
| 09:41:53.390 -> Position: -738 |
| 09:41:53.530 -> Position: -738 |
| 09:41:53.715 -> Position: -738 |
| 09:41:53.808 -> Position: 2 |
| 09:41:53.948 -> Position: -2 |
| 09:41:54.040 -> Position: -2 |
| 09:41:54.132 -> Position: -2 |
| 09:41:54.224 -> Position: -2 |
| 09:41:54.316 -> Position: -2 |
| 09:41:54.410 -> Position: -2 |
| 09:41:54.551 -> Position: -2 |
| 09:41:54.644 -> Position: -2 |
| 09:41:54.736 -> Position: -2 |
| 09:41:54.829 -> Position: -2 |
| 09:41:54.922 -> Position: -2 |
| 09:41:55.015 -> Position: -807 |
| 09:41:55.152 -> Position: -771 |
| 09:41:55.245 -> Position: -771 |
| 09:41:55.338 -> Position: -771 |
| 09:41:55.431 -> Position: -771 |
| 09:41:55.523 -> Position: -771 |
| 09:41:55.616 -> Position: -771 |
| 09:41:55.754 -> Position: -771 |
| 09:41:55.846 -> Position: -771 |
| 09:41:55.939 -> Position: -771 |
| 09:41:56.031 -> Position: -771 |
| 09:41:56.123 -> Position: -771 |
| 09:41:56.261 -> Position: -771 |
| 09:41:56.353 -> Position: -771 |
| 09:41:56.445 -> Position: -771 |
| 09:41:56.538 -> Position: -771 |
| 09:41:56.630 -> Position: -771 |
| 09:41:56.724 -> Position: -771 |
| 09:41:56.863 -> Position: -771 |
| 09:41:56.955 -> Position: -771 |

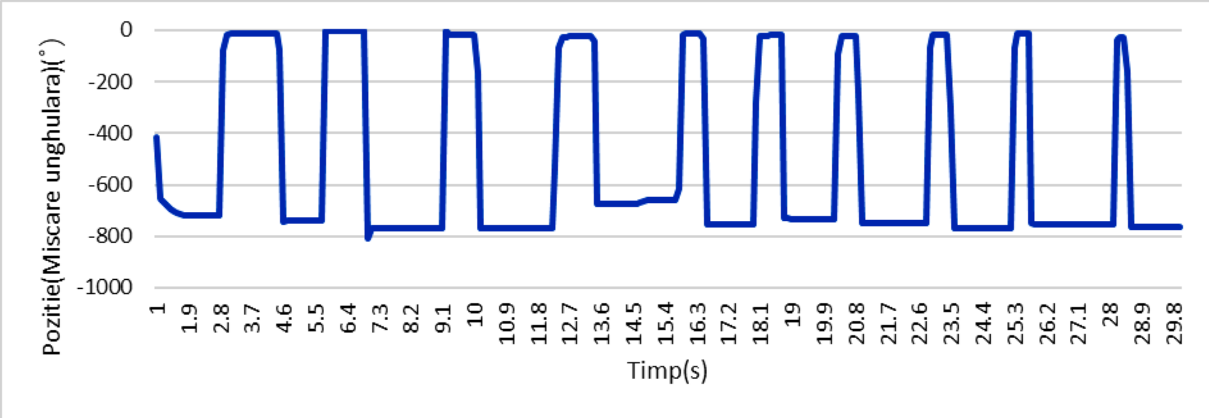
Pozitie(Miscare unghulara)(°)
0
-200
-400
-600
-800
-1000
1
1.9
2.8
3.7
4.6
5.5
6.4
7.3
8.2
9.1
10
10.9
11.8
12.7
13.6
14.5
15.4
16.3
17.2
18.1
19
19.9
20.8
21.7
22.6
23.5
24.4
25.3
26.2
27.1
28
28.9
29.8
Timp(s)

## Appendix 5. The final shape of the gripper

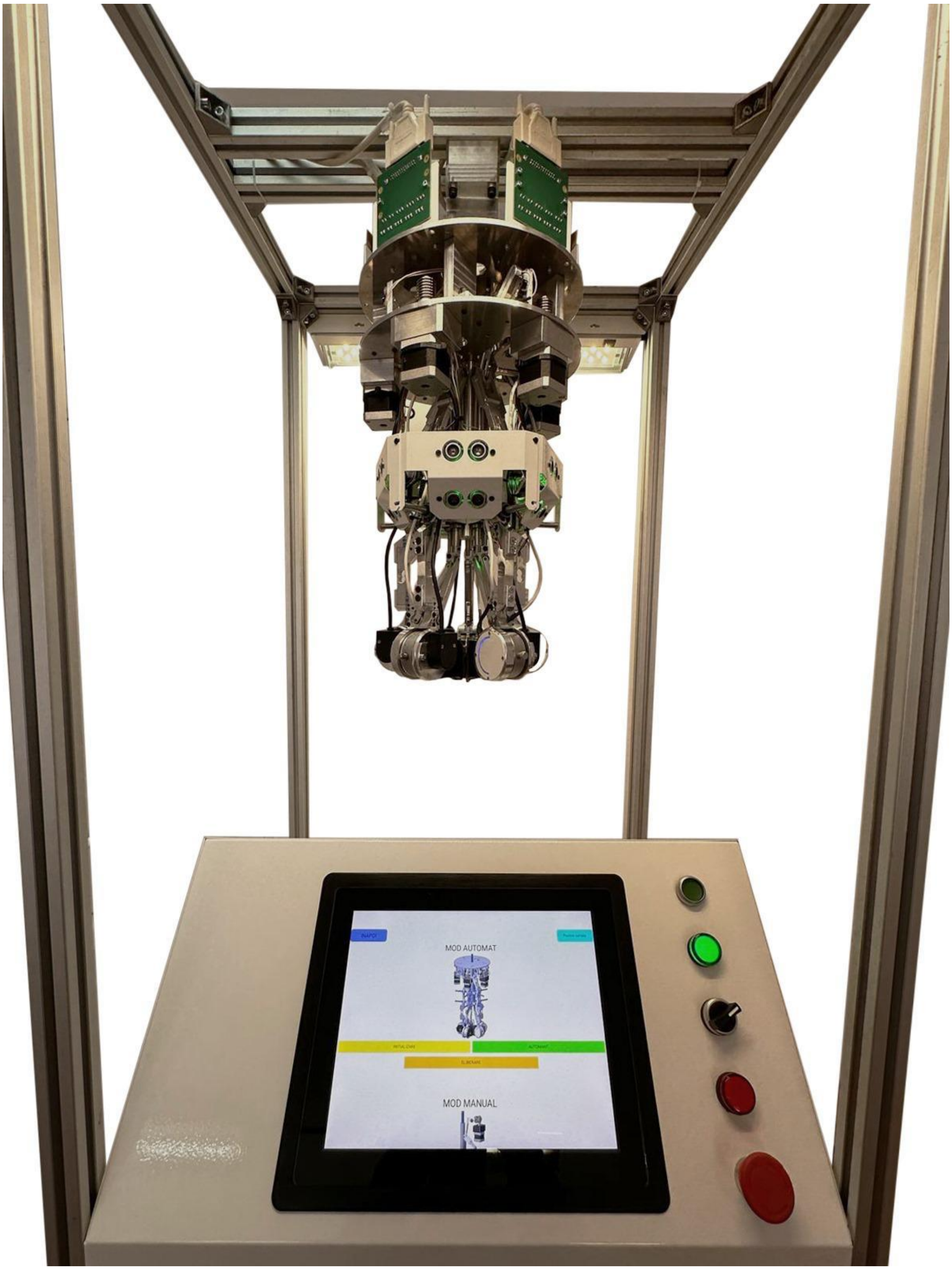
MOD AUTOMAT
MOD MANUAL